



THE STUDY OF INTERPLAY BETWEEN SPIN DENSITY WAVE AND SUPERCONDUCTIVITY IN FERROPNICTIDES

By
WUBISHET AHMED

A THESIS PRESENTED TO THE SCHOOL OF GRADUATE STUDIES ADDIS ABABA
UNIVERSITY IN PARTIAL FULFILLMENT OF THE
REQUIREMENTS FOR THE DEGREE OF
MASTER OF SCIENCE IN PHYSICS

ADDIS ABABA, ETHIOPIA

JUNE, 2011

ADDIS ABABA UNIVERSITY
DEPARTMENT OF
PHYSICS

The undersigned hereby certify that they have read and recommend to the School of Graduate Studies for acceptance a thesis entitled **“THE STUDY OF INTERPLAY BETWEEN SPIN DENSITY WAVE AND SUPERCONDUCTIVITY IN FERROPNICTIDES”** by **WUBISHET AHMED** in partial fulfillment of the requirements for the degree of **Master of Science in Physics**.

Dated: JUNE,2011

Approved by the examination committee

Advisor:

Prof.P.Singh

Examiners:

Prof.V.N.Mal'nev

Prof.Javed Mazher

ADDIS ABABA UNIVERSITY

Date: **JUNE,2011**

Author: **WUBISHET AHMED**

Title: **THE STUDY OF INTERPLAY BETWEEN SPIN
DENSITY WAVE AND SUPERCONDUCTIVITY IN
FERROPNICTIDES**

Department: **Physics**

Degree: **M.Sc.** Convocation: **JUNE** Year: **2011**

Permission is herewith granted to Addis Ababa University to circulate and to have copied for non-commercial purposes, at its discretion, the above title upon the request of individuals or institutions.

Signature of Author

THE AUTHOR RESERVES OTHER PUBLICATION RIGHTS, AND NEITHER THE THESIS NOR EXTENSIVE EXTRACTS FROM IT MAY BE PRINTED OR OTHERWISE REPRODUCED WITHOUT THE AUTHOR'S WRITTEN PERMISSION.

THE AUTHOR ATTESTS THAT PERMISSION HAS BEEN OBTAINED FOR THE USE OF ANY COPYRIGHTED MATERIAL APPEARING IN THIS THESIS (OTHER THAN BRIEF EXCERPTS REQUIRING ONLY PROPER ACKNOWLEDGEMENT IN SCHOLARLY WRITING) AND THAT ALL SUCH USE IS CLEARLY ACKNOWLEDGED.

Table of Contents

Table of Contents	v
List of Figures	vi
Abstract	vii
Acknowledgements	viii
1 Introduction	1
2 Review Literature	9
2.1 Introduction	9
2.2 Phase Diagrams	13
2.2.1 1111 materials	13
2.2.2 122 materials	16
2.2.3 11 materials	20
2.3 Magnetic order	21
2.3.1 1111 materials	22
2.3.2 122 materials	25
2.3.3 11 materials	26
2.4 Spin density wave state	27
2.4.1 The coexistence of SDW and SC	28
3 Mathematical Techniques	30
3.1 Green's function formalism	30
3.1.1 Green's functions formulation with reduced Hamiltonian	32
4 Theoretical Formulation	36
4.1 The model Hamiltonian	36
4.2 Equations of motion	37
4.2.1 For superconducting order parameter and transition temperature	47
4.2.2 For the spin density wave order parameter and temperature	58
4.2.3 For pure superconducting state	67
4.2.4 For pure SDW State	68

5 Results and Discussions	69
6 Conclusion	76
Bibliography	78

List of Figures

1.1	Graph of resistance against temperature for a mercury wire.	2
2.1	Crystal structure of the 1111, 122, 111, and 11 materials.	10
2.2	Experimentally determined phase diagram for $BaFe_{2-x}Co_xAs_2$ and $Ba_{1-x}K_xFe_2As_2$	18
2.3	(a) Resulting phase diagram of $Ba(Fe_{1-x}Co_x)_2As_2$ with inclusion of high resolution x-ray diffraction measurements in the region where superconductivity and magnetism coexist. (b) Shows the reentrant nature of the structural phase transition.	19
2.4	Experimentally determined phase diagram for $e)Fe_{1.03}Te_{1-x}Se_x$	21
2.5	(a) In-plane magnetic structure for the 1111 and 122 parent compounds.(b) Magnetic structure for 11 materials	22
5.1	A graph of energy gap (Δ) Vs Temperature(T) for doped $LaFeAsO_{1-x}F_x$ (Blue color), $Ba(Fe_{1-x}Co_x)_2As_2$ (Red color) and $Fe_{1.03}Te_{1-x}Se_x$ (Yellow color) .	70
5.2	A graph of magnetic ordering temperature (T_{SDW}) Vs magnetic order parameter (Δ_{SDW}) for doped $LaFeAsO_{1-x}F_x$ (Blue color), $Ba(Fe_{1-x}Co_x)_2As_2$ (Red color) and $Fe_{1.03}Te_{1-x}Se_x$ (Yellow color)	71
5.3	A graph of superconducting transition temperature (T_C) Vs magnetic order parameter (Δ_{SDW}) for doped $LaFeAsO_{1-x}F_x$ (Blue color), $Ba(Fe_{1-x}Co_x)_2As_2$ (Red color) and $Fe_{1.03}Te_{1-x}Se_x$ (Yellow color)	72
5.4	A graph of magnetic ordering temperature (T_{SDW}) Vs superconducting order parameter (Δ_S) for doped $LaFeAsO_{1-x}F_x$ (Blue color), $Ba(Fe_{1-x}Co_x)_2As_2$ (Red color) and $Fe_{1.03}Te_{1-x}Se_x$ (Yellow color)	72
5.5	The phase diagram of the SDW and SC for doped $Ba(Fe_{1-x}Co_x)_2As_2$. . .	73
5.6	The phase diagram of the SDW and SC for doped $LaFeAsO_{1-x}F_x$	74
5.7	The phase diagram of the SDW and SC for doped $Fe_{1.03}Te_{1-x}Se_x$	75

Abstract

This work focuses on the study of interplay between superconductivity and spin density wave in Fe- based superconductors. The effect of magnetic ordering state on transition temperature (T_C) has been investigated in Fe-based superconductors with in the BCS theory, irrespective of the pairing mechanism.

The expression for the transition temperatures (T_c and T_{SDW}) as a function of superconducting order parameter (Δ_S) and magnetic order parameter (Δ_{SDW}) has been obtained using the model Hamiltonian for the system and Green's function technique and their application have been studied. And their values has been calculated numerically for suitable values of system parameters.

The interplay of magnetic ordering state and superconductivity have been found crucial for enhancing T_C . It is also found that the presence of magnetic ordering state does not increase T_C rather it decreases, but the suppression of this state should increase the superconducting transition temperature (T_C).

On the other hand, for suitable value of the parameters, we report the magnetic order dependent phase diagrams Which shows the interplay of superconductivity and spin density wave in some Fe based superconductors.

The results are in general agreement with experimental observations and theoretical models of ferropnictides.

Acknowledgements

I would like to express my heart full gratitude to my advisor and instructor Prof.P.Singh for his guidance, assistance, supervision and contribution of valuable suggestions. His scientific excitement, integral view on research and overly enthusiasm, has made a deep impression on me. Finally I express my sincere gratitude and appreciation for all my friends for their contribution.

Chapter 1

Introduction

The Rocky Road To High Temperature Superconductivity

Superconductivity is a phenomena occurring in a certain materials at low temperature, characterized by the complete absence of electrical resistance. The story of high temperature superconductivity has its Genesis in the stars, particularly in one star, our sun. In the 1860's unusual spectral lines were observed from the emitted light of the hot incandescent gases in the chromosphere's of the sun. These spectral lines appeared unrelated to any then known substances on earth. The gas was given the name Helium deriving from the Greek Words Helios—sun. At the turn of the century, helium was discovered on earth, and in 1908, the Deutsch scientist, Kamerlingh ones, succeeded in liquefying helium gas at a temperature a few degrees above absolute zero. This set the stage for the discovery of superconductivity.

In 1911 superconductivity was first observed in mercury by Dutch physicist Heike Kamerlingh Onnes of Leiden University [6]. When he cooled it to the temperature of liquid helium, 4.2 degrees Kelvin (-452 F, -269 C), its resistance suddenly disappeared. The Kelvin scale represents an "absolute" scale of temperature. Current was flowing through the mercury wire and nothing was stopping it, the resistance was zero. (See Figure 1.1 which shows a graph of resistance against temperature of a mercury wire which Onnes produced.) According to Onnes, "Mercury has passed into a new state, which on account of its extraordinary electrical properties may be called the super-conductive state". The

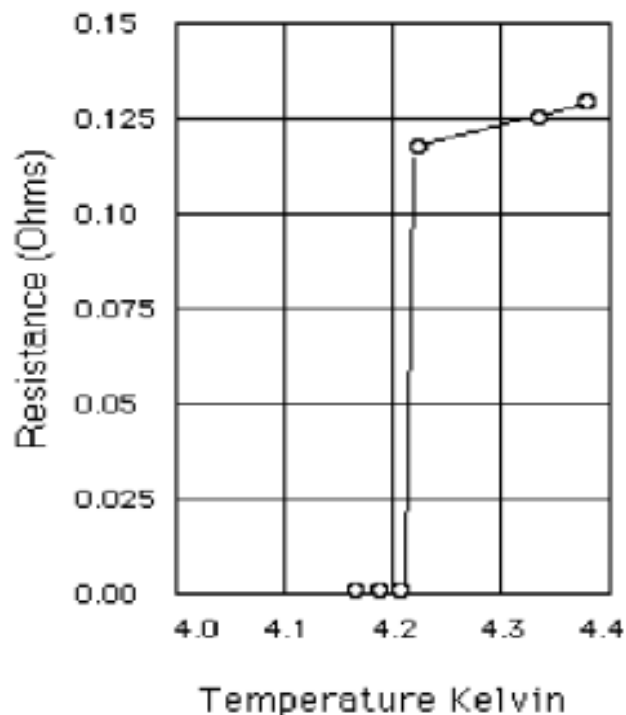


Figure 1.1: Graph of resistance against temperature for a mercury wire.

experiment left no doubt about the disappearance of the resistance of a mercury wire. Kamerlingh Onnes called this newly discovered state, **Superconductivity**. The temperature at which this transition starts is called the critical temperature (T_c). In one of Onnes experiments he started a current flowing through a loop of lead wire cooled to 4 K. A year later the current was still flowing without significant current loss. Onnes found that the superconductor exhibited what he called persistent currents, electric currents that continued to flow without an electric potential driving them. Onnes had discovered superconductivity, and was awarded the Nobel Prize in 1913.

Superconductors, materials that have no resistance to the flow of electricity, are one of the last great frontiers of scientific discovery. Not only have the limits of superconductivity not yet been reached, but the theories that explain superconductor behavior seem to be constantly under review. Whenever a new scientific discovery is made, researchers must strive to explain their theories. By 1933 Walther Meissner and R. Ochsenfeld discovered

that superconductors are more than a perfect conductor of electricity, they also have an interesting magnetic property of excluding a magnetic field[7].

Because of Faraday's law, the magnetic field inside a superconductor cannot change because there is no emf due to the lack of electric resistance. Thus to prevent this, a current is induced in the superconductor which cancels out the external field.

A superconductor will not allow a magnetic field to penetrate its interior. It causes currents to flow that generate a magnetic field inside the superconductor that just balances the field that would have otherwise penetrated the material. This effect, called the Meissner effect, causes a phenomenon that is a very popular demonstration of superconductivity. The Meissner Effect will occur only if the magnetic field is relatively small. If the magnetic field becomes too great, it penetrates the interior of the metal and the metal loses its superconductivity. The Meissner effect is so strong that a magnet can actually be levitated over a super-conductive material.[7]

In subsequent decades other superconducting metals, alloys and compounds were discovered. In 1941, niobium-nitride was found by Aschermann, Friederich, Justi and Kramer to super conduct at 16 K. In 1953 vanadium-silicon displayed super-conductive properties at 17.5 K. And, in 1962 scientists at Westinghouse developed the first commercial superconducting wire, an alloy of niobium and titanium ($NbTi$).

The first widely-accepted theoretical understanding of superconductivity was advanced in 1957 by American physicists John Bardeen, Leon Cooper, and John Schrieffer. They developed a model that has since stood as a good mental picture of why superconductors behave as they do. The model is expressed in terms of advanced ideas of the science of quantum mechanics, but the main idea of the model suggests that electrons in a superconductor condense into a quantum ground state and travel together collectively and coherently. In 1972, Bardeen, Cooper, and Schrieffer received the Nobel Prize in Physics for their theory of superconductivity, which is now known as the BCS theory, after the initials of their last names.[8]

The mathematically-complex BCS theory explained superconductivity at temperatures close to absolute zero for elements and simple alloys. However, at higher temperatures and with different superconductor systems, the BCS theory has subsequently become inadequate to fully explain how superconductivity is occurring.

Another significant theoretical advancement came in 1962 when Brian D. Josephson, a graduate student at Cambridge University, predicted that electrical current would flow between two superconducting materials - even when they are separated by a non-superconductor or insulator. His prediction was later confirmed and won him a share of the 1973 Nobel Prize in Physics. This tunneling phenomenon is today known as the "Josephson effect".

Rapid cooling techniques leading ultimately to film preparation techniques (sputtering, thermal evaporation, E- beam evaporation, etc.) were developed leading to the discovery in 1971 of a record high Tc of 23 k in Nb_3Ge . Researchers next turned to preparation of Nb_3Si which was expected to have a Tc near 30 k. Where as $NbGe$ had an of stoichiometric equilibrium A 15 phase, Nb_3Si had none. In addition to film growth techniques, high pressure synthesis techniques were used in attempts to produce this material[27].

A significant advance on the road to high Tc materials occurred in 1972 when superconductivity was discovered in $PbMO_6S_8$ a ternary superconductor. The significance of this discovery was that it broke the hold of binary super conductors as being the only high Tc materials. Most of the empirical rules developed for the binaries were invalid for the ternaries and synthesis become much more sophisticated.

In the late 1970s and early 1980s superconductivity was discovered in the heavy fermions systems and in nearly magnetic systems[28].Such researches become fashionable even though these systems did not necessarily have high Tc value. New pairing interactions were sought with the hope of eventually using the new interaction for high Tc superconductors.

The next major mile stone in this direct route to high Tc occurred in 1973 when

Johnston discovered super conductivity in $LiTiO_3$ at temperature as high as 13 k[29]. Thus removing the belief that super conductivity in the oxide materials was limited to very low temperatures. In 1975 ,superconductivity was discovered in $PbBiBaO_3$ at 14 k to represent another member to the growing class of higher temperature oxides[30].

There were many reports of high temperature superconductors in organic materials in the early 1970s. In 1973, Heeger reported super conducting fluctuations in $TTF-TCNQ$ molecules at temperature as high as 77 k. It was claimed that an electronically driven structural transformation (Pieierls instability) occurred at temperature slightly higher than the supper conducting Tc; hence bulk super conductivity was not observed.[31]

The 1980's were a decade of unrivaled discovery in the field of superconductivity. In 1964 Bill Little of Stanford University had suggested the possibility of organic (carbon-based) superconductors. The first of these theoretical superconductors was successfully synthesized in 1980 by Danish researcher Klaus Bechgaard of the University of Copenhagen and 3 French team members. $(TMTSF)_2PF_6$ had to be cooled to an incredibly cold 1.2 K transition temperature and subjected to high pressure to super-conduct.

Many new phenomena have been seen in these organic materials in addition to superconductivity. At present the maximum Tc (under pressure) is 8 k in $\beta - (BEDT - TTF)_2I_3$. There is some evidence that the mechanism for super conductivity in the organic materials is not the electron- phonon interaction and there are also speculations that P wave pairing interactions are occurring[33].

Shortly thereafter, super conductivity was discovered in $SrTiO_3$ the first oxide super conductors and the first perovskite superconducting materials[34]. Although Tc of these materials were below 1 k, history must regard these reports as major milestones in the road to high temperature superconductivity since they started the interest in these types of materials, which persisted on a limited basis until the discoveries of super conductivity as in $LaBaCuO_5$ [36] and $YBaCuO$ [35].

Then, in 1986, a truly breakthrough discovery was made in the field of superconductivity. Georg Bednorz and Alex Müller, working at IBM in Zurich Switzerland, were experimenting with a particular class of metal oxide ceramics called perovskites. Bednorz and Müller surveyed hundreds of different oxide compounds. Working with ceramics of lanthanum, barium, copper, and oxygen they found indications of superconductivity at 35 K, a startling 12 K above the old record for a superconductor. What made this discovery so remarkable was that ceramics are normally insulators. They don't conduct electricity well at all.[36]

Müller and Bednorz discovery triggered a flurry of activity in the field of superconductivity. In January of 1987 a research team at the University of Alabama-Huntsville substituted Yttrium for Lanthanum in the Müller and Bednorz molecule and achieved an incredible 92 K T_c. For the first time a material (today referred to as YBCO) had been found that would superconduct at temperatures warmer than liquid nitrogen - a commonly available coolant. Additional milestones have since been achieved using exotic - and often toxic - elements in the base perovskite ceramic.

The world record T_c of 138 K is now held by a thallium-doped, mercuric-cuprate comprised of the elements Mercury, Thallium, Barium, Calcium, Copper and Oxygen. The T_c of this ceramic superconductor was confirmed by Dr. Ron Goldfarb at the National Institute of Standards and Technology-Colorado in February of 1994. Under extreme pressure its T_c can be coaxed up even higher - approximately 25 to 30 degrees more at 300,000 atmospheres.

In recent years, many discoveries regarding the novel nature of superconductivity have been made. In 1997 researchers found that at a temperature very near absolute zero an alloy of gold and indium was both a superconductor and a natural magnet. Conventional wisdom held that a material with such properties could not exist. Since then, over a half-dozen such compounds have been found. Recent years have also seen the discovery of the first high-temperature superconductor that does not contain any copper (2000), and the

first all-metal perovskite superconductor (2001).

Also in 2001 a material that had been sitting on laboratory shelves for decades was found to be an extraordinary new superconductor. Japanese researchers measured the transition temperature of magnesium diboride at 39 Kelvin - far above the highest T_c of any of the elemental or binary alloy superconductors. While 39 K is still well below the T_c's of the "warm" ceramic superconductors, subsequent refinements in the way MgB_2 is fabricated have paved the way for its use in industrial applications. Laboratory testing has found MgB_2 will outperform $NbTi$ and Nb_3Sn wires in high magnetic field applications like MRI. Laboratory testing has found MgB_2 will outperform $NbTi$ and Nb_3Sn wires in high magnetic field applications like MRI.

The most recent "family" of superconductors to be discovered is the "pnictides". The first report of superconductivity in an iron pnictide, specifically in F-doped $LaOFeP$ below 5 K in 2006 [1], was hardly noticed and only two years later, On 23rd February, 2008, a group from Tokyo Institute of technology published paper in (JACS) Journal of the American society, in which they reported that the fluorine doped lanthanum Oxide Iron Arsenide super conducts at 26 K. The discovery of superconductivity below a critical temperature (T_c) at 26 K in $LaO_{1-x}FxFeAs$ gave birth to what many have already christened the iron age of high-temperature superconductivity.

After the publication of this paper within month a Chinese group from Beijing reported that they replaced Lanthanum (La) with Cerium (Ce) and boosted T_c to 41 k. Another group from china replaced Lanthanum (La) with samarium (Sm) and raised T_c to 43 k. By replacing La with rare earth ions of smaller radii the critical temperature increased from 26 K in $LaOFFeAs$ to 55 K in $SmOFFeAs$ within a couple of days.

Since the discovery of cuprates in 1986 no other material has reached a superconducting transition as high as 55 K. The discovery in early 2008 of the new class of high temperature superconductors has broken the monopoly in the cuprates in the physics of high temperature superconducting compounds. At present dozens of HTSC compounds

are known to have of superconducting transitions Tc temperatures exceeding 24 K.

The iron age of high-temperature superconductivity is not only providing a new class of high-Tc compounds, it could also provide the clearest examples of magnetism-mediated superconductivity. The interplay between Superconductivity and magnetism has been an interesting topic in condensed matter physics. Therefore, in this study we attempt to investigate theoretically the interplay between superconductivity and spin density wave in ferropnictide superconductors.

Therefore, we present a model study for the interplay between SDW and SC which incorporates two competing physical processes involving the electron-hole (SDW) like pairing of opposite spins with a net momentum difference (Q) between the conjugates and electron-electron (SC) pairing of opposite spins with zero total momentum. Such a model study can also provide an important understanding regarding the effect of the presence of antiferromagnetic (SDW) order on the pairing symmetry of the superconducting state.

Our main concern therefore boils down to study of the phase diagram, comprising of the magnetic ordering temperature and superconducting transition temperature as a function of magnetic order parameter (Δ_{SDW}). Interestingly enough, we obtain the phase diagram which resembles to most of Fe pnictide superconductors.

The rest of the paper is arranged as follows. In chapter 2 we provide the experimental studies of magnetism in the Fe based superconductors and its influence on superconductivity. In chapter 3 we present the Greens function technique (Retarded double time) we are using to solve the self consistent gap equations. Chapter 4 contains the mean field model Hamiltonian for the interplay between Sc and SDW together with the respective gap equations and transition temperatures. Chapter 5 is devoted to discuss the results obtained from our model calculations and finally we conclude in chapter 6.

Chapter 2

Review Literature

2.1 Introduction

The first report of superconductivity in an iron pnictides, specifically in F-doped LaOFeP below 5 K in 2006 , was hardly noticed and only two years later, when F-doped LaOFeAs was reported to super conduct below 28 K, the potential of iron pnictides as high-temperature superconducting materials was realized [41]. Following this discovery, more than 50 new iron superconductors with the same basic structure were discovered with T_c reaching up to 56 K .The common motive is a planar FeAs layer in which the Fe atoms form a square lattice, tetrahe- drally coordinated with As atoms placed alternately above and below the hollow centers of the squares. Instead of As, the ligand could be another pnictogen (P) or a chalcogen (X=Se or Te), but for simplicity, in this paper we shall refer to it as As.[55]

These superconductors are divided in four main families depending on their 3D crystal structure This structure is shown in Fig. 2.1 [31]: The iron chalcogenides are simple tetragonal (st) with the FeX layers stacked on top of each other (11 family). The iron pnictides have the FeAs layers separated by alkali metals (111 family), or by rare-earth oxygen/fluoride blocking layers (1111 family as in Fig.2.1), in st stacking, or by alkali-earth metals (122 family) in body-centered tetragonal (bct) stacking.

The discovery of superconductivity in F doped LaFeAsO with T_C of 26 K [1] created

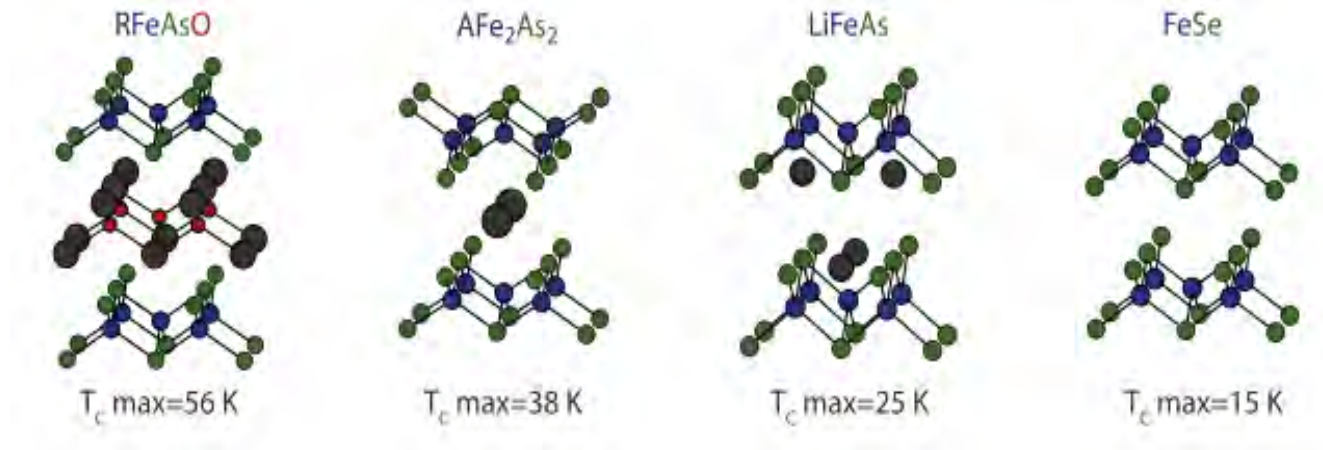


Figure 2.1: Crystal structure of the 1111, 122, 111, and 11 materials.

a flurry of excitement in the condensed matter physics community. Substitutional replacement of the rare earth ion led to a rapid increase in the superconducting transition temperature. Denoting the chemical formula of these so-called 1111 materials by $RFeAsO$, F doping resulted in the following optimal transition temperatures: 52 K for $R = Nd$ [2], 52 K for $R = Pr$ [3], 55 K for $R = Sm$ [4], 41 K for $R = Ce$ [5], 36–50 K for $R = Gd$ [68], 46 K for $R = Tb$ [9], and 45 K for $R = Dy$ [9]. To date, the highest transition temperature for the Fe-based superconductors is 56 K observed in a sample of $Gd_{1-x}Th_xFeAsO$ [10].

These superconducting transition temperatures make the Fe-based materials second only to the cuprates and they, therefore, represent the second family of high- T_c superconductors. It was later shown that F doping was not necessary and similar transition temperatures could be obtained for the case of oxygen deficient $RFeAsO_{1-y}$: 28 K for $R = La$ [11, 12], 42 K for Ce [11], 53 K for Nd [11–13], 48 K for Pr [11, 12], 55 K for Sm [11], 53 K for Gd [14, 12], 52 K for Tb and Dy [12]. Both the F doped and oxygen deficient samples show the same trend for T_c as a function of rare earth ion. Crystal structure of the 1111, 122, 111, and 11 materials. At room temperature, the $RFeAsO$ materials crystallize in the $P 4/nmm$ tetragonal space group resulting in a layered structure with $FeAs$ and RO layers [15] (see figure 2.1 above). This layered structure is reminiscent of the cuprates with $FeAs$ planes taking the place of the CuO layers. The square planar arrangement of

(likely) magnetic Fe is similar to the cuprates and leads one to naturally speculate that magnetism may play an essential role in the superconducting pairing. Shortly after the initial activity on the 1111 materials, superconductivity was also discovered in related materials possessing identical FeAs layers with differing spacers.

The discovery of superconductivity with T_c of 38 K in $Ba_{1-x}KxFe_2As_2$ [16] was of particular interest as it was quickly realized that large single crystals of these 122 materials could be grown (unlike the 1111 family). Structurally, at room temperature, the 122 materials exhibit the $ThCr_2Si_2$ crystal structure (space group I 4/mmm). As is clearly shown in figure 2.1 above, the FeAs layers are very similar to the 1111 materials although neighboring layers along the c-axis have an inverted arsenic coordination.

For both the 1111 [17] and 122 [18] materials, it was quickly realized that replacement of Fe with Co would also result in superconductivity, albeit with a reduced T_C when compared with doping between FeAs planes. Such behavior is in contrast to that observed in the cuprates where disorder in the copper oxide plane was found to destroy superconductivity. Superconductivity was also discovered in the 122 materials upon electron doping on the Fe site with Ni [19], Rh [20, 21], Ir [21] and Pd [20, 21] or by isoelectronic replacement of Fe with Ru [22, 23]. Interestingly, electron doping with Cu [24] or hole doping with Cr [25] does not yield superconductivity. The large number of potential dopants together with the availability of single crystal samples has made the 122 family of compounds the topic of considerable experimental focus.

Superconductivity was also discovered in LiFeAs [37–39] and $Na_{1-x}FeAs$ [40] (111 materials) sharing the same FeAs plane with Li or Na as the spacer as shown in figure 2.1 above. Transition temperatures of 18 K (for LiFeAs) and 12–25 K (for $Na_{1-x}FeAs$) [40] have been observed dependent on the precise Na concentration. Interestingly, superconductivity seems to appear in the 111 materials in purely stoichiometric material without chemical doping. Finally, the Fe(Se, Te) family of compounds (11 materials) also exhibits superconductivity with a maximum transition temperature (under ambient pressure) of

15 K. The alpha phase of FeSe is a superconductor with a transition temperature of 8 K [42].

Structurally, the FeSe plane is very similar to the FeAs plane in the aforementioned materials (see figure 2.1 above) indicating that the presence of As is not a requirement for superconductivity. Band structure calculations [43] suggested that FeTe may have enhanced superconducting properties. However, pure $FeTe$ is not a superconductor [41] but is complicated by the presence of excess Fe, i.e. the actual chemical formula is $Fe_{1+y}Te$ [44]. It has been suggested that this excess Fe is magnetic and may act as a pair breaking moment destroying superconductivity [45]. Nonetheless, the doped material, $Fe_{1+y}Te_{1-x}Sex$ does exhibit an enhanced T_c of 15 K with the maximum transition temperature observed for x near 0.5 [41].

The structures of the 1111, 122, 111, and 11 families of materials are shown in figure 2.1 above. The common feature is the presence of an identical FeAs (or FeSe) plane. An interesting trend can be seen in figure 1—the larger the separation between layers, the higher the observed optimal transition temperature. Two-dimensional (2D) magnetism occurs in the regions of highest T_c and, thus, may be favorable for superconductivity. This trend led to attempts at further separating the FeAs layers and superconductivity with fairly high transition temperatures have been observed in Sr_2VO_3FeAs with a spacer of Sr_2VO_3 and T_c of 37.2 K [46], and doped $Sr_2Sc_{0.4}Ti_{0.6}FeAsO_3$ with a spacer of $Sr_2Sc_{0.4}Ti_{0.6}O_3$ and T_C onset of 45 K (although the resistivity does not reach zero until 7 K) [47]. Although these temperatures still do not exceed the 56 K in the 1111 materials, they are quite high particularly in the case of Sr_2VO_3FeAs as this material is nominally stoichiometric. There is hope that doping of this and related materials could lead to an increase in transition temperature.

Shortly after the discovery of superconductivity in $LaFeAsO_{1-x}Fx$, calculations indicated that conventional electron–phonon coupling was insufficient to explain the high transition temperatures [48], as was later verified experimentally [49]. As will be explained

below, a ubiquitous magnetically ordered state is present indicating magnetism in close proximity to superconductivity leading one to naturally consider the interplay between magnetism and superconductivity in these materials. In the following section, we will review experimental studies of magnetism in the Fe- based compounds and its influence on superconductivity.

2.2 Phase Diagrams

2.2.1 1111 materials

The first evidence for the importance of magnetism in the Fe-based superconductors was the concentration dependent phase diagram presented with the initial discovery of superconductivity in F doped LaFeAsO [1]. An additional phase was clearly present at low F concentration which vanished at doping levels where superconductivity appears although the exact nature of this phase was unclear. It was soon shown that the undoped LaFeAsO parent compound exhibited spin-density wave (SDW) order below about 150 K [15, 50] consistent with a $\sqrt{2} \times \sqrt{2} \times 2$ unit cell.

Unexpectedly, *LaFeAsO* also exhibited a structural phase transition [15] at a temperature slightly above the magnetic ordering temperature. The low temperature structure was originally described by the monoclinic P 112/n space group [15] but it was later clarified that the correct low temperature space group is the orthorhombic Cmma [51] (note that both notations accurately describe the observed structure). There is clear competition between magnetism and superconductivity as the magnetically ordered state is destroyed in the fluorine doped, superconducting samples [15, 50].

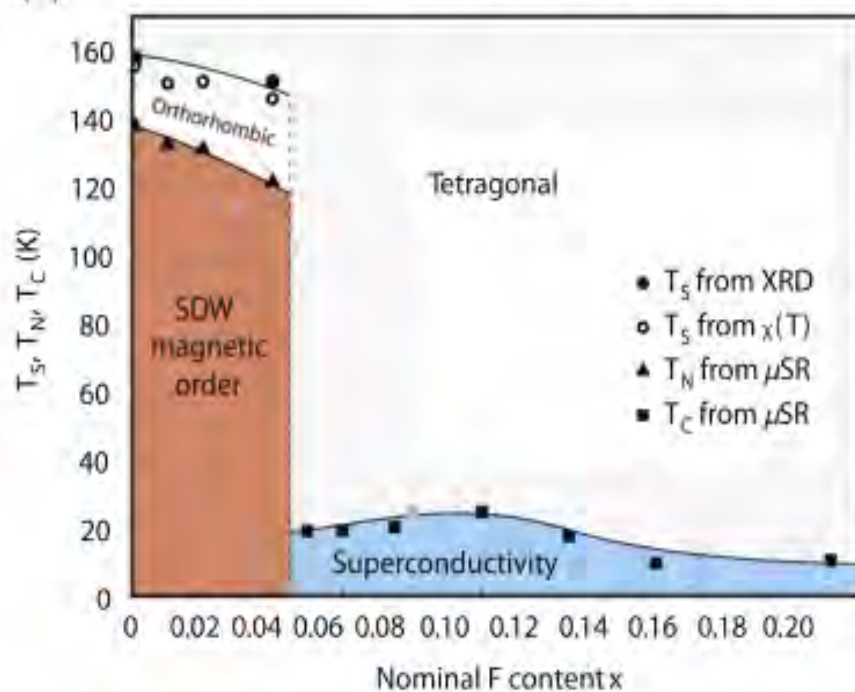
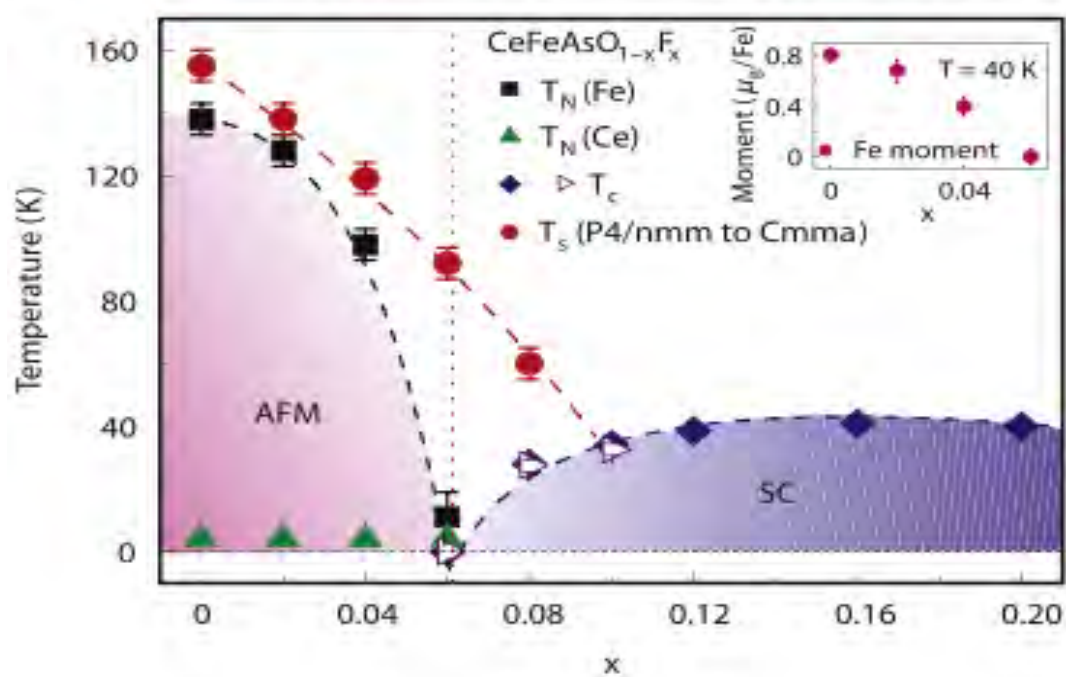
The phase diagram of *RFeAsO_{1-x}Fx* as a function of doping has been carefully studied for R = La [52] (figure 2.2(a)), Ce [53] (figure 2.2(b)), Pr [56] and Sm [54, 57] (figure 2.2(c)). The phase diagrams were experimentally determined using the following techniques: R = La, μ SR, ^{57}Fe Mossbauer spectroscopy and x-ray diffraction [52]; R = Ce,

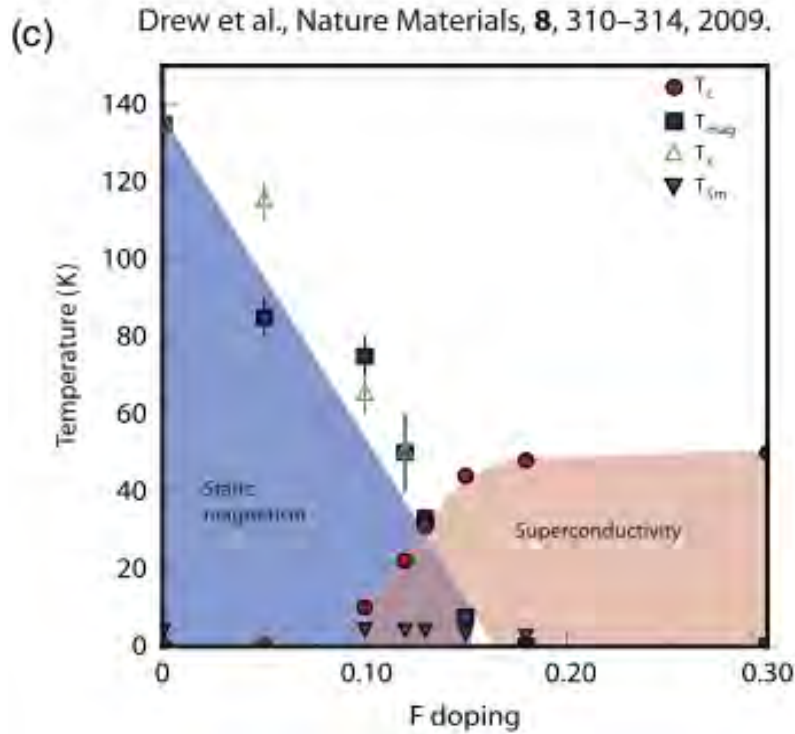
neutron diffraction, resistivity and magnetization [53]; R = Pr, x-ray diffraction, resistivity and magnetization [56]; R = Sm, μ SR [54] and x-ray diffraction [57]. For R = Nd, a partial phase diagram [58] was determined using resistivity measurements. In all cases measured, the $x = 0$ parent compounds show a structural phase transition at a temperature slightly above the transition to magnetic ordering with a typical structural transition at 150 K and SDW ordering at about 140 K.

In general, doping causes a suppression of both the structural and magnetic phase transitions and as these are suppressed, superconductivity emerges. The fundamental difference between materials with different rare earths comes in the behavior near the emergence of superconductivity. For R = La and Pr, the structural and magnetic transitions vanish in an abrupt step-like manner as a function of doping at the onset of superconductivity [52, 56], as shown in figure 2.2(a) for the case of R = La. For the case of R = Ce, the magnetic transition appears to vanish continuously to very low temperatures and superconductivity emerges at a concentration where this transition has been completely suppressed [53] (see figure 2.2(b)).

However, the structural transition has some range of concentrations where superconductivity coexists with this phase transition [53]. Finally, the case of R = Sm, shown in figure 2.2(c), looks similar to R = Ce in that the transitions are suppressed gradually and there appears to be overlap between the structural transition and superconductivity [57]. However, unlike the case of Ce, the Sm phase diagram shows a region where magnetic ordering coexists with superconductivity [54]. This suggests that the destruction of long range magnetic order is not a necessary condition for the emergence of superconductivity.

Figure 2.2 Experimentally determined phase diagram for (a) $LaFeAsO_{1-x}Fx$, b) $CeFeAsO_{1-x}Fx$ and c) $SmFeAsO_{1-x}Fx$

(a) Luetkens et al., Nature Materials, **8**, 305–309, 2009.(b) Zhao et al., Nature Materials, **7**, 953–959, 2008



2.2.2 122 materials

As mentioned previously, the AFe_2As_2 family of materials has numerous doping possibilities. The basic behavior of the superconducting materials can be described by considering the phase diagrams for $Ba_{1-x}K_xFe_2As_2$ (hole doping between the FeAs planes) and $BaFe_{2-x}Co_xAs_2$ (electron doping within the FeAs plane). Both materials share the same $BaFe_2As_2$ parent compound. As in the case of the 1111 parent compounds, Ba-122 exhibits both a structural phase transition (in this case from the room temperature tetragonal $I4/mmm$ space group to the low temperature orthorhombic $Fmmm$ space group [59, 60]) and the magnetic transition to a long range ordered, SDW state.

However, unlike the 1111 materials, both the structural and magnetic phase transitions occur at the same temperature in the Ba-122 parent compound [59–61]. Doping with either K [62, 63] or Co [34, 64, 65] causes a suppression of the structural and SDW transitions as in the 1111 materials. For Co doping, as x increases, the two transitions no longer appear at the same temperature with the structural transition occurring first

upon cooling [64] as shown in figure 2.3(d). In both cases, superconductivity emerges as the SDW order is suppressed. For K doping, the superconducting region starts for $x \sim 0.1$ and the maximum T_c of 38 K is reached for $x \sim 0.4$ [62, 63]. For $Ba(Fe_{1-x}Co_x)_2As_2$, superconductivity is first observed for $x \sim 0.03$ and the maximum T_c of 23 K is seen for $x \sim 0.07$ [34, 65]. Interestingly, for both K and Co doping, there is a region of the phase diagram where the SDW state and structural transition coexist with superconductivity.

Coexistence of superconductivity and magnetism has been a recurring theme in the study of superconducting materials [68–71]. For the doped 122 materials, the question of whether the SDW and superconducting states are microscopically coexisting or phase separated has received considerable attention experimentally. For hole doping with K, ^{75}As NMR [72], μSR [73] and magnetic force microscopy [73] consistently indicate distinct regions which are magnetically ordered and nonmagnetic regions as expected for microscopic phase separation. Furthermore, analysis of micro strain measured with x-ray and neutron diffraction was interpreted as being consistent with electronic phase separation [74].

Although most measurements on the K doped samples are consistent with a phase separation scenario, ^{75}Fe -Mössbauer measurements indicate a sample which is completely magnetically ordered as expected with microscopic coexistence of the SDW and superconducting states [75]. For the case of Co doping, both ^{75}As NMR [76] and μSR measurements [77] indicate that all the Fe sites participate in the magnetic order as would be expected for coexistence of superconductivity and SDW order. One ^{75}As NMR study directly compared the cases of K and Co doping and concluded phase coexistence for Co doped samples and separation for the case of K doping [78]. Finally, we note neutron diffraction measurements on Co doped samples [66, 67] showed that the magnetic Bragg peak intensity of the SDW state is suppressed on entering the superconducting state.

This certainly shows a very strong interaction between the superconducting and SDW

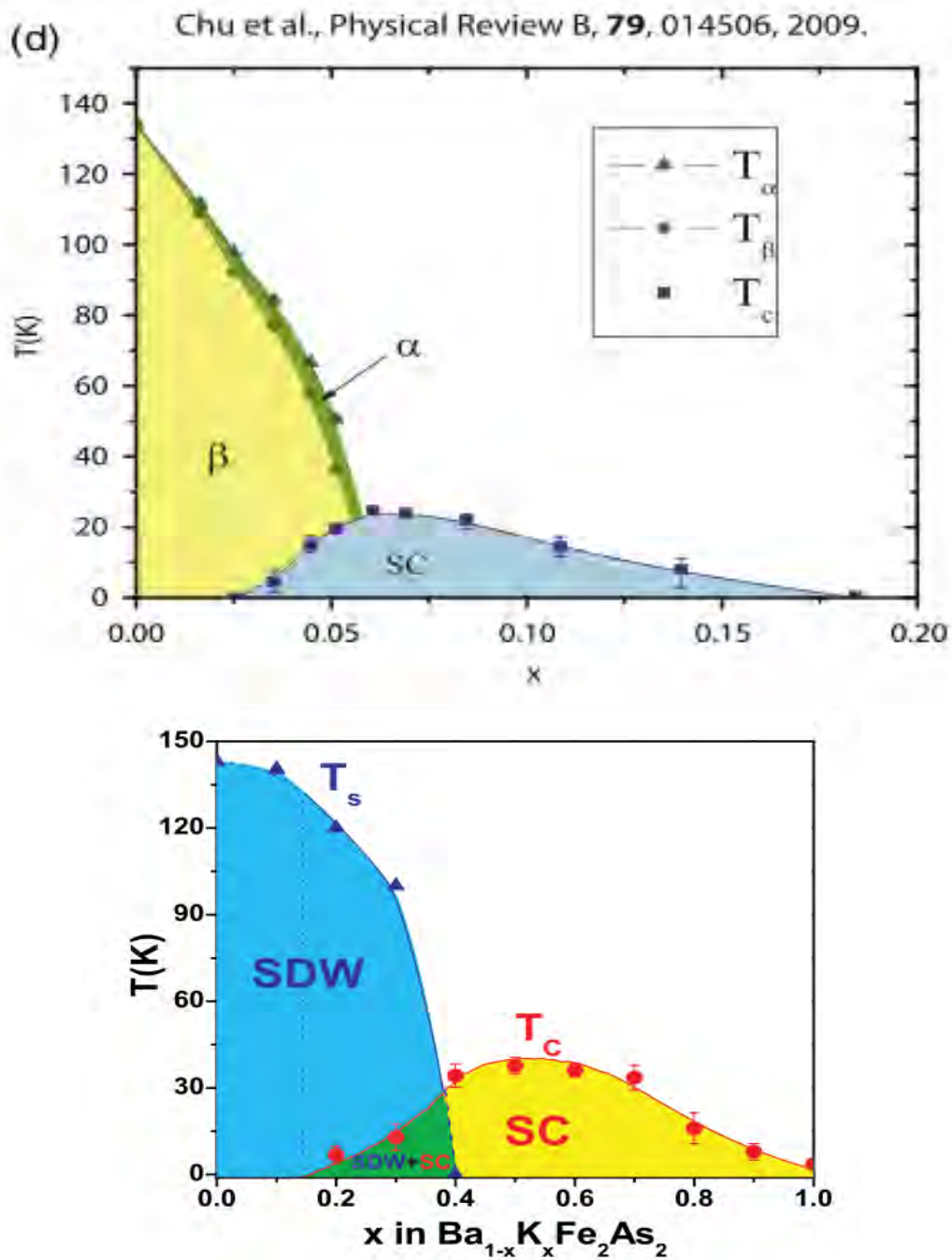


Figure 2.2: Experimentally determined phase diagram for $BaFe_{2-x}Co_xAs_2$ and $Ba_{1-x}K_xFe_2As_2$

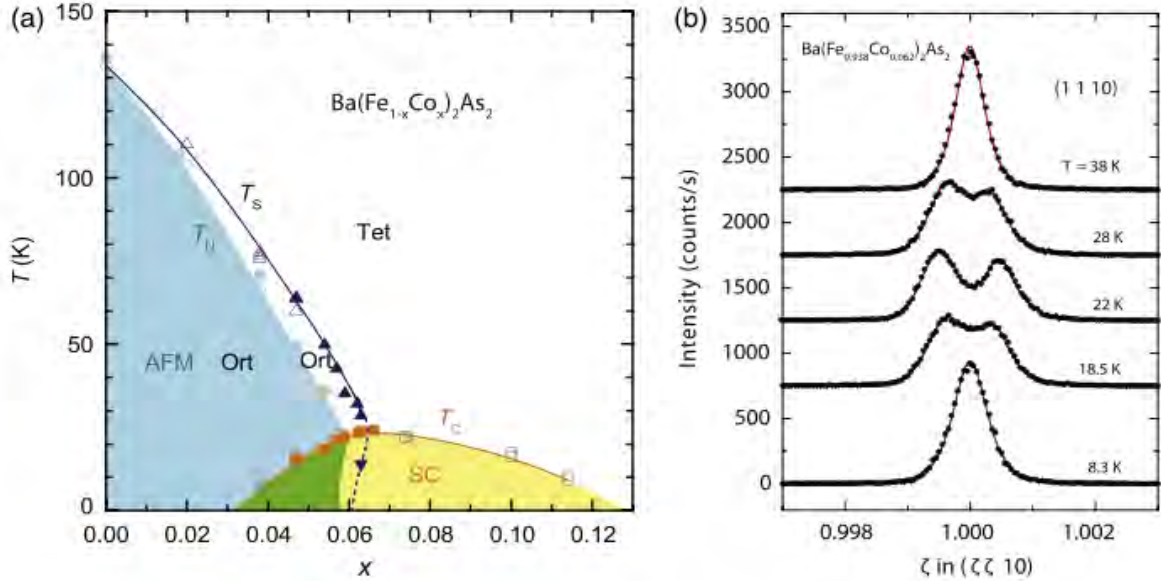


Figure 2.3: (a) Resulting phase diagram of $Ba(Fe_{1-x}Co_x)_2As_2$ with inclusion of high resolution x-ray diffraction measurements in the region where superconductivity and magnetism coexist. (b) Shows the reentrant nature of the structural phase transition.

states. It could be interpreted that this suppression is due to the same electrons participating in both the SDW and superconductivity favoring a phase coexistence scenario. However, in a phase separation scenario, a proximity effect could cause the superconducting regions to interfere with the SDW regions causing a reduction in the SDW volume consistent with the observed Bragg peak intensity reduction. Hence, it is difficult to make any strong conclusions about the implications of this observation for the question of phase coexistence. Interestingly, the details of the phase diagram in the region where the structural and magnetic transitions cross the superconducting dome have recently been explored with high resolution x-ray diffraction [79]. These measurements indicate that the shape of the line in the x - T phase diagram representing the tetragonal to orthorhombic transition changes on entering the superconducting state and bends to lower values of x [79] as shown in figure 2.4(a). As such, clear reentrant behavior is seen in a crystal of $Ba(Fe_{0.938}Co_{0.062})_2As_2$ where the system transforms from tetragonal to orthorhombic and back to tetragonal on cooling [79] (see figure 2.4(b)). This shows a strong interaction

between the structural transition and superconductivity and it was proposed that the interaction was actually one between magnetism and superconductivity with the influence on the structural transition resulting from magneto-elastic coupling [79].

2.2.3 11 materials

Finally, we discuss the phase diagram of the $FeSexTe_{1-x}$ family of materials. As mentioned previously, these materials form with excess Fe with the largest amount of extra Fe observed near the Te-rich side of the phase diagram. Initial measurements of the $Fe_{1+y}Te_{1-x}Sex$ [41] family of compounds showed superconductivity with T_c as high as 15 K for $x \sim 0.5$ existing for all values of x except very near $x = 0$ where superconductivity is destroyed. This suggests a different phase diagram from other Fe-based superconductors. However, single crystal specific heat measurements on the Te-rich side of the phase diagram indicate bulk superconductivity only for concentrations near $x = 0.5$ [80]. With this in mind, the phase moment diagram was re-investigated and indicated magnetic order for small x which coexists with superconductivity over a range of concentrations [55] (see figure 2.5(e)) in a manner very similar to the doped 122 materials and $SmFeAsO_{1-x}Fx$. As mentioned previously, materials with low Se concentrations have a tendency to form with excess Fe. Measurements of the phase diagram with samples intentionally grown with $Fe_{1.1}$ [81] show an additional spin glass phase which coexists with superconductivity over much of the measured concentration range. This shows the sensitivity of these materials to stoichiometry and, in particular, the amount of excess Fe present.

Although, as discussed above, there are some differences in the concentration dependent phase diagrams of various Fe-based superconductors, inspection of phase diagrams for pnictides family shows that there are some common features. All materials exhibit a SDW state at low concentrations and this state is suppressed with doping allowing for the emergence of superconductivity. This shows strong similarity to the generic cuprates phase diagram and is evidence for the interplay of magnetism and superconductivity in

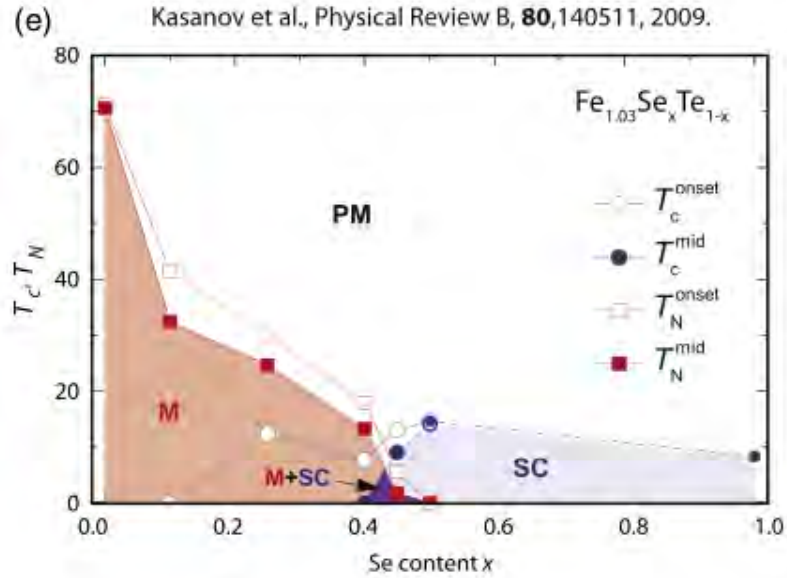


Figure 2.4: Experimentally determined phase diagram for e) $\text{Fe}_{1.03}\text{Te}_{1-x}\text{Se}_x$

the Fe-based materials.

2.3 Magnetic order

The parent compounds of both the 1111 and 122 materials are metals which exhibit SDW order. The high temperature ($T > T_N$) paramagnetic state is characterized by magnetic susceptibility with an unusual linear temperature dependence ($\chi \propto T$) [82, 31, 83–86]. This behavior is neither Pauli- nor CurieWeiss-like and is reminiscent of the ($T > T_{SDW}$) behavior of metallic Cr [87]. In the following section, we will provide an overview of the magnetic order which evolves out of this unusual paramagnetic state in the 1111, 122, and 11 family of materials. Examination of the magnetic ordering can shed light on the magnetic interactions and the nature (local moment or itinerant) of the magnetism in these materials.

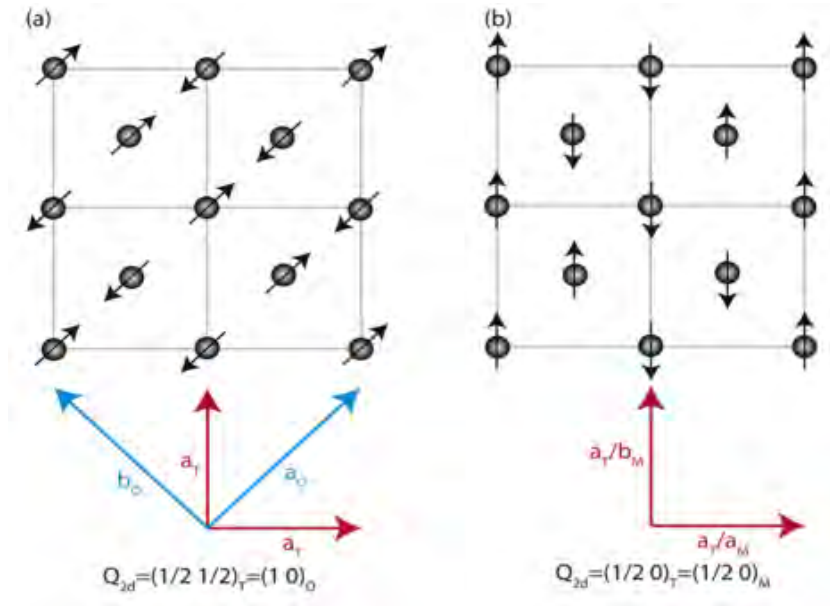


Figure 2.5: (a) In-plane magnetic structure for the 1111 and 122 parent compounds.(b) Magnetic structure for 11 materials

2.3.1 1111 materials

As discussed above, it is well established that the undoped parent compounds exhibit some form of antiferromagnetic long range order. This was first observed in LaFeAsO where the magnetic structure was characterized by the ordering wave vector $(\frac{1}{2}\frac{1}{2}\frac{1}{2})_T = (10\frac{1}{2})_o$ (where the subscripts T and O refer to the tetragonal and orthorhombic structures, respectively) and the low temperature ordered magnetic moment was $0.36 \mu\beta$ [15]. At this point, we note that the ordering wave vector in the orthorhombic cell (i.e. $(10\frac{1}{2})_o$) differs from the wave vector listed in [15] as the later wave vector is relative to the unit cell of the magnetic structure where the unit cell is doubled along the c-axis. The observed wave vector is consistent with a magnetic unit cell of size $\sqrt{2}a \times \sqrt{2}a \times 2c$ relative to the tetragonal cell. This ordering is consistent with stripe-like anti-ferromagnetic order with ferro-magnetically coupled chains along the tetragonal (110) direction coupled anti-ferromagnetically along the in- plane perpendicular direction (see figure 2.6(a) above). The doubling of the unit cell along the c-axis indicates antiferromagnetic interactions between neighboring planes. The magnetic moment direction could not be uniquely determined

in this measurement but the observed intensity is consistent with moments lying in the $a-b$ plane. The magnetic moment observed is much smaller than the $2.2 \mu\text{B}$ moment observed in metallic Fe. Measurements of $\text{LaFeAsO}_{1-x}\text{Fx}$ shows that the magnetic moment is rather independent of concentration for $x < 0.03$ and is zero for $x > 0.05$ [88]. More concentration points are required to determine how abruptly the magnetic moment vanishes with fluorine concentrations between 3 and 5 percent.

The nature of the ordered state in these materials has been a topic of considerable study. The calculated Fermi surface for LaFeAsO consists of electron cylinders near the M point and hole cylinders and a 3D hole pocket around the Γ point [89]. Further investigations indicated good nesting of these components separated by the 2D wave vector $(\frac{1}{2}\frac{1}{2})_T$ consistent with the observed magnetic structure [90, 91]. This led to the suggestion that the observed antiferromagnetic state is a SDW induced by Fermi surface nesting [91]. In addition to this Fermi surface nesting scenario, it has been proposed that near-neighbor and next- near-neighbor interactions between local Fe moments are both antiferromagnetic and of comparable strength leading to magnetic frustration [92–94].

Changes of the ordered magnetic structure with different rare earth elements (RFeAsO) have been extensively studied with neutron diffraction as well as local probe methods. The ordering wave vector of $(\frac{1}{2}\frac{1}{2}\frac{1}{2})_T$ observed for $\text{R} = \text{La}$ [15] is also observed for $\text{R} = \text{Nd}$ [98]. However, for $\text{R} = \text{Ce}$ [53] and $\text{R} = \text{Pr}$ [99] the ordering is described by the wave vector $(\frac{1}{2}\frac{1}{2}0)_T$ suggesting ferromagnetic coupling between planes. This suggests rather weak inter-plane coupling which is strongly influenced by the rare earth ion and the associated induced structural changes. Unfortunately, for the case of $\text{R} = \text{Sm}$, the high absorption cross-section for Sm makes neutron scattering measurements very difficult.

A particularly interesting case is that of Ce where neutron scattering indicated a much larger magnetic moment of $0.8 \mu\text{B}$ [53] more than twice the size of any other rare earth. Thus, on the basis of these neutron diffraction results, the Fe moment size varies considerably with rare earth element. However, a contradictory picture is obtained

from ^{57}Fe Mossbauer measurements. Such measurements for $\text{R} = \text{La}$ indicate an internal magnetic field of 4.86 T [103], 5.19 T [50], and 5.3 T [104]. For the other rare earths, the internal field was measured to be 5.2 T [105] and 5.3 T [106] for $\text{R} = \text{Nd}$, 5.06 T [106] for $\text{R} = \text{Ce}$, and 4.99 T [106] for $\text{R} = \text{Pr}$.

For the parent compounds with magnetic rare earth ions (i.e. Pr, Ce, Nd, and Sm), the rare earth moments order at low temperatures. The Pr moments in PrFeAsO order below 14 K [99, 101] with a fairly complex ordered structure with Pr spins along the c -axis [99]. There is coupling between the Pr and Fe moments and the ordered moments at 5 K were reported to be $0.84 \mu\text{B}$ for Pr and $0.48 \mu\text{B}$ for Fe [99] (an independent measurement indicated moments at 1.4 K of $0.83 \mu\text{B}$ for Pr and $0.53 \mu\text{B}$ for Fe [101]). Note that the Fe moment is enhanced from the value of $0.35 \mu\text{B}$ observed for temperatures above the Pr ordering temperature [101]. Ce moments in CeFeAsO order below ~ 4 K with moments lying primarily in the $a-b$ plane [53]. As in the case of Pr, significant coupling between the Fe and Ce moments is observed with low temperature ordered moments of $0.83 \mu\text{B}$ and $0.94 \mu\text{B}$ for Ce and Fe respectively which can be compared to the Fe moment of $0.8 \mu\text{B}$ at 40 K [53]. Nd spins in NdFeAsO order below 2 K and form a collinear arrangement with antiferromagnetic coupling along the orthorhombic b axis [102]. The ordered moments below 2 K were found to be $1.55 \mu\text{B}$ for Nd and $0.9 \mu\text{B}$ for Fe indicating a strong enhancement when compared to the Fe ordered moment of $0.25 \mu\text{B}$ observed for temperatures between the Fe and Pr ordering temperatures [98]. Finally, despite the large absorption cross-section of Sm, low temperature measurements on SmFeAsO indicated Sm order at 1.6 K [100]. The determined Sm spin structure is quite different than the other rare earths in that ferromagnetic sheets of Sm moments are stacked antiferromagnetically along the c -axis and the ordered Sm moment is $0.6 \mu\text{B}$ [100]. In contrast, the cases of Pr, Ce, and Nd have rare earth moments coupled antiferromagnetically along the b axis despite differences in the moment direction [99, 53, 102]. Note that for all measured cases, the Fe ordering arrangement exhibits ferromagnetic coupling along the orthorhombic b

axis with an antiferromagnetic arrangement along the a-axis.

2.3.2 122 materials

The temperature dependent structure of the AFe_2As_2 parent compounds has been carefully studied for $BaFe_2As_2$ [59, 60], $SrFe_2As_2$ [84, 114, 113], $CaFe_2As_2$ [120] and $EuFe_2As_2$ [114]. In all cases the room temperature tetragonal space group is $I4/mmm$ and the materials transform to a low temperature orthorhombic $Fmmm$ space group with a 45 rotated cell in the a b plane. The room temperature $I4/mmm$ space group is different than the $P4/nmm$ space group of the 1111 materials in that it contains two FeAs layers per unit cell. In contrast to the 1111 materials, the 122 parent compounds exhibit a structural and magnetic transition at the same temperature as shown in measurements on $BaFe_2As_2$ [60, 110], $SrFe_2As_2$ [111–113, 121], and $CaFe_2As_2$ [115].

Neutron diffraction experiments on the 122 materials find larger ordered magnetic moments than in the 1111 materials which are fairly consistent for different members of the AFe_2As_2 family with $0.99 \mu B$ [110] observed in single crystal measurements on $BaFe_2As_2$ (grown with Sn flux), $0.87 \mu B$ [60] in powder measurements on $BaFe_2As_2$, $0.94 \mu B$ in single crystals of $SrFe_2As_2$, $1.01 \mu B$ [112] in powder measurements on $SrFe_2As_2$ and $0.8 \mu B$ in single crystals of $CaFe_2As_2$. This consistency of the ordered moment occurs despite a large variation in transition temperatures ranging from 90 K in $BaFe_2As_2$ grown with Sn flux [110] to 220 K in crystals of $SrFe_2As_2$ [111].

Finally we discuss the evolution of the magnetic structure with doping. Most measurements have focused on $Ba(Fe_{1-x}Co_x)_2As_2$ as the crystals are considered to be homogeneous. Neutron scattering measurements have indicated a magnetic structure characterized by the same $(101)_O$ wave vector as the $BaFe_2As_2$ parent compound for concentrations of $x = 0.04$ [67] and $x = 0.047$ [66]. However, NMR measurements on a sample with $x = 0.06$ indicate a distribution of internal fields [76] and $^{57}\text{Mossbauer}$ measurements on single crystals with x as high as 0.045 indicate a distribution of hyperfine fields [122].

Both observations [76, 122], as well as NMR measurements on other underdoped samples [127], were taken as evidence that the SDW order evolves from commensurate for the parent compound to incommensurate in the presence of Co doping. Modeling the NMR line shape yields the prediction of a small incommensuration with magnitude ~ 0.04 [76].

2.3.3 11 materials

The structural and magnetic properties of the 11 family of compounds is complicated by extreme sensitivity to stoichiometry and the presence of excess Fe. As an example, nearly stoichiometric $FeSe_{0.97}$ crystallizes in the P 4/nmm tetragonal space group while a small variation in concentration to $FeSe_{1.06}$ induces a phase change and the material exhibits a hexagonal structure [128]. Furthermore, superconductivity in $Fe_{1.01}Se$ with $T_c \sim 8$ K is destroyed by increasing the amount of excess Fe and no superconductivity is observed down to 0.6 K in samples of $Fe_{1.03}Se$ [129]. The phase of interest with respect to superconductivity is the α phase (curiously this phase is occasionally referred to in the literature as the β phase). Magnetic ordering is observed in samples close to the Te endpoint member of the $Fe_{1+y}Te_{1-x}Sex$ family. Structurally, $Fe_{1+y}Te$ exhibits the PbO crystal structure with a space group of P 4/nmm at room temperature for values of y ranging from 0.068 to 0.14 [44, 117]. At low temperatures, a first-order structural transition is observed (transition temperature ~ 65 K [130]) and the low temperature space group is the monoclinic P 21 /m for samples of $Fe_{1.076}Te$ [44] and $Fe_{1.0681}Te$ [117]. On the other hand, a small change in x to $Fe_{1.141}Te$ Te changes the low temperature unit cell to orthorhombic with the Pmmn space group [44] again providing evidence for sensitivity to stoichiometry. In both the orthorhombic and monoclinic unit cells, there is no cell doubling or cell rotation when compared to the tetragonal cell and, hence, the Miller indices of Bragg reflections are the same for all unit cells [44].

The wave vector observed in the 11 materials is different than that observed in the 1111 or 122 materials with an in-plane wave vector of $(\frac{1}{2}0)_T$ as opposed to $(\frac{1}{2}\frac{1}{2})_T$ seen in

both the 1111 and 122 compounds. Interestingly, this happens despite calculated Fermi surfaces that are very similar suggesting that the 11 materials should be susceptible to a nesting instability with the same $(\frac{1}{2}\frac{1}{2})_T$ nesting wave vector [43]. Calculations indicate that excess Fe in these materials is magnetic [45], consistent with the conclusions of neutron structure refinements [44].

2.4 Spin density wave state

The SDW state is a kind of antiferromagnetic state with the electronic spin density forming a static wave. The density varies perpendicularly as a function of position with no net magnetisation in the entire volume. The SDW transition occurs when the spatial spin density modulation is due to delocalization or itinerant electrons rather than the localized one. Usually in the normal state the density $\rho_{\uparrow}(\vec{r})$ of electron spins polarized upward with respect to any quantization axis is completely cancelled by ρ_{\downarrow} of downward polarized spins.

In the SDW state, however, the difference $\sigma(r) = \rho_{\uparrow}(\vec{r}) - \rho_{\downarrow}(\vec{r})$ is finite and modulate in space as a function of the position vector \vec{r} in the SDW state. Such tendency of forming SDW ground state takes place when a system possesses nested pieces of FS together with intermediate coulomb correlation. In the case of the SDW transition it is the wave vector dependent static magnetic susceptibility which develops a singularity at $\vec{q} = \vec{Q}$ i.e., $\chi(q, \omega)|_{\vec{q} = \vec{Q}, \omega = 0} = \langle\langle S^+(q, t); S^-(-q, t) \rangle\rangle_{\omega|_q = Q, \omega = 0} \rightarrow \infty$ where S^{\pm} are the spin raising and lowering operators and \vec{Q} is known as the nesting wave vector which determines the periodicity of the SDW. This singularity in the magnetic susceptibility is an artifact of the nesting property of the FS given by

$$\epsilon_{\vec{k}} = -\epsilon_{\vec{k}+\vec{Q}}$$

2.4.1 The coexistence of SDW and SC

Usually, magnetism and superconductivity are expected to be mutually exclusive phenomena i.e, they are unlikely to occur simultaneously in the same compound. Superconductivity (including in the high temperature superconductors) is known to be due to Cooper pair formation of electrons of opposite spins and momenta whereas magnetism requires spin polarisation. Therefore, naturally one order would inhibit the other.

Furthermore, like superconductivity (electron-electron pairing), the transverse SDW state is also a result of condensation of electron-hole pairs of opposite spins but with a momentum difference of Q between the conjugates. Hence, when any of the orders (either the SC or the SDW) set in, the FS is unstable with respect to that condensate state.

In other words, if one of the phases (say SDW) sets in first, and exists all over the FS, then there will be no carrier available to form Cooper pairs and hence no superconductivity. This would also be equally true in case of the SDW state, had the superconductivity appeared first. However, in reality we do see the coexistence of the two phases as is already discussed earlier. In what follows we discuss two different scenarios where both the presence of SDW state and SC coexist.

A. The case of an isotropic SDW-state : SC can arise over the SDW background

If the nesting of the FS is perfect the entire FS could be isotropically gapped due to the formation of the SDW state transforming the system from a metal to an insulator. In order to build superconductivity over such an insulating phase one needs to dope the system with charge carriers.

In the event of doping the system with holes, or equivalently removal of electrons from the lower filled (valence) SDW band, there will be deviation from perfect nesting of the FS resulting in a local suppression of the SDW gap. This is so because, the gain in electronic energy resulting from the formation of the SDW state is lowered due to removal of

electrons from the valence band. This local suppression of the SDW gap acts as a potential well for the injected hole, in which it gets self-trapped forming the so called spin bag.

On creating two holes it is energetically favourable for them to dig a deeper well and stay together provided the two holes have opposite spins to avoid Pauli exclusion principle. This is however nothing but a local Cooper pair and if such bags with two holes of opposite spins move coherently, the system will be superconducting. This is the essence of Schrieffer's spin bag model for high temperature superconductivity and hence is an example where superconductivity can arise over the SDW state.

B. Anisotropic SDW state : SC can coexist with SDW

The above case is however, physically reasonable only when the hole concentration is very small. But in reality superconductivity in most of the systems (specially high T_c systems) appears only after large doping. So, it is likely that the SDW state will be completely suppressed in particular directions of the FS whereas it would still exist in the rest of the FS which still nests (anisotropic SDW). Such situation may also appear due to particular topology of the FS of a system without doping i.e., the system may have nested pieces of FS only in certain direction and no nesting in other direction resulting in an anisotropic SDW state.

In the regions of the FS where the SDW gap vanishes (i.e., the lower and upper SDW bands merge together), the pairing interaction between the SDW quasi particles can take place leading to superconductivity. In both the cases discussed above, the origin of superconductivity is fundamentally different from that in conventional superconductors.

In contrast, in the cases where nesting is not perfect either due to peculiar topology of the FS or due to doping, the SDW gap will appear only in the nested part of the FS allowing for the superconducting instability in the rest of the FS. But in such a case, the origin of superconducting pairing may arise be due to any other mechanism including the BCS phonon exchange.

Chapter 3

Mathematical Techniques

In this chapter we will review the Green's function formalism which is used to obtain the expressions for superconducting transition temperature T_C , magnetic ordering temperature T_{SDW} and order parameters (Δ_S and Δ_{SDW}).

3.1 Green's function formalism

The Green's functions are useful because they are flexible enough to describe the effects of retarded interactions and all the quantities of physical interest can be derived from them. Green's functions or propagators play the most important part in the field theoretical treatment of the many body problem. There are different types of Greens functions; one particle, two particle...n particle, advanced, retarded, casual, zero temperature, finite temperature, real time, imaginary-time and so on.

In our discussion we used only the retarded Double-time Green's function. It is defined as

$$G_r(t, t') \equiv \langle\langle \hat{A}(t); \hat{B}(t') \rangle\rangle \quad (3.1.1)$$

$$= -i\theta(t, t') \langle [\hat{A}(t), \hat{B}(t')] \rangle \quad (3.1.2)$$

where $\langle\langle \dots \rangle\rangle$ is the abbreviated notation for the Green functions, and $\langle \dots \rangle$ denotes averaging over a ground canonical ensemble $\theta(t, t')$ is the step function. $\hat{A}(t), \hat{B}(t')$ are operators in the Heisenberg representation which can be expressed as the product of the quantized

field operators ,that is, $\hat{A}(t) = \exp(iHt)A(0)\exp(-iHt), h = 1$

$$\theta(t) = \begin{cases} 0, & t < 0; \\ 1, & t > 0 \end{cases} \quad (3.1.3)$$

also $[A, B]$ is a commutator or anti commutator that is $[A, B] = AB - \eta BA, \eta = \pm$ the sign of η is positive if A and B are both Bose operator and negative if they are Fermi operators. In order to obtain the equation of motion we differentiate equation (3.1.1) with respect to t as,

$$i \frac{d}{dt} G_r(t-t') = i \frac{d}{dt} \langle \langle \hat{A}(t); \hat{B}(t) \rangle \rangle \quad (3.1.4)$$

$$= \delta(t-t') \langle [\hat{A}(t); \hat{B}(t')] \rangle + \langle \langle [\hat{A}(t); \hat{H}]; \hat{B}(t') \rangle \rangle \quad (3.1.5)$$

Taking use of between heavy side step function $\theta(t)$ and Dirac δ function,

$$\theta(t) = \int_{-\infty}^t \delta(t) dt,$$

therefore $\frac{d}{dt} \theta(t) = \delta(t)$. It is known that $A(t)$ and $B(t')$ satisfy equation of the form $i \frac{d}{dt} = [\hat{A}; \hat{H}]$ Now equation of motion becomes,

$$i \frac{d}{dt} G_r(t-t') = \delta(t-t') \langle [\hat{A}(t); \hat{B}(t')] \rangle + \langle \langle [\hat{A}(t); \hat{H}]; \hat{B}(t') \rangle \rangle$$

To solve this equation it is convenient to work with Fourier transform of this equation .A care full analysis shows that the function depends on t and t' through $(t-t')$. Thus we can write $G_r(t, t') = G_r(t-t')$.

Now let $G_r(\omega)$ be the Fourier transform of $G_r(t-t')$ such that,

$$G_r(t-t') = \int_{-\infty}^{\infty} G_r(\omega) e^{-i\omega(t-t')} d\omega$$

$$G_r(\omega) = \frac{1}{2\pi} \int_{-\infty}^{\infty} G_r(t-t') e^{i\omega(t-t')} d(t-t')$$

and the δ function can be defined as

$$\delta(t-t') = \frac{1}{2\pi} \int_{-\infty}^{\infty} e^{-i\omega(t-t')} d\omega$$

Then equation (3.1.5) becomes,

$$\omega G_r(\omega) = \langle [\hat{A}(t); \hat{B}(t')] \rangle + \langle \langle [\hat{A}(t); \hat{H}]; \hat{B}(t') \rangle \rangle_\omega \quad (3.1.6)$$

since the Fourier transform of $G(t)$ is

$$G(t) = \int G(\omega) \exp(-i\omega t) d\omega$$

from which we can show that $\frac{\partial}{\partial t} = -i\omega$ Fourier transform of $G(t)$. Then $\omega G(\omega)$ can be written as

$$\omega \langle \langle A, B \rangle \rangle_\omega = \langle [\hat{A}(t); \hat{B}(t')] \rangle + \langle \langle [\hat{A}(t); \hat{H}]; \hat{B}(t') \rangle \rangle_\omega \quad (3.1.7)$$

since $\langle \langle A, B \rangle \rangle_\omega$ denotes the Fourier transform of the green's functions involving the operator A and B. It satisfies the equation of motion (3.1.5), where the double brackets $\langle \langle \dots \rangle \rangle$ indicates the Fourier transform of the corresponding Green function. The single brackets $\langle \dots \rangle$ indicate the thermal average over the canonical, that is

$$\langle F \rangle = \frac{\text{Tr} \exp(-\beta H) F}{\text{Tr} \exp(\beta H)} \quad (3.1.8)$$

Where $\beta = \frac{1}{(k_B T)}$, k_B is the Boltzmann constant. H is the Hamiltonian of the system considered.

From the analytical properties of the Green's function it follows that the correlation function $\langle \hat{B}(t'); \hat{A}(t) \rangle$ can be obtained from the equation of Green's functions by

$$\langle \hat{B}(t'); \hat{A}(t) \rangle = i \lim_{\epsilon \rightarrow 0} \int_{-\infty}^{\infty} \frac{\left(\langle \langle A; B \rangle \rangle_{\hbar\omega+i\epsilon} - \langle \langle A; B \rangle \rangle_{\hbar\omega-i\epsilon} \right)}{\exp(\beta\hbar\omega) - 1} \quad (3.1.9)$$

3.1.1 Green's functions formulation with reduced Hamiltonian

To solve the properties of superconductivity, we will use BCS-type Hamiltonian (or reduced Hamiltonian), which is given below

$$\hat{H} = \sum_{k,\sigma} \epsilon_k C_{k\sigma}^\dagger C_{k\sigma} - \sum_{k,k'} V_{k,k'} C_{k\uparrow}^\dagger C_{-k\downarrow}^\dagger C_{k'\downarrow} C_{-k'\uparrow} \quad (3.1.10)$$

where $V(k, k')$ define the matrix element of the interaction potential. $C_{k\sigma}^\dagger(C_{k\sigma})$ is the creation(annihilation) operator of an electron specified by the wave vector k and the spin σ . ϵ_k is the energy of the one electron measured relative to the chemical potential. To get the equation of motion we apply Green's function techniques;

Defining;

$$G_{k,k'}^{\uparrow\uparrow} = \langle\langle C_{k\uparrow}, C_{k'\uparrow}^\dagger \rangle\rangle \quad (3.1.11)$$

And writing the equation of motion for $\langle\langle C_{k\uparrow}, C_{k'\uparrow}^\dagger \rangle\rangle$;

$$\omega \langle\langle C_{k\uparrow}, C_{k'\uparrow}^\dagger \rangle\rangle = \delta_{kk'} + \langle\langle [C_{k\uparrow}, H_{BCS}]; C_{k'\uparrow}^\dagger \rangle\rangle \quad (3.1.12)$$

Now let us eliminate $[C_{k\uparrow}, H_{BCS}]$ Using the Hamiltonian (3.1.10)

$$[C_{k\uparrow}, H_{BCS}] = [C_{k\uparrow}, \sum_{k,\sigma} \epsilon_k C_{k\sigma}^\dagger C_{k\sigma} - \sum_{k,k'} V_{k,k'} C_{k\uparrow}^\dagger C_{-k\downarrow}^\dagger C_{k'\downarrow} C_{-k'\uparrow}] \quad (3.1.13)$$

Evaluating the relevant commutator $[C_{k\uparrow}, H_{BCS}]$ using the Hamiltonian (3.1.10), we finally obtain after decoupling higher order Greens functions in to lower order using mean field approximation;

$$\begin{aligned} (w - \epsilon_k) \langle\langle C_{k\uparrow}, C_{k'\uparrow}^\dagger \rangle\rangle &= \delta_{kk'} - V \sum_{k,k'} \langle\langle C_{-k\downarrow}^\dagger C_{k'\downarrow} C_{-k'\uparrow}; C_{k\uparrow}^\dagger \rangle\rangle \\ &= \delta_{kk'} - V \sum_{k,k'} \langle C_{k'\downarrow}, C_{-k'\uparrow} \rangle \langle\langle C_{-k\downarrow}^\dagger, C_{k\uparrow}^\dagger \rangle\rangle \end{aligned} \quad (3.1.14)$$

From the relation

$$\Delta = V \sum_{k,k'} \langle C_{k'\downarrow}, C_{-k'\uparrow} \rangle = V \sum_{k,k'} \langle C_{-k\downarrow}^\dagger, C_{k\uparrow}^\dagger \rangle$$

Where Δ is the energy gap

Therefore equation (3.1.12) becomes;

$$(w - \epsilon_k) \langle\langle C_{k\uparrow}, C_{k'\uparrow}^\dagger \rangle\rangle = \delta_{kk'} - \Delta \langle\langle C_{-k\downarrow}^\dagger, C_{k\uparrow}^\dagger \rangle\rangle \quad (3.1.15)$$

Which is the equation of motion for $\langle\langle C_{k\uparrow}, C_{k'\uparrow}^\dagger \rangle\rangle$.

Now let us calculate the 2nd equation of motion for $\langle\langle C_{-k\downarrow}^\dagger, C_{k'\uparrow}^\dagger \rangle\rangle$; Similarly the equation of Green function $\langle\langle C_{-k\downarrow}^\dagger, C_{k'\uparrow}^\dagger \rangle\rangle$ can be obtained as before by evaluating the relevant commutators. Finally we obtain;

$$\begin{aligned} (\omega + \epsilon_k) \langle\langle C_{-k\downarrow}^\dagger, C_{k\uparrow}^\dagger \rangle\rangle &= -V \sum_k \langle\langle C_{k\uparrow}^\dagger C_{-k\downarrow}^\dagger C_{k\uparrow}, C_{k\uparrow}^\dagger \rangle\rangle \\ &= -V \sum_{k'} \langle C_{k'\uparrow}^\dagger C_{-k'\downarrow}^\dagger \rangle \langle\langle C_{k\uparrow}, C_{k\uparrow}^\dagger \rangle\rangle \end{aligned} \quad (3.1.16)$$

But, $\Delta = V \sum_k \langle C_{k\uparrow}^\dagger C_{-k\downarrow}^\dagger \rangle$, therefore;

$$(\omega + \epsilon_k) \langle\langle C_{-k\downarrow}^\dagger, C_{k\uparrow}^\dagger \rangle\rangle = -\Delta \langle\langle C_{k\uparrow}, C_{k\uparrow}^\dagger \rangle\rangle \quad (3.1.17)$$

From equation (3.1.15) and (3.1.17), we have;

$$(w - \epsilon_k) \langle\langle C_{k\uparrow}, C_{k'\uparrow}^\dagger \rangle\rangle = \delta_{kk'} - \Delta \langle\langle C_{-k\downarrow}^\dagger, C_{k'\uparrow}^\dagger \rangle\rangle \quad (3.1.18)$$

$$(\omega + \epsilon_k) \langle\langle C_{-k\downarrow}^\dagger, C_{k'\uparrow}^\dagger \rangle\rangle = -\Delta \langle\langle C_{k\uparrow}, C_{k'\uparrow}^\dagger \rangle\rangle \quad (3.1.19)$$

Since $\delta_{kk'} = 1$ iff $k = k'$, then

$$\langle\langle C_{k\uparrow}, C_{k\uparrow}^\dagger \rangle\rangle = \frac{1}{w - \epsilon_k} \left(1 - \Delta \langle\langle C_{-k\downarrow}^\dagger, C_{k\uparrow}^\dagger \rangle\rangle \right) \quad (3.1.20)$$

substituting equation (3.1.20) in equation (3.1.19) yields

$$\langle\langle C_{-k\downarrow}^\dagger, C_{k\uparrow}^\dagger \rangle\rangle = -\frac{\Delta}{\omega^2 - \epsilon_k^2 - \Delta^2} \quad (3.1.21)$$

The superconducting order parameter Δ can be given by the relation,

$$\Delta = \frac{V}{\beta} \sum_{k,n} \langle\langle C_{-k\downarrow}^\dagger, C_{k\uparrow}^\dagger \rangle\rangle \quad (3.1.22)$$

Then equation (3.1.22) becomes;

$$\Delta = \frac{V}{\beta} \sum_{k,n} -\frac{\Delta}{\omega_n^2 - \epsilon_k^2 - \Delta^2}$$

then let us define

$$\omega_n = \frac{(2n+1)i\pi}{\beta}, \quad \epsilon_k^2 + \Delta^2 = \tilde{E}_k^2$$

so,

$$\Delta = V\Delta\beta \sum_{k,n} \frac{1}{(2n+1)^2\pi^2 + \beta^2\tilde{E}_k^2} \quad (3.1.23)$$

and from the relation,

$$\frac{\tanh(\frac{x}{2})}{2x} = \sum_{n=-\infty}^{-\infty} \frac{1}{(2n+1)^2\pi^2 + \beta^2\tilde{x}^2}$$

Equation (3.1.23) becomes, Where, $x = \beta\tilde{E}_k$

$$\frac{1}{V} = \sum_n \frac{\tanh(\frac{\beta\tilde{E}_k}{2})}{2\beta\tilde{E}_k}$$

Changing the summation in to an integral with cut off energy $\pm\hbar\omega_D$ from the Fermi level, we get;

$$1 = N(0)V \int_{\pm\hbar\omega_D}^{\pm\hbar\omega_D} \frac{\tanh(\frac{\beta\sqrt{\epsilon_k^2 + \Delta^2}}{2})}{2\sqrt{\epsilon_k^2 + \Delta^2}} d\epsilon_k$$

as $T \rightarrow T_c, \Delta \rightarrow 0$

$$\frac{1}{N(0)V} = \int_0^\infty \frac{\tanh(\frac{\epsilon_k}{2k_B T_c})}{\epsilon_k}$$

Integrating gives

$$T_c = 1.14 \frac{\tilde{\epsilon}_k}{k_B} e^{-\frac{1}{\lambda}}$$

Where $\lambda = N(0)V$, and $N(0)$ is the density of state at the fermi level

Then, $\tilde{\epsilon}_k = \hbar\omega_D$

$$T_c = 1.14 \frac{\hbar\omega_D}{k_B} e^{-\frac{1}{\lambda}}$$

And from the relation, $\theta_D = \frac{\hbar\omega_D}{k_B}$ Therefore ,

$$T_c = 1.14\theta_D e^{-\frac{1}{\lambda}} \quad (3.1.24)$$

Chapter 4

Theoretical Formulation

4.1 The model Hamiltonian

The purpose of this work is to study theoretically the interplay between spin density wave and superconductivity in Fe-based superconductors and to find the expression for the superconducting transition temperatures and magnetic ordering temperatures as a function of order parameters.

We take the following Hamiltonian as with ref.[113] to describe the interplay between superconductivity and spin density wave.

$$\hat{H} = \hat{H}_1 + \hat{H}_2 \quad (4.1.1)$$

Where;

$$\hat{H}_1 = \sum_{k,\sigma} \epsilon_k C_{k\sigma}^\dagger C_{k\sigma} - \sum_{k,k'} V_{k,k'} C_{k\uparrow}^\dagger C_{-k\downarrow}^\dagger C_{k'\downarrow} C_{-k'\uparrow} \quad (4.1.2)$$

$$\hat{H}_2 = I \sum_{k,Q} C_{k\uparrow}^\dagger C_{k+Q\downarrow} C_{k'\downarrow}^\dagger C_{k'-Q\uparrow} \quad (4.1.3)$$

Where, $C_{k\sigma}^\dagger$ ($C_{k\sigma}$) are creation (annihilation) operators of an electron having the wave vector k and spin σ . In equation (4.1.1) the first term represents for the one electron energy, while the second term describes BCS type. The term (4.1.3) represent the on site Coulomb interaction; $I = \frac{U}{N}$ with U being the on site Coulomb energy and N the number of the molecules.

4.2 Equations of motion

In our present analysis to obtain the self-consistent expression for order parameter and transition temperatures(T_C and T_{SDW}) as a function of order parameter (Δ_S and Δ_{SDW}) respectively, we apply Green's function technique.

Defining

$$G_{k,k'}^{\uparrow\uparrow} = \langle\langle C_{k\uparrow}, C_{k'\uparrow}^\dagger \rangle\rangle \quad (4.2.1)$$

And writing equation of motion;

$$\omega \langle\langle C_{k\uparrow}, C_{k'\uparrow}^\dagger \rangle\rangle = \langle[C_{k\uparrow}, C_{k'\uparrow}^\dagger]\rangle + \langle\langle [C_{k\uparrow}, \hat{H}]; C_{k'\uparrow}^\dagger \rangle\rangle \quad (4.2.2)$$

First let us calculate the commutator $[C_{k\uparrow}, H]$ using the Hamiltonian(4.1.2) then, the equation of motion for $\langle\langle C_{k\uparrow}, C_{k'\uparrow}^\dagger \rangle\rangle$ is given by ;

$$\omega \langle\langle C_{k\uparrow}, C_{k'\uparrow}^\dagger \rangle\rangle = \delta_{kk'} + \langle\langle [C_{k\uparrow}, \hat{H}]; C_{k'\uparrow}^\dagger \rangle\rangle \quad (4.2.3)$$

Using the commutation relations,

$$[\hat{A}; \hat{B} + \hat{C}] = [\hat{A}, \hat{B}] + [\hat{A}, \hat{C}] \quad (4.2.4)$$

$$[\hat{A}; \hat{B}\hat{C}] = [\hat{A}; \hat{B}]\hat{C} + \hat{B}[\hat{A}; \hat{C}] \quad (4.2.5)$$

$$[\hat{A}\hat{B}; \hat{C}] = \hat{A}[\hat{B}; \hat{C}] + [\hat{A}; \hat{C}]\hat{B} \quad (4.2.6)$$

$$[\hat{A}; \hat{B}\hat{C}] = \{\hat{A}; \hat{B}\}\hat{C} - \hat{B}\{\hat{A}; \hat{C}\} \quad (4.2.7)$$

$$[\hat{A}\hat{B}; \hat{C}] = \hat{A}\{\hat{B}; \hat{C}\} - \{\hat{A}; \hat{C}\}\hat{B} \quad (4.2.8)$$

and

$$[C_{k\sigma}, C_{k'\sigma}^\dagger] = \delta_{kk'} = 1, \text{ if } k = k', \text{ Otherwise } 0. \quad (4.2.9)$$

$$[C_{k\sigma}, C_{k\sigma}] = [C_{k\sigma}^\dagger, C_{k\sigma}^\dagger] = 0 \quad (4.2.10)$$

Now let us eliminate $[C_{k\uparrow}, H]$ Therefore

$$[C_{k\uparrow}, H] = [C_{k\uparrow}; \left(\sum_{k,\sigma} \epsilon_k C_{k\sigma}^\dagger C_{k\sigma} - \sum_{k,k'} V_{k,k'} C_{k\uparrow}^\dagger C_{-k\downarrow}^\dagger C_{k'\downarrow} C_{-k'\uparrow} + U \sum_{k,Q} C_{k\uparrow}, C_{k\uparrow}^\dagger C_{k+Q\downarrow} C_{k'\downarrow}^\dagger C_{k'-Q\uparrow} \right)]$$

Then;

$$[C_{k\uparrow}, H] = \sum_{k,\sigma} \epsilon_k [C_{k\uparrow}; C_{k\sigma}^\dagger C_{k\sigma}] - V \sum_{k,k'} [C_{k\uparrow}; C_{k\uparrow}^\dagger C_{-k\downarrow}^\dagger C_{k'\downarrow} C_{-k'\uparrow}] + U \sum_{k,Q} [C_{k\uparrow}; C_{k\uparrow}^\dagger C_{k+Q\downarrow} C_{k'\downarrow}^\dagger C_{k'-Q\uparrow}] \quad (4.2.11)$$

$$= \sum_{k,\sigma} \epsilon_k [C_{k\uparrow}; C_{k\sigma}^\dagger C_{k\sigma}] - V \sum_{k,k'} \left([C_{k\uparrow}, C_{k\uparrow}^\dagger C_{-k\downarrow}^\dagger] C_{k'\downarrow} C_{-k'\uparrow} + C_{k\uparrow}^\dagger C_{-k\downarrow}^\dagger [C_{k\uparrow}, C_{k'\downarrow} C_{-k'\uparrow}] \right) \\ + U \sum_{k,Q} \left([C_{k\uparrow}; C_{k\uparrow}^\dagger C_{k+Q\downarrow}] C_{k'\downarrow}^\dagger C_{k'-Q\downarrow} + C_{k\uparrow}^\dagger C_{k+Q\downarrow} [C_{k\uparrow}, C_{k'\downarrow}^\dagger C_{k'-Q\uparrow}] \right) \quad (4.2.12)$$

$$= \sum_{k\sigma} \epsilon_k \left(\{C_{k\uparrow}, C_{k\uparrow}^\dagger\} C_{k\sigma} + \{C_{k\uparrow}, C_{k\sigma}\} C_{k\sigma}^\dagger \right) - V \sum_{k,k'} \{C_{k\uparrow}, C_{k\uparrow}^\dagger\} C_{-k\downarrow}^\dagger C_{k'\downarrow} C_{-k'\uparrow} + C_{k\uparrow}^\dagger \{C_{k\uparrow}, C_{-k\downarrow}^\dagger\} C_{k'\downarrow} C_{-k'\uparrow} \\ + C_{k\uparrow}^\dagger C_{-k\downarrow}^\dagger \{C_{k\uparrow}, C_{k'\downarrow}\} C_{-k'\uparrow} + C_{k\uparrow}^\dagger C_{-k\downarrow}^\dagger C_{k'\downarrow} \{C_{k\uparrow}, C_{-k'\uparrow}\} \quad (4.2.13)$$

$$+ U \sum_{k,Q} \left(\{C_{k\uparrow}, C_{k\uparrow}^\dagger\} C_{k+Q\downarrow} C_{k'\downarrow}^\dagger C_{k'-Q\uparrow} - C_{k\uparrow}^\dagger \{C_{k\uparrow}, C_{k+Q\downarrow}\} C_{k'\downarrow}^\dagger C_{k'-Q\uparrow} + C_{k\uparrow}^\dagger C_{k+Q\downarrow} \{C_{k\uparrow}, C_{k'\downarrow}^\dagger\} C_{k'-Q\uparrow} \right. \\ \left. - C_{k\uparrow}^\dagger C_{k+Q\downarrow} C_{k'\downarrow}^\dagger \{C_{k\uparrow}, C_{k'-Q\uparrow}\} \right)$$

since $\{C_{k\sigma}, C_{k\sigma}\} = \{C_{k\sigma}^\dagger, C_{k\sigma}^\dagger\} = 0$, $\{C_{k\sigma}, C_{k'\sigma}^\dagger\} = \delta_{kk'} = 1$, *iff* $k = k'$

$$[C_{k\uparrow}, H] = \sum_{k\sigma} \epsilon_k \{C_{k\uparrow}, C_{k\uparrow}^\dagger\} C_{k\sigma} - V \sum_{k,k'} \{C_{k\uparrow}, C_{k\uparrow}^\dagger\} C_{-k\downarrow}^\dagger C_{k'\downarrow} C_{-k'\uparrow} \quad (4.2.14)$$

$$+ U \sum_{k,Q} \{C_{k\uparrow}, C_{k\uparrow}^\dagger\} C_{k+Q\downarrow} C_{k'\downarrow}^\dagger C_{k'-Q\downarrow} \\ = \epsilon_k C_{k\uparrow} - V \sum_{k'} C_{-k\downarrow}^\dagger C_{k'\downarrow} C_{-k'\uparrow} + U \sum_{k',Q} C_{k+Q\downarrow} C_{k'\downarrow}^\dagger C_{k'-Q\uparrow} \quad (4.2.15)$$

In general our equation of motion becomes;

$$\omega \langle\langle C_{k\uparrow}, C_{k'\uparrow}^\dagger \rangle\rangle = 1 + \langle\langle \left(\epsilon_k C_{k\uparrow} - V \sum_{k'} C_{-k\downarrow}^\dagger C_{k'\downarrow} C_{-k'\uparrow} + U \sum_{k',Q} C_{k+Q\downarrow} C_{k'\downarrow}^\dagger C_{k'-Q\uparrow} \right); C_{k\uparrow}^\dagger \rangle\rangle$$

since $k = k'$, Then $\delta_{kk'} = 1$

Substituting equation (4.2.15) in equation (4.2.3) yields;

$$= 1 + \langle\langle \epsilon_k C_{k\uparrow}, C_{k\uparrow}^\dagger \rangle\rangle - V \sum_{k'} \langle\langle C_{-k\downarrow}^\dagger C_{k'\downarrow} C_{-k'\uparrow}, C_{k\uparrow}^\dagger \rangle\rangle + U \sum_{k',Q} \langle\langle C_{k+Q\downarrow} C_{k'\downarrow}^\dagger C_{k'-Q\uparrow}; C_{k\uparrow}^\dagger \rangle\rangle$$

Rearranging and defining the energy gaps (Δ_S and Δ_{SDW})

$$= 1 + \epsilon_k \langle \langle C_{k\uparrow}, C_{k\uparrow}^\dagger \rangle \rangle - V \sum_{k,k'} \langle C_{k'\downarrow}, C_{-k'\uparrow} \rangle \langle \langle C_{-k\uparrow}^\dagger, C_{k\uparrow}^\dagger \rangle \rangle + U \sum_{k',Q} \langle C_{k'\downarrow}^\dagger, C_{k'-Q\uparrow} \rangle \langle \langle C_{k+Q\downarrow}, C_{k\uparrow}^\dagger \rangle \rangle \quad (4.2.16)$$

Defining;

$$\Delta_S = V \sum_{k'} \langle C_{k'\downarrow}, C_{-k'\uparrow} \rangle, \quad \Delta_{SDW} = U \sum_{k',Q} \langle C_{k'\downarrow}^\dagger, C_{k'-Q\uparrow} \rangle$$

Then we have;

$$(\omega - \epsilon_k) \langle \langle C_{k\uparrow}, C_{k\uparrow}^\dagger \rangle \rangle = 1 - \Delta_S \langle \langle C_{-k\downarrow}^\dagger, C_{k\uparrow}^\dagger \rangle \rangle + \Delta_{SDW} \langle \langle C_{k+Q\downarrow}, C_{k\uparrow}^\dagger \rangle \rangle \quad (4.2.17)$$

Similarly the equation of motion of Greens function $\langle \langle C_{-k\downarrow}^\dagger, C_{k'\uparrow}^\dagger \rangle \rangle$ can be obtained as before by evaluating the relevant commutators. Then the equation of motion for $\langle \langle C_{-k\downarrow}^\dagger, C_{k'\uparrow}^\dagger \rangle \rangle$ becomes;

$$\omega \langle \langle C_{-k\downarrow}^\dagger, C_{k'\uparrow}^\dagger \rangle \rangle = \langle \langle [C_{-k\downarrow}^\dagger, \hat{H}]; C_{k'\uparrow}^\dagger \rangle \rangle \quad (4.2.18)$$

Then solving for the commutator $[C_{-k\downarrow}^\dagger, \hat{H}]$;

$$[C_{-k\downarrow}^\dagger, \hat{H}] = [C_{-k\downarrow}^\dagger; \left(\sum_{k,\sigma} \epsilon_k C_{k\sigma}^\dagger C_{k\sigma} - \sum_{k,k'} V_{k,k'} C_{k\uparrow}^\dagger C_{-k\downarrow}^\dagger C_{k'\downarrow} C_{-k'\uparrow} + U \sum_{k,Q} C_{k\uparrow}^\dagger C_{k+Q\downarrow} C_{k'\downarrow}^\dagger C_{k'-Q\uparrow} \right)] \quad (4.2.19)$$

Similarly using the commutation relations (from equation (4.2.4) to (4.2.10)) we have;

$$\begin{aligned} [C_{-k\downarrow}^\dagger, \hat{H}] &= \sum_{k,\sigma} \epsilon_k [C_{-k\downarrow}^\dagger, C_{k\sigma}^\dagger C_{k\sigma}] - V \sum_{k,k'} [C_{-k\downarrow}^\dagger, C_{k\uparrow}^\dagger C_{-k\downarrow}^\dagger C_{k'\downarrow} C_{-k'\uparrow}] \\ &\quad + U \sum_{k,Q} [C_{-k\downarrow}^\dagger, C_{k\uparrow}^\dagger C_{k+Q\downarrow} C_{k'\downarrow}^\dagger C_{k'-Q\uparrow}] \\ &= \sum_{k,\sigma} \epsilon_k [C_{-k\downarrow}^\dagger, C_{k\sigma}^\dagger C_{k\sigma}] - V \sum_{k,k'} \left([C_{-k\downarrow}^\dagger, C_{k\uparrow}^\dagger C_{-k\downarrow}^\dagger] C_{k'\downarrow} C_{-k'\uparrow} + C_{k\uparrow}^\dagger C_{-k\downarrow}^\dagger [C_{-k\downarrow}^\dagger, C_{k'\downarrow} C_{-k'\uparrow}] \right) \\ &\quad + U \sum_{k,Q} \left([C_{-k\downarrow}^\dagger, C_{k\uparrow}^\dagger C_{k+Q\downarrow}] C_{k'\downarrow}^\dagger C_{k'-Q\uparrow} + C_{k\uparrow}^\dagger C_{k+Q\downarrow} [C_{-k\downarrow}^\dagger, C_{k'\downarrow}^\dagger C_{k'-Q\uparrow}] \right) \\ &= \sum_{k,\sigma} \epsilon_k (\{C_{-k\downarrow}^\dagger, C_{k\sigma}^\dagger\} C_{k\sigma} - C_{k\sigma}^\dagger \{C_{-k\downarrow}^\dagger, C_{k\sigma}\}) \end{aligned} \quad (4.2.21)$$

$$-V \sum_{k,k'} \left(C_{k\uparrow}^\dagger C_{-k\downarrow}^\dagger \{C_{-k\downarrow}^\dagger, C_{k'\downarrow}\} C_{-k'\uparrow} - C_{k\uparrow}^\dagger C_{-k\downarrow}^\dagger C_{k'\downarrow} \{C_{-k\downarrow}^\dagger, C_{-k'\uparrow}\} \right) \quad (4.2.22)$$

$$+U \sum_{k,Q} \left(\{C_{-k\downarrow}^\dagger, C_{k\uparrow}^\dagger\} C_{k+Q\downarrow} C_{k'\downarrow}^\dagger C_{k'-Q\uparrow} - C_{k\uparrow}^\dagger \{C_{-k\downarrow}^\dagger, C_{k+Q\downarrow}\} C_{k'\downarrow}^\dagger C_{k'-Q\uparrow} \right. \\ \left. + C_{k\uparrow}^\dagger C_{k+Q\downarrow} \{C_{-k\downarrow}^\dagger, C_{k'\downarrow}^\dagger\} C_{k'-Q\uparrow} - C_{k\uparrow}^\dagger C_{k+Q\downarrow} C_{k'\downarrow}^\dagger \{C_{-k\downarrow}^\dagger, C_{k'-Q\downarrow}\} \right)$$

since $\{C_{k\sigma}, C_{k\sigma}\} = \{C_{k\sigma}^\dagger, C_{k\sigma}^\dagger\} = 0$, $\{C_{k\sigma}, C_{k'\sigma}^\dagger\} = \delta_{kk'} = 1$, *iff* $k = k'$

$$= - \sum_{k,\sigma} \epsilon_k (C_{k\sigma}^\dagger \{C_{-k\downarrow}^\dagger, C_{k\sigma}\}) - V \sum_{k,k'} \left(C_{k\uparrow}^\dagger C_{-k\downarrow}^\dagger \{C_{-k\downarrow}^\dagger, C_{k'\downarrow}\} C_{-k'\uparrow} \right) \\ + U \sum_{k,Q} \left(\{C_{k\uparrow}, C_{k\uparrow}^\dagger\} C_{k+Q\downarrow} C_{k'\downarrow}^\dagger C_{k'-Q\downarrow} \right) \quad (4.2.23)$$

$$[C_{-k\downarrow}^\dagger, \hat{H}] = -\epsilon_{-k} C_{-k\downarrow}^\dagger - V \sum_{k'} C_{k'\uparrow}^\dagger C_{-k'\downarrow}^\dagger C_{k\uparrow} - U \sum_{k',Q} C_{-k-Q\uparrow}^\dagger C_{k'\downarrow}^\dagger C_{k'-Q\uparrow} \quad (4.2.24)$$

We can also obtain the equation of motion for higher order Green's function $\langle\langle C_{-k\downarrow}^\dagger, C_{k\uparrow}^\dagger \rangle\rangle$, then substituting equation (4.2.24) in to (4.2.18) yields;

$$\omega \langle\langle C_{-k\downarrow}^\dagger, C_{k\uparrow}^\dagger \rangle\rangle = \langle\langle \left(-\epsilon_{-k} C_{-k\downarrow}^\dagger - V \sum_k C_{k\uparrow}^\dagger C_{-k\downarrow}^\dagger C_{k\uparrow} - U \sum_{k',Q} C_{-k-Q\uparrow}^\dagger C_{k'\downarrow}^\dagger C_{k'-Q\uparrow} \right); C_{k\uparrow}^\dagger \rangle\rangle \\ = -\epsilon_{-k} \langle\langle C_{-k\downarrow}^\dagger, C_{k\uparrow}^\dagger \rangle\rangle - V \sum_{k'} \langle\langle C_{k\uparrow}^\dagger C_{-k'\downarrow}^\dagger C_{k'\uparrow}, C_{k\uparrow}^\dagger \rangle\rangle - U \sum_{k',Q} \langle\langle C_{-k-Q\uparrow}^\dagger C_{k'\downarrow}^\dagger C_{k'-Q\uparrow}; C_{k\uparrow}^\dagger \rangle\rangle$$

Rearranging and defining the energy gaps

$$(\omega + \epsilon_{-k}) \langle\langle C_{-k\downarrow}^\dagger, C_{k\uparrow}^\dagger \rangle\rangle = -V \sum_k \langle C_{k\uparrow}^\dagger C_{-k\downarrow}^\dagger \rangle \langle\langle C_{k\uparrow}, C_{k\uparrow}^\dagger \rangle\rangle - U \sum_{k,Q} \langle C_{k'\downarrow}^\dagger C_{k'-Q\uparrow} \rangle \langle\langle C_{-k-Q\uparrow}^\dagger; C_{k\uparrow}^\dagger \rangle\rangle \quad (4.2.25)$$

Then from the relation

$$\Delta_S^* = V \sum_k \langle C_{k\uparrow}^\dagger C_{-k\downarrow}^\dagger \rangle \quad \Delta_{SDW}^* = U \sum_{k,Q} \langle C_{k'\downarrow}^\dagger C_{k'-Q\uparrow} \rangle$$

We get;

$$(\omega + \epsilon_{-k}) \langle\langle C_{-k\downarrow}^\dagger, C_{k\uparrow}^\dagger \rangle\rangle = -\Delta_S^* \langle\langle C_{k\uparrow}, C_{k\uparrow}^\dagger \rangle\rangle - \Delta_{SDW}^* \langle\langle C_{-k-Q\uparrow}^\dagger; C_{k\uparrow}^\dagger \rangle\rangle \quad (4.2.26)$$

Similarly the equation of motion of Green's function $\langle\langle C_{k+Q\downarrow}, C_{k'\uparrow}^\dagger \rangle\rangle$ can be obtained as before by evaluating the relevant commutators.

writing the equation of motion,

$$\omega \langle\langle C_{k+Q\downarrow}, C_{k'\uparrow}^\dagger \rangle\rangle = \langle [C_{k+Q\downarrow}, C_{k'\uparrow}^\dagger] \rangle + \langle\langle [C_{k+Q\downarrow}, \hat{H}]; C_{k'\uparrow}^\dagger \rangle\rangle \quad (4.2.27)$$

$$\omega \langle\langle C_{k+Q\downarrow}, C_{k'\uparrow}^\dagger \rangle\rangle = \delta_{k+Q, k'} + \langle\langle [C_{k+Q\downarrow}, \hat{H}]; C_{k'\uparrow}^\dagger \rangle\rangle \quad (4.2.28)$$

Evaluating the commutator $[C_{k+Q\downarrow}, \hat{H}]$ using the Hamiltonian (4.1.1)

$$[C_{k+Q\downarrow}, \hat{H}] = [C_{k+Q\downarrow}, \sum_{k,\sigma} \epsilon_k C_{k\sigma}^\dagger C_{k\sigma} - \sum_{k,k'} V_{k,k'} C_{k\uparrow}^\dagger C_{-k\downarrow}^\dagger C_{k'\downarrow} C_{-k'\uparrow} + U \sum_{k,Q} C_{k\uparrow}^\dagger C_{k+Q\downarrow} C_{k'\downarrow}^\dagger C_{k'-Q\uparrow}] \quad (4.2.29)$$

using the commutation relations

$$\begin{aligned} [C_{k+Q\downarrow}, \hat{H}] &= \sum_{k,\sigma} \epsilon_k [C_{k+Q\downarrow}, C_{k\sigma}^\dagger C_{k\sigma}] - \sum_{k,k'} V_{k,k'} \left([C_{k+Q\downarrow}, C_{k\uparrow}^\dagger C_{-k\downarrow}^\dagger] C_{k'\downarrow} C_{-k'\uparrow} + C_{k\uparrow}^\dagger C_{-k\downarrow}^\dagger [C_{k+Q\downarrow}, C_{k'\downarrow} C_{-k'\uparrow}] \right) \\ &\quad + U \sum_{k,Q} \left([C_{k+Q\downarrow}, C_{k\uparrow}^\dagger C_{k+Q\downarrow}] C_{k'\downarrow}^\dagger C_{k'-Q\uparrow} + C_{k\uparrow}^\dagger C_{k+Q\downarrow} [C_{k+Q\downarrow}, C_{k'\downarrow}^\dagger C_{k'-Q\uparrow}] \right) \\ &= \sum_{k,\sigma} \epsilon_k \{C_{k+Q\downarrow}, C_{k'\sigma}^\dagger\} C_{k\sigma} - C_{k\sigma}^\dagger \{C_{k+Q\downarrow}, C_{k\sigma}\} \\ &\quad - \sum_{k,k'} V_{k,k'} \left(\{C_{k+Q\downarrow}, C_{k\uparrow}^\dagger\} C_{-k\downarrow}^\dagger - C_{k\uparrow}^\dagger \{C_{k+Q\downarrow}, C_{-k\downarrow}^\dagger\} \right) C_{k'\downarrow} C_{-k'\uparrow} \\ &\quad + C_{k\uparrow}^\dagger C_{-k\downarrow}^\dagger \left(\{C_{k+Q\downarrow}, C_{k'\downarrow}\} C_{-k'\uparrow} - C_{k'\downarrow} \{C_{k+Q\downarrow}, C_{-k'\uparrow}\} \right) \\ &\quad + U \sum_{k,Q} \left(\{C_{k+Q\downarrow}, C_{k\uparrow}^\dagger\} C_{k+Q\downarrow} - C_{k\uparrow}^\dagger \{C_{k+Q\downarrow}, C_{k+Q\downarrow}\} \right) C_{k'\downarrow}^\dagger C_{k'-Q\uparrow} \\ &\quad + C_{k\uparrow}^\dagger C_{k+Q\downarrow} \left(\{C_{k+Q\downarrow}, C_{k'\downarrow}^\dagger\} C_{k'-Q\uparrow} - C_{k'\downarrow}^\dagger \{C_{k+Q\downarrow}, C_{k'-Q\uparrow}\} \right) \end{aligned}$$

since, $\{C_{k\sigma}, C_{k'\sigma}^\dagger\} = \delta_{kk'} = 1$, iff $k = k'$, Otherwise 0.

And $\{C_{k\sigma}, C_{k'\sigma}\} = \{C_{k\sigma}^\dagger, C_{k'\sigma}^\dagger\} = 0$

$$\begin{aligned} [C_{k+Q\downarrow}, \hat{H}] &= \sum_{k,\sigma} \epsilon_k \{C_{k+Q\downarrow}, C_{k'\sigma}^\dagger\} C_{k\sigma} + V \sum_{k,k'} C_{k\uparrow}^\dagger \{C_{k+Q\downarrow}, C_{-k\downarrow}^\dagger\} C_{k'\downarrow} C_{-k'\uparrow} \\ &\quad + U \sum_{k,Q} C_{k\uparrow}^\dagger C_{k+Q\downarrow} \{C_{k+Q\downarrow}, C_{k'\downarrow}^\dagger\} C_{k'-Q\uparrow} \end{aligned} \quad (4.2.30)$$

$$= \epsilon_{k+Q} C_{k+Q\downarrow} + V \sum_{k'} C_{-k-Q\uparrow}^\dagger C_{k'\downarrow} C_{-k'\uparrow} - U \sum_{k',Q} C_{k'\uparrow}^\dagger C_{k'+Q\downarrow} C_{-k\downarrow}^\dagger \quad (4.2.31)$$

Substituting equation (4.2.31) in to equation (4.2.28) yields;

$$\begin{aligned} \omega \langle \langle C_{k+Q\downarrow}, C_{k'\uparrow}^\dagger \rangle \rangle &= \delta_{k+Q,k'} + \langle \langle \left(\epsilon_{k+Q} C_{k+Q\downarrow} + V \sum_{k,k'} C_{-k-Q\uparrow}^\dagger C_{k'\downarrow} C_{-k'\uparrow} + U \sum_{k',Q} C_{k'\uparrow}^\dagger C_{k'+Q\downarrow} C_{k\uparrow} \right); C_{k'\uparrow}^\dagger \rangle \rangle \\ (\omega - \epsilon_{k+Q}) \langle \langle C_{k+Q\downarrow}, C_{k'\uparrow}^\dagger \rangle \rangle &= \delta_{k+Q,k'} + V \sum_{k,k'} \langle \langle C_{-k-Q\uparrow}^\dagger C_{k'\downarrow} C_{-k'\uparrow}; C_{k'\uparrow}^\dagger \rangle \rangle + U \sum_{k',Q} \langle \langle C_{k'\uparrow}^\dagger C_{k'+Q\downarrow} C_{k\uparrow}; C_{k'\uparrow}^\dagger \rangle \rangle \\ (\omega - \epsilon_{k+Q}) \langle \langle C_{k+Q\downarrow}, C_{k'\uparrow}^\dagger \rangle \rangle &= \delta_{k+Q,k'} + V \sum_{k,k'} \langle C_{k'\downarrow} C_{-k'\uparrow} \rangle \langle \langle C_{-k-Q\uparrow}^\dagger; C_{k'\uparrow}^\dagger \rangle \rangle + U \sum_{k',Q} \langle C_{k'\uparrow}^\dagger C_{k'+Q\downarrow} \rangle \langle \langle C_{k\uparrow}; C_{k'\uparrow}^\dagger \rangle \rangle \end{aligned} \quad (4.2.32)$$

Defining the order parameters i.e;

$$\Delta_S^{**} = V \sum_{k,k'} \langle C_{k'\downarrow} C_{-k'\uparrow} \rangle, \text{ and } \Delta_{SDW}^{**} = U \sum_{k',Q} \langle C_{k'\uparrow}^\dagger C_{k'+Q\downarrow} \rangle$$

Equation (4.2.32) becomes;

$$(\omega - \epsilon_{k+Q}) \langle \langle C_{k+Q\downarrow}, C_{k'\uparrow}^\dagger \rangle \rangle = \delta_{k+Q,k'} + \Delta_S^{**} \langle \langle C_{-k-Q\uparrow}^\dagger; C_{k'\uparrow}^\dagger \rangle \rangle + \Delta_{SDW}^{**} \langle \langle C_{k\uparrow}; C_{k'\uparrow}^\dagger \rangle \rangle \quad (4.2.33)$$

similarly the equation of Green's functions $\langle \langle C_{-k-Q\uparrow}^\dagger, C_{k'\uparrow}^\dagger \rangle \rangle$ can be obtained as before by evaluating the relevant commutator. Writting the equation of motion

$$\omega \langle \langle C_{-k-Q\uparrow}^\dagger, C_{k'\uparrow}^\dagger \rangle \rangle = \langle \langle [C_{-k-Q\uparrow}^\dagger, \hat{H}]; C_{k'\uparrow}^\dagger \rangle \rangle \quad (4.2.34)$$

Evaluating the commutator $[C_{-k-Q\uparrow}^\dagger, \hat{H}]$ using the Hamiltonian(4.1.1)

$$[C_{-k-Q\uparrow}^\dagger, \hat{H}] = [C_{-k-Q\uparrow}^\dagger, \left(\sum_{k,\sigma} \epsilon_k C_{k\sigma}^\dagger C_{k\sigma} - \sum_{k,k'} V_{k,k'} C_{k\uparrow}^\dagger C_{-k\downarrow}^\dagger C_{k'\downarrow} C_{-k'\uparrow} + U \sum_{k,Q} C_{k\uparrow}^\dagger C_{k+Q\downarrow} C_{k'\downarrow}^\dagger C_{k'-Q\uparrow} \right)] \quad (4.2.35)$$

Using the commutation relations;

$$\begin{aligned} [C_{-k-Q\uparrow}^\dagger, \hat{H}] &= \sum_{k,\sigma} \epsilon_k [C_{-k-Q\uparrow}^\dagger, C_{k\sigma}^\dagger C_{k\sigma}] \\ &- \sum_{k,k'} V_{k,k'} [C_{-k-Q\uparrow}^\dagger, C_{k\uparrow}^\dagger C_{-k\downarrow}^\dagger] C_{k'\downarrow} C_{-k'\uparrow} + [C_{-k-Q\uparrow}^\dagger, C_{k'\downarrow} C_{-k'\uparrow}] C_{k\uparrow}^\dagger C_{-k\downarrow}^\dagger \end{aligned} \quad (4.2.36)$$

$$\begin{aligned}
& +U \sum_{k,Q} \left([C_{-k-Q\uparrow}^\dagger, C_{k\uparrow}^\dagger C_{k+Q\downarrow}] C_{k'\downarrow}^\dagger C_{k'-Q\uparrow} + C_{k\uparrow}^\dagger C_{k+Q\downarrow} [C_{-k-Q\uparrow}^\dagger, C_{k'\downarrow}^\dagger C_{k'-Q\uparrow}] \right) \\
& = - \sum_{k,\sigma} \epsilon_k C_{k\sigma}^\dagger \{C_{-k-Q\uparrow}^\dagger, C_{k\sigma}\} + \sum_{k,k'} V_{k,k'} (\{C_{-k-Q\uparrow}^\dagger, C_{-k'\uparrow}\} C_{k'\downarrow}^\dagger) C_{k\uparrow}^\dagger C_{-k\downarrow}^\dagger \\
& \quad - U \sum_{k,Q} C_{k\uparrow}^\dagger C_{k+Q\downarrow} \{C_{-k-Q\uparrow}^\dagger, C_{k'-Q\uparrow}\} C_{k'\downarrow}^\dagger
\end{aligned}$$

since, $\{C_{k\sigma}, C_{k'\sigma}^\dagger\} = \delta_{kk'} = 1, \text{ if } k = k', \text{ Otherwise } 0.$

And $\{C_{k\sigma}, C_{k'\sigma}^\dagger\} = \{C_{k\sigma}^\dagger, C_{k'\sigma}\} = 0$

$$[C_{-k-Q\uparrow}^\dagger, \hat{H}] = -\epsilon_{-k-Q} C_{-k-Q\uparrow}^\dagger + V \sum_{k'} C_{k'\uparrow}^\dagger C_{-k'\downarrow}^\dagger C_{k+Q\downarrow} - U \sum_{k',Q} C_{k'\uparrow}^\dagger C_{k'+Q\downarrow} C_{-k\downarrow}^\dagger \quad (4.2.37)$$

Substituting equation (4.2.37) in equation (4.2.34) yields;

$$\begin{aligned}
\omega \langle\langle C_{-k-Q\uparrow}^\dagger, C_{k'\uparrow}^\dagger \rangle\rangle & = \langle\langle \left(-\epsilon_{-k-Q} C_{-k-Q\uparrow}^\dagger + V \sum_{k'} C_{k'\uparrow}^\dagger C_{-k'\downarrow}^\dagger C_{k+Q\downarrow} - U \sum_{k',Q} C_{k'\uparrow}^\dagger C_{k'+Q\downarrow} C_{-k\downarrow}^\dagger \right); C_{k'\uparrow}^\dagger \rangle\rangle \\
(\omega + \epsilon_{-k-Q}) \langle\langle C_{-k-Q\uparrow}^\dagger, C_{k'\uparrow}^\dagger \rangle\rangle & = V \sum_{k'} \langle\langle C_{k'\uparrow}^\dagger C_{-k'\downarrow}^\dagger C_{k+Q\downarrow}; C_{k'\uparrow}^\dagger \rangle\rangle - U \sum_{k',Q} \langle\langle C_{k'\uparrow}^\dagger C_{k'+Q\downarrow} C_{-k\downarrow}^\dagger; C_{k'\uparrow}^\dagger \rangle\rangle \\
(\omega + \epsilon_{-k-Q}) \langle\langle C_{-k-Q\uparrow}^\dagger, C_{k'\uparrow}^\dagger \rangle\rangle & = V \sum_{k'} \langle C_{k'\uparrow}^\dagger C_{-k'\downarrow}^\dagger \rangle \langle\langle C_{k+Q\downarrow}; C_{k'\uparrow}^\dagger \rangle\rangle - U \sum_{k',Q} \langle C_{k'\uparrow}^\dagger C_{k'+Q\downarrow} \rangle \langle\langle C_{-k\downarrow}^\dagger; C_{k'\uparrow}^\dagger \rangle\rangle
\end{aligned}$$

Defining the order parameters;

$$\Delta_S^{***} = V \sum_{k'} \langle C_{k'\uparrow}^\dagger C_{-k'\downarrow}^\dagger \rangle, \text{ and } \Delta_{SDW}^{***} = U \sum_{k',Q} \langle C_{k'\uparrow}^\dagger C_{k'+Q\downarrow} \rangle$$

$$(\omega + \epsilon_{-k-Q}) \langle\langle C_{-k-Q\uparrow}^\dagger, C_{k'\uparrow}^\dagger \rangle\rangle = \Delta_S^{***} \langle\langle C_{k+Q\downarrow}; C_{k'\uparrow}^\dagger \rangle\rangle - \Delta_{SDW}^{***} \langle\langle C_{-k\downarrow}^\dagger; C_{k'\uparrow}^\dagger \rangle\rangle \quad (4.2.38)$$

Generally we have four coupled equations of motion, they are;

$$(\omega - \epsilon_k) \langle\langle C_{k\uparrow}, C_{k'\uparrow}^\dagger \rangle\rangle = \delta_{k,k'} - \Delta_S \langle\langle C_{-k\downarrow}^\dagger; C_{k'\uparrow}^\dagger \rangle\rangle + \Delta_{SDW} \langle\langle C_{k+Q\downarrow}; C_{k'\uparrow}^\dagger \rangle\rangle \quad (4.2.39)$$

$$(\omega + \epsilon_{-k}) \langle\langle C_{-k\downarrow}^\dagger, C_{k'\uparrow}^\dagger \rangle\rangle = -\Delta_S \langle\langle C_{k\uparrow}; C_{k'\uparrow}^\dagger \rangle\rangle - \Delta_{SDW} \langle\langle C_{-k-Q\uparrow}^\dagger; C_{k'\uparrow}^\dagger \rangle\rangle \quad (4.2.40)$$

$$(\omega - \epsilon_{k+Q}) \langle\langle C_{k+Q\downarrow}, C_{k'\uparrow}^\dagger \rangle\rangle = \delta_{k+Q,k'} + \Delta_S \langle\langle C_{-k-Q\uparrow}^\dagger; C_{k'\uparrow}^\dagger \rangle\rangle + \Delta_{SDW} \langle\langle C_{k\uparrow}; C_{k'\uparrow}^\dagger \rangle\rangle \quad (4.2.41)$$

$$(\omega + \epsilon_{-k-Q}) \langle\langle C_{-k-Q\uparrow}^\dagger, C_{k'\uparrow}^\dagger \rangle\rangle = \Delta_S \langle\langle C_{k+Q\downarrow}; C_{k'\uparrow}^\dagger \rangle\rangle - \Delta_{SDW} \langle\langle C_{-k\downarrow}^\dagger; C_{k'\uparrow}^\dagger \rangle\rangle \quad (4.2.42)$$

we have assumed that

$$\Delta_{SDW} = \Delta_{SDW}^* = \Delta_{SDW}^{**} = \Delta_{SDW}^{***}$$

$$\Delta_S = \Delta_S^* = \Delta_S^{**} = \Delta_S^{***}$$

$$\epsilon_{-k} = \epsilon_k, -\epsilon_k = \epsilon_{k+Q}, \epsilon_{-k-Q} = -\epsilon_k,$$

$$\frac{\omega - \epsilon_k}{\omega + \epsilon_k} \cong 1, k = k' \implies \delta_{k,k'} = 1, \delta_{k+Q,k'} = 0$$

Rearranging;

$$\langle\langle C_{k\uparrow}, C_{k'\uparrow}^\dagger \rangle\rangle = \frac{1}{\omega - \epsilon_k} \left(1 - \Delta_S \langle\langle C_{-k\downarrow}^\dagger; C_{k'\uparrow}^\dagger \rangle\rangle + \Delta_{SDW} \langle\langle C_{k+Q\downarrow}^\dagger; C_{k'\uparrow}^\dagger \rangle\rangle \right) \quad (4.2.43)$$

$$\langle\langle C_{-k\downarrow}^\dagger, C_{k'\uparrow}^\dagger \rangle\rangle = \frac{1}{(\omega + \epsilon_{-k})} \left(-\Delta_S \langle\langle C_{k\uparrow}; C_{k'\uparrow}^\dagger \rangle\rangle - \Delta_{SDW} \langle\langle C_{-k-Q\uparrow}^\dagger; C_{k'\uparrow}^\dagger \rangle\rangle \right) \quad (4.2.44)$$

$$\langle\langle C_{k+Q\downarrow}, C_{k'\uparrow}^\dagger \rangle\rangle = \frac{1}{\omega - \epsilon_{k+Q}} \left(\Delta_S \langle\langle C_{-k-Q\uparrow}^\dagger; C_{k'\uparrow}^\dagger \rangle\rangle + \Delta_{SDW} \langle\langle C_{k\uparrow}; C_{k'\uparrow}^\dagger \rangle\rangle \right) \quad (4.2.45)$$

$$\langle\langle C_{-k-Q\uparrow}^\dagger, C_{k'\uparrow}^\dagger \rangle\rangle = \frac{1}{\omega + \epsilon_{-k-Q}} \left(\Delta_S \langle\langle C_{k+Q\downarrow}; C_{k'\uparrow}^\dagger \rangle\rangle - \Delta_{SDW} \langle\langle C_{-k\downarrow}^\dagger; C_{k'\uparrow}^\dagger \rangle\rangle \right) \quad (4.2.46)$$

Substituting equation (4.2.46) and (4.2.43) in to (4.2.44), yields;

$$\begin{aligned} (\omega + \epsilon_{-k}) \langle\langle C_{-k\downarrow}^\dagger, C_{k'\uparrow}^\dagger \rangle\rangle &= \frac{-\Delta_S}{(\omega - \epsilon_k)} \left(1 - \Delta_S \langle\langle C_{-k\downarrow}^\dagger; C_{k'\uparrow}^\dagger \rangle\rangle + \Delta_{SDW} \langle\langle C_{k+Q\downarrow}^\dagger; C_{k'\uparrow}^\dagger \rangle\rangle \right) \\ &\quad - \frac{\Delta_{SDW}}{(\omega + \epsilon_{-k-Q})} \left(\Delta_S \langle\langle C_{k+Q\downarrow}; C_{k'\uparrow}^\dagger \rangle\rangle - \Delta_{SDW} \langle\langle C_{-k\downarrow}^\dagger; C_{k'\uparrow}^\dagger \rangle\rangle \right) \\ \frac{\Delta_S}{(\omega - \epsilon_k)} &= \left[\frac{\Delta_S^2}{(\omega - \epsilon_k)} + \frac{\Delta_{SDW}^2}{(\omega + \epsilon_{-k-Q})} - (\omega + \epsilon_{-k}) \right] \langle\langle C_{-k\downarrow}^\dagger; C_{k'\uparrow}^\dagger \rangle\rangle \\ &\quad - \Delta_S \Delta_{SDW} \left[\frac{1}{(\omega - \epsilon_k)} + \frac{1}{(\omega + \epsilon_{-k-Q})} \right] \langle\langle C_{k+Q\downarrow}; C_{k'\uparrow}^\dagger \rangle\rangle \end{aligned}$$

Similarly substituting equation (4.2.43) and (4.2.46) in to (4.2.45), yields;

$$\begin{aligned} (\omega - \epsilon_{k+Q}) \langle\langle C_{k+Q\downarrow}, C_{k'\uparrow}^\dagger \rangle\rangle &= \frac{\Delta_S}{\omega + \epsilon_{-k-Q}} \left[\Delta_S \langle\langle C_{k+Q\downarrow}; C_{k'\uparrow}^\dagger \rangle\rangle - \Delta_{SDW} \langle\langle C_{-k\downarrow}^\dagger; C_{k'\uparrow}^\dagger \rangle\rangle \right] \\ &\quad + \frac{\Delta_{SDW}}{\omega - \epsilon_k} \left[1 - \Delta_S \langle\langle C_{-k\downarrow}^\dagger; C_{k'\uparrow}^\dagger \rangle\rangle + \Delta_{SDW} \langle\langle C_{k+Q\downarrow}^\dagger; C_{k'\uparrow}^\dagger \rangle\rangle \right] \\ -\frac{\Delta_{SDW}}{\omega - \epsilon_k} &= \left[\frac{\Delta_S^2}{\omega + \epsilon_{-k-Q}} + \frac{\Delta_{SDW}}{\omega - \epsilon_k} - (\omega + \epsilon_{k+Q}) \right] \langle\langle C_{k+Q\downarrow}, C_{k'\uparrow}^\dagger \rangle\rangle \end{aligned}$$

$$-\Delta_{SDW}\Delta_S \left[\frac{1}{\omega + \epsilon_{-k-Q}} + \frac{1}{\omega - \epsilon_k} \right] \langle\langle C_{-k\downarrow}^\dagger, C_{k'\uparrow}^\dagger \rangle\rangle$$

Rearranging the above equations yields;

$$-\Delta_S = \left[\omega^2 - \epsilon_k^2 - (\Delta_S^2 + \Delta_{SDW}^2) \right] \langle\langle C_{-k\downarrow}^\dagger, C_{k'\uparrow}^\dagger \rangle\rangle + 2\Delta_S\Delta_{SDW} \langle\langle C_{k+Q\downarrow}, C_{k'\uparrow}^\dagger \rangle\rangle \quad (4.2.47)$$

$$\Delta_{SDW} = \left[\omega^2 - \epsilon_k^2 - (\Delta_S^2 + \Delta_{SDW}^2) \right] \langle\langle C_{k+Q\downarrow}, C_{k'\uparrow}^\dagger \rangle\rangle + 2\Delta_S\Delta_{SDW} \langle\langle C_{-k\downarrow}^\dagger, C_{k'\uparrow}^\dagger \rangle\rangle \quad (4.2.48)$$

Solving for $\langle\langle C_{-k\downarrow}^\dagger, C_{k'\uparrow}^\dagger \rangle\rangle$

$$\langle\langle C_{-k\downarrow}^\dagger, C_{k'\uparrow}^\dagger \rangle\rangle = \frac{-\Delta_S \left[\omega^2 - \epsilon_k^2 - (\Delta_S^2 + \Delta_{SDW}^2) + 2\Delta_{SDW}^2 \right]}{\left[\omega^2 - \epsilon_k^2 - (\Delta_S^2 + \Delta_{SDW}^2) \right]^2 - (2\Delta_{SDW}\Delta_S)^2} \quad (4.2.49)$$

Similarly, solving for $\langle\langle C_{k+Q\downarrow}, C_{k'\uparrow}^\dagger \rangle\rangle$

$$\langle\langle C_{k+Q\downarrow}, C_{k'\uparrow}^\dagger \rangle\rangle = \frac{\Delta_{SDW} \left[\omega^2 - \epsilon_k^2 - (\Delta_S^2 + \Delta_{SDW}^2) + 2\Delta_S^2 \right]}{\left[\omega^2 - \epsilon_k^2 - (\Delta_S^2 + \Delta_{SDW}^2) \right]^2 - (2\Delta_{SDW}\Delta_S)^2} \quad (4.2.50)$$

Applying factorization theorem for equation (4.2.49) above we have;

$$\begin{aligned} & \frac{-\Delta_S \left[\omega^2 - \epsilon_k^2 - (\Delta_S^2 + \Delta_{SDW}^2) \right]}{\left[\left(\omega^2 - \epsilon_k^2 - (\Delta_S^2 + \Delta_{SDW}^2) \right) - (2\Delta_{SDW}\Delta_S) \right] \left[\left(\omega^2 - \epsilon_k^2 - (\Delta_S^2 + \Delta_{SDW}^2) \right) + (2\Delta_{SDW}\Delta_S) \right]} \\ = & \frac{A}{\left[\left(\omega^2 - \epsilon_k^2 - (\Delta_S^2 + \Delta_{SDW}^2) \right) + (2\Delta_{SDW}\Delta_S) \right]} + \frac{B}{\left[\left(\omega^2 - \epsilon_k^2 - (\Delta_S^2 + \Delta_{SDW}^2) \right) - (2\Delta_{SDW}\Delta_S) \right]} \\ & A + B = -\Delta_S, 2\Delta_S\Delta_{SDW}(B - A) = 0 \end{aligned}$$

$$A = \frac{-\Delta_S}{2}$$

and

$$B = \frac{-\Delta_S}{2}$$

$$-2\Delta_S\Delta_{SDW}^2$$

$$\left[\left(\omega^2 - \epsilon_k^2 - (\Delta_S^2 + \Delta_{SDW}^2) \right) - (2\Delta_{SDW}\Delta_S) \right] \left[\left(\omega^2 - \epsilon_k^2 - (\Delta_S^2 + \Delta_{SDW}^2) \right) + (2\Delta_{SDW}\Delta_S) \right]$$

$$= \frac{A}{\left[\left(\omega^2 - \epsilon_k^2 - (\Delta_S^2 + \Delta_{SDW}^2) \right) + (2\Delta_{SDW}\Delta_S) \right]} + \frac{B}{\left[\left(\omega^2 - \epsilon_k^2 - (\Delta_S^2 + \Delta_{SDW}^2) \right) - (2\Delta_{SDW}\Delta_S) \right]}$$

$$A + B = 0, 2\Delta_S\Delta_{SDW}(B - A) = -\Delta_{SDW}(2\Delta_S\Delta_{SDW})$$

$$A = \frac{-\Delta_{SDW}}{2}$$

and

$$B = \frac{\Delta_{SDW}}{2}$$

Finally we will have;

$$\langle\langle C_{-k\downarrow}^\dagger, C_{k'\uparrow}^\dagger \rangle\rangle = \frac{-\Delta_S}{\left[\left(\omega^2 - \epsilon_k^2 - (\Delta_S^2 + \Delta_{SDW}^2) \right) + (2\Delta_{SDW}\Delta_S) \right]}$$

$$- \frac{\Delta_S}{\left[\left(\omega^2 - \epsilon_k^2 - (\Delta_S^2 + \Delta_{SDW}^2) \right) - (2\Delta_{SDW}\Delta_S) \right]}$$

$$+ \frac{\Delta_{SDW}}{\left[\left(\omega^2 - \epsilon_k^2 - (\Delta_S^2 + \Delta_{SDW}^2) \right) + (2\Delta_{SDW}\Delta_S) \right]} - \frac{\Delta_{SDW}}{\left[\left(\omega^2 - \epsilon_k^2 - (\Delta_S^2 + \Delta_{SDW}^2) \right) - (2\Delta_{SDW}\Delta_S) \right]}$$

Collecting the terms which have similar denominator we obtain;

$$\langle\langle C_{-k\downarrow}^\dagger, C_{k'\uparrow}^\dagger \rangle\rangle = \frac{-(\Delta_S + \Delta_{SDW})}{2[\omega^2 - \epsilon_k^2 - (\Delta_S + \Delta_{SDW})^2]} - \frac{(\Delta_S - \Delta_{SDW})}{2[\omega^2 - \epsilon_k^2 - (\Delta_S - \Delta_{SDW})^2]} \quad (4.2.51)$$

In similar fashion, applying factorization theorem for $\langle\langle C_{k+Q\downarrow}, C_{k'\uparrow}^\dagger \rangle\rangle$

$$\frac{\Delta_{SDW} \left[\omega^2 - \epsilon_k^2 - (\Delta_S^2 + \Delta_{SDW}^2) \right]}{\left[\left(\omega^2 - \epsilon_k^2 - (\Delta_S^2 + \Delta_{SDW}^2) \right) - (2\Delta_{SDW}\Delta_S) \right] \left[\left(\omega^2 - \epsilon_k^2 - (\Delta_S^2 + \Delta_{SDW}^2) \right) + (2\Delta_{SDW}\Delta_S) \right]}$$

$$= \frac{A}{\left[\left(\omega^2 - \epsilon_k^2 - (\Delta_S^2 + \Delta_{SDW}^2) \right) + (2\Delta_{SDW}\Delta_S) \right]} + \frac{B}{\left[\left(\omega^2 - \epsilon_k^2 - (\Delta_S^2 + \Delta_{SDW}^2) \right) - (2\Delta_{SDW}\Delta_S) \right]}$$

$$A + B = \Delta_{SDW}, B = A$$

$$A = \frac{\Delta_{SDW}}{2}$$

and

$$B = \frac{\Delta_{SDW}}{2}$$

$$\begin{aligned}
& \frac{2\Delta_S^2\Delta_{SDW}}{\left[\left(\omega^2 - \epsilon_k^2 - (\Delta_S^2 + \Delta_{SDW}^2)\right) - (2\Delta_{SDW}\Delta_S)\right]\left[\left(\omega^2 - \epsilon_k^2 - (\Delta_S^2 + \Delta_{SDW}^2)\right) + (2\Delta_{SDW}\Delta_S)\right]} \\
&= \frac{A}{\left[\left(\omega^2 - \epsilon_k^2 - (\Delta_S^2 + \Delta_{SDW}^2)\right) + (2\Delta_{SDW}\Delta_S)\right]} + \frac{B}{\left[\left(\omega^2 - \epsilon_k^2 - (\Delta_S^2 + \Delta_{SDW}^2)\right) - (2\Delta_{SDW}\Delta_S)\right]} \\
& \quad A + B = 0, (B - A) = \Delta_S \\
& \quad A = \frac{-\Delta_S}{2}
\end{aligned}$$

and

$$B = \frac{\Delta_S}{2}$$

Therefore;

$$\begin{aligned}
\langle\langle C_{k+Q\downarrow}^\dagger, C_{k\uparrow}^\dagger \rangle\rangle &= \frac{\Delta_{SDW}}{\left[\left(\omega^2 - \epsilon_k^2 - (\Delta_S^2 + \Delta_{SDW}^2)\right) + (2\Delta_{SDW}\Delta_S)\right]} \\
&+ \frac{\Delta_{SDW}}{\left[\left(\omega^2 - \epsilon_k^2 - (\Delta_S^2 + \Delta_{SDW}^2)\right) - (2\Delta_{SDW}\Delta_S)\right]} \\
&- \frac{\Delta_S}{\left[\left(\omega^2 - \epsilon_k^2 - (\Delta_S^2 + \Delta_{SDW}^2)\right) + (2\Delta_{SDW}\Delta_S)\right]} + \frac{\Delta_S}{\left[\left(\omega^2 - \epsilon_k^2 - (\Delta_S^2 + \Delta_{SDW}^2)\right) - (2\Delta_{SDW}\Delta_S)\right]}
\end{aligned}$$

Rearranging yields;

$$\langle\langle C_{k+Q\downarrow}^\dagger, C_{k\uparrow}^\dagger \rangle\rangle = \frac{(\Delta_S + \Delta_{SDW})}{2[\omega^2 - \epsilon_k^2 - (\Delta_S + \Delta_{SDW})^2]} + \frac{(\Delta_{SDW} - \Delta_S)}{2[\omega^2 - \epsilon_k^2 - (\Delta_S - \Delta_{SDW})^2]} \quad (4.2.52)$$

4.2.1 For superconducting order parameter and transition temperature

Using equation (4.2.51),

$$\langle\langle C_{-k\downarrow}^\dagger, C_{k\uparrow}^\dagger \rangle\rangle = \frac{-(\Delta_S + \Delta_{SDW})}{2[\omega^2 - \epsilon_k^2 - (\Delta_S + \Delta_{SDW})^2]} - \frac{(\Delta_S - \Delta_{SDW})}{2[\omega^2 - \epsilon_k^2 - (\Delta_S - \Delta_{SDW})^2]}$$

Where Δ_S is the superconducting order parameter (analogues to the BCS order parameter) and Δ_{SDW} is the magnetic order parameter.

Using the relation for Δ_S i.e;

$$\Delta_S = \frac{V}{\beta} \sum_{k,n} \langle \langle C_{-k\downarrow}^\dagger, C_{k\uparrow}^\dagger \rangle \rangle$$

And the sum may be changed in to an integral by introducing the density of states, $N(\epsilon)$,

$$\frac{1}{V} \sum_k \longrightarrow \frac{1}{(2\pi)^3} \int d^3k = \int_{-E_F}^{\infty} d\epsilon N(\epsilon)$$

The summation with respect to k and n extends over all allowed pair states. Therefore;

$$\Delta_S = \frac{V}{\beta} \sum_{k,n} \left\{ \frac{-(\Delta_S + \Delta_{SDW})}{2[\omega_n^2 - \epsilon_k^2 - (\Delta_S + \Delta_{SDW})^2]} - \frac{(\Delta_S - \Delta_{SDW})}{2[\omega^2 - \epsilon_k^2 - (\Delta_S - \Delta_{SDW})^2]} \right\} N(\epsilon) d\epsilon$$

$$\Delta_S = \frac{V}{\beta} \sum_{k,n} \int_{-\epsilon_F}^{\infty} d\epsilon N(\epsilon) \left[\frac{-(\Delta_S + \Delta_{SDW})}{2[\omega_n^2 - \epsilon_k^2 - (\Delta_S + \Delta_{SDW})^2]} - \frac{(\Delta_S - \Delta_{SDW})}{2[\omega^2 - \epsilon_k^2 - (\Delta_S - \Delta_{SDW})^2]} \right]$$

Attractive interaction is effective for the region $-\hbar\omega_b < \epsilon < \hbar\omega_b$, Assuming the density of states doesn't vary over this integral. Then the expression becomes;

$$\Delta_S = 2N(\epsilon) \frac{V}{\beta} \sum_{k,n} \int_0^{\hbar\omega_b} d\epsilon \left[\frac{-(\Delta_S + \Delta_{SDW})}{2[\omega_n^2 - \epsilon_k^2 - (\Delta_S + \Delta_{SDW})^2]} - \frac{(\Delta_S - \Delta_{SDW})}{2[\omega^2 - \epsilon_k^2 - (\Delta_S - \Delta_{SDW})^2]} \right]$$

Now changing $\omega \longrightarrow \omega_n$, and using the Matsubara frequency; $\omega_n = \frac{(2n+1)\pi}{\beta}$, $\omega_n^2 = -\frac{(2n+1)^2\pi^2}{\beta^2}$;

$$2\Delta_S = 2N(0) \frac{V}{\beta} \sum_n \int_0^{\hbar\omega_b} d\epsilon \left[\frac{-(\Delta_S + \Delta_{SDW})}{\left[-\frac{(2n+1)^2\pi^2}{\beta^2} - \epsilon_k^2 - (\Delta_S + \Delta_{SDW})^2 \right]} \right]$$

$$-2N(0) \frac{V}{\beta} \sum_n \int_0^{\hbar\omega_b} d\epsilon \left[\frac{-(\Delta_S - \Delta_{SDW})}{\left[-\frac{(2n+1)^2\pi^2}{\beta^2} - \epsilon_k^2 - (\Delta_S - \Delta_{SDW})^2 \right]} \right]$$

Let $\tilde{E}_1^2 = \epsilon_k^2 + (\Delta_S + \Delta_{SDW})^2$, and $\tilde{E}_2^2 = \epsilon_k^2 + (\Delta_S - \Delta_{SDW})^2$ therefore;

$$2\Delta_S = 2N(0)V\beta \sum_n \int_0^{\hbar\omega_b} d\epsilon \left[\frac{(\Delta_S + \Delta_{SDW})}{\left[(2n+1)^2\pi^2 + \beta^2\tilde{E}_1^2 \right]} + \frac{(\Delta_S - \Delta_{SDW})}{\left[(2n+1)^2\pi^2 + \beta^2\tilde{E}_2^2 \right]} \right]$$

Using the relation ;

$$\frac{\tanh\left(\frac{x}{2}\right)}{2x} = \sum_n \frac{1}{(2n+1)^2\pi^2 + x^2}$$

So We can rewrite the above equation as follows ,Where $x = \beta\tilde{E}$ and $x = \beta\tilde{E}_2$

$$2\Delta_S = 2N(0)V\beta \sum_n \int_0^{\hbar\omega_b} d\epsilon \left\{ (\Delta_S + \Delta_{SDW}) \frac{\tanh\left(\frac{\beta\tilde{E}_1}{2}\right)}{2\beta\tilde{E}_1} + (\Delta_S - \Delta_{SDW}) \frac{\tanh\left(\frac{\beta\tilde{E}_2}{2}\right)}{2\beta\tilde{E}_2} \right\}$$

Let $N(0)V = \lambda$;

$$\begin{aligned} \frac{2\Delta_S}{\lambda} = & \sum_n \int_0^{\hbar\omega_b} d\epsilon \left\{ \left[\frac{\Delta_S + \Delta_{SDW}}{\sqrt{\epsilon_k^2 + (\Delta_S + \Delta_{SDW})^2}} \right] \tanh\left(\frac{\beta\sqrt{\epsilon_k^2 + (\Delta_S + \Delta_{SDW})^2}}{2}\right) \right\} \\ & + \left\{ \left[\frac{\Delta_S - \Delta_{SDW}}{\sqrt{\epsilon_k^2 + (\Delta_S - \Delta_{SDW})^2}} \right] \tanh\left(\frac{\beta\sqrt{\epsilon_k^2 + (\Delta_S - \Delta_{SDW})^2}}{2}\right) \right\} \end{aligned} \quad (4.2.53)$$

Let us study the above equation for the case $T \rightarrow T_C$

As $T \rightarrow T_C$, $\Delta_S \rightarrow 0$

Using equation (4.2.53),

$$\begin{aligned} \frac{2}{\lambda} = & \int_0^{\hbar\omega_b} d\epsilon \left[\frac{\left(1 + \frac{\Delta_{SDW}}{\Delta_S}\right)}{\sqrt{\epsilon_k^2 + (\Delta_S + \Delta_{SDW})^2}} \right] \tanh\left(\frac{\beta\sqrt{\epsilon_k^2 + (\Delta_S + \Delta_{SDW})^2}}{2}\right) \\ & + \int_0^{\hbar\omega_b} d\epsilon \left[\frac{\left(1 - \frac{\Delta_{SDW}}{\Delta_S}\right)}{\sqrt{\epsilon_k^2 + (\Delta_S - \Delta_{SDW})^2}} \right] \tanh\left(\frac{\beta\sqrt{\epsilon_k^2 + (\Delta_S - \Delta_{SDW})^2}}{2}\right) \end{aligned} \quad (4.2.54)$$

$$\text{let, } \frac{2}{\lambda} = I + L \quad (4.2.55)$$

Where

$$\begin{aligned} I = & \int_0^{\hbar\omega_b} d\epsilon \left[\frac{\left(1 + \frac{\Delta_{SDW}}{\Delta_S}\right)}{\sqrt{\epsilon_k^2 + (\Delta_S + \Delta_{SDW})^2}} \tanh\left(\frac{\beta\sqrt{\epsilon_k^2 + (\Delta_S + \Delta_{SDW})^2}}{2}\right) \right] \\ L = & \int_0^{\hbar\omega_b} d\epsilon \left[\frac{\left(1 - \frac{\Delta_{SDW}}{\Delta_S}\right)}{\sqrt{\epsilon_k^2 + (\Delta_S - \Delta_{SDW})^2}} \tanh\left(\frac{\beta\sqrt{\epsilon_k^2 + (\Delta_S - \Delta_{SDW})^2}}{2}\right) \right] \end{aligned}$$

LET US SOLVE FOR I

$$\begin{aligned}
I &= \int_0^{\hbar\omega_b} d\epsilon \left[\frac{1}{\sqrt{\epsilon_k^2 + (\Delta_S + \Delta_{SDW})^2}} \right] \tanh \left\{ \frac{\beta \sqrt{\epsilon_k^2 + (\Delta_S + \Delta_{SDW})^2}}{2} \right\} \\
&+ \int_0^{\hbar\omega_b} d\epsilon \left[\frac{\Delta_{SDW}}{\Delta_S \sqrt{\epsilon_k^2 + (\Delta_S - \Delta_{SDW})^2}} \right] \tanh \left\{ \frac{\beta \sqrt{\epsilon_k^2 + (\Delta_S + \Delta_{SDW})^2}}{2} \right\} \quad (4.2.56)
\end{aligned}$$

At $T = T_C, \Delta_S = 0$

The first integral of equation (4.2.56) can be calculated as follows using the relation, $\tanh\left(\frac{x}{2}\right) = \sum_n \frac{1}{(2n+1)^2\pi^2 + x^2}$, where $\omega_n = \frac{(2n+1)\pi}{\beta}$

For $\Delta_S = 0$

$$\begin{aligned}
&\int_0^{\hbar\omega_b} d\epsilon \left[\frac{1}{\sqrt{\epsilon_k^2 + \Delta_{SDW}^2}} \right] \tanh \left\{ \frac{\beta \sqrt{\epsilon_k^2 + \Delta_{SDW}^2}}{2} \right\} \\
&= \int_0^{\hbar\omega_b} d\epsilon \frac{2}{\beta} \sum_{n=-\infty}^{\infty} \frac{1}{\omega_n^2 + \epsilon_k^2 + \Delta_{SDW}^2} \quad (4.2.57)
\end{aligned}$$

Using Laplace's transform and Matsubara frequency, $\omega_n = \frac{(2n+1)\pi}{\beta}$, the above integral becomes;

$$\begin{aligned}
&= \int_0^{\hbar\omega_b} d\epsilon \frac{2}{\beta} \sum_{n=-\infty}^{\infty} \frac{1}{\omega_n^2 + \epsilon^2} - \int_0^{\hbar\omega_b} \Delta_{SDW}^2 d\epsilon \frac{2}{\beta} \sum_{n=-\infty}^{\infty} \frac{1}{(\omega_n^2 + \epsilon^2)^2} + \dots \\
&= \int_0^{\hbar\omega_b} d\epsilon \frac{\tanh\left(\frac{\beta\epsilon}{2}\right)}{\epsilon} - \int_0^{\hbar\omega_b} \Delta_{SDW}^2 d\epsilon \frac{2}{\beta} \sum_{n=-\infty}^{\infty} \frac{1}{\left\{ \left(\frac{(2n+1)\pi}{\beta} \right)^2 + \epsilon^2 \right\}^2} + \dots
\end{aligned}$$

But the sum becomes;

$$\sum_{n=-\infty}^{\infty} \frac{1}{\left\{ \left(\frac{(2n+1)\pi}{\beta} \right)^2 + \epsilon^2 \right\}^2} = 2 \sum_{n=0}^{\infty} \frac{1}{\left\{ \left(\frac{(2n+1)\pi}{\beta} \right)^2 + \epsilon^2 \right\}^2}$$

And from the expression;

$$2 \sum_{n=0}^{\infty} \frac{1}{(a^2 + \epsilon^2)^2} = 2 \sum_{n=0}^{\infty} \frac{1}{a^4 \left(1 + \frac{\epsilon^2}{a^2} \right)^2} = 2 \sum_{n=0}^{\infty} \frac{1}{a^4 (1 + x^2)^2}$$

Where,

$$x^2 = \frac{\epsilon^2}{a^2} \quad a = \frac{(2n+1)\pi}{\beta}$$

Then,

$$\begin{aligned} & \int_0^{\hbar\omega_b} d\epsilon \left[\frac{1}{\sqrt{\epsilon_k^2 + \Delta_{SDW}^2}} \right] \tanh \left\{ \frac{\beta\sqrt{\epsilon_k^2 + \Delta_{SDW}^2}}{2} \right\} \\ &= \int_0^{\hbar\omega_b} d\epsilon \frac{\tanh\left(\frac{\beta\epsilon}{2}\right)}{\epsilon} - \int_0^{\hbar\omega_b} \Delta_{SDW}^2 d\epsilon \frac{2}{\beta} \sum_{n=0}^{\infty} \frac{1}{a^4 (1+x^2)^2} \end{aligned}$$

Let

$$\begin{aligned} I_1 &= \int_0^{\hbar\omega_b} d\epsilon \frac{\tanh\left(\frac{\beta\epsilon}{2}\right)}{\epsilon} \\ I_2 &= - \int_0^{\hbar\omega_b} \Delta_{SDW}^2 d\epsilon \frac{4}{\beta} \sum_{n=0}^{\infty} \frac{1}{a^4 (1+x^2)^2} \end{aligned}$$

Now let us evaluate I_1 ;

$$I_1 = \int_0^{\hbar\omega_b} d\epsilon \frac{\tanh\left(\frac{\beta\epsilon}{2}\right)}{\epsilon}$$

Let $Y = \frac{\beta\epsilon}{2}$ and $d\epsilon = \frac{2}{\beta}dY$

$$\begin{aligned} I_1 &= \int_0^y d\epsilon \frac{\tanh y}{y} \\ &= \ln y \tanh y \Big|_0^y - \int_0^y \frac{\ln y}{\text{Cosh}^2 y} dy \end{aligned}$$

At low temperature, $\tanh y = \tanh\left(\frac{\hbar\omega}{2k_B T}\right) \rightarrow 1$

$$I_1 = \ln y - \ln\left(\frac{\pi}{4}\right)e^{-c}$$

$$I_1 = \ln y - \ln\left(\frac{\pi}{4\gamma}\right)$$

Where γ is the Euler's constant. $\gamma = 1.78$

$$I_1 = \ln 1.13 \left(\frac{\hbar\omega_b}{k_B T_C} \right) \quad (4.2.58)$$

For the second integral I_2 , i.e;

$$I_2 = - \int_0^{\hbar\omega_b} \Delta_{SDW}^2 d\epsilon \frac{4}{\beta} \sum_{n=0}^{\infty} \frac{1}{a^4 (1+x^2)^2}$$

Where $x^2 = \frac{\epsilon^2}{a^2}$, $x = \frac{\epsilon}{a}$, $d\epsilon = a dx$, $a^2 = \left(\frac{(2n+1)\pi}{\beta} \right)^2$

$$I_2 = -\frac{4\Delta_{SDW}^2}{\beta} \sum_{n=0}^{\infty} \frac{1}{a^4} \int_0^{\hbar\omega_b} a dx \frac{1}{(1+x^2)^2} + \dots$$

$$I_2 = -\frac{4\Delta_{SDW}^2}{\beta} \sum_{n=0}^{\infty} \frac{1}{a^3} \int_0^{\hbar\omega_b} dx \frac{1}{(1+x^2)^2} + \dots$$

But, $a^3 = \left(\frac{(2n+1)\pi}{\beta} \right)^3$

$$I_2 = -4\Delta_{SDW}^2 \sum_{n=0}^{\infty} \frac{\beta^2}{[(2n+1)\pi]^3} \int_0^{\hbar\omega_b} \frac{1}{(1+x^2)^2} dx + \dots$$

$$I_2 = -\frac{4\beta^2\Delta_{SDW}^2}{\pi^3} \sum_{n=0}^{\infty} \frac{1}{[2n+1]^3} \int_0^{\hbar\omega_b} \frac{1}{(1+x^2)^2} dx + \dots$$

From the laws series and Zeta function;

$$I_2 = -\left\{ \frac{4\beta^2\Delta_{SDW}^2}{\pi^3} \right\} \left\{ \frac{7}{8}\zeta(3) \right\} \left\{ \frac{\pi}{4} \right\}$$

Where ζ is Zeta function; and

$$\int_0^{\hbar\omega_b} \frac{1}{(1+x^2)^2} dx = \frac{\pi}{4}, \sum_{n=0}^{\infty} \frac{1}{[2n+1]^p} = (1-2^{-p})\zeta(p),$$

So,

$$\sum_{n=0}^{\infty} \frac{1}{[2n+1]^3} = \frac{7}{8}\zeta(3); \zeta(3) = 1.202$$

Therefore,

$$I_2 = -\left(\frac{\Delta_{SDW}}{\pi k_B T_C} \right)^2 \frac{8.414}{8} \quad (4.2.59)$$

Therefore equation (4.2.57) becomes the sum of equation (4.2.58) and (4.2.59) i.e;

$$\begin{aligned} \int_0^{\hbar\omega_b} d\epsilon \left[\frac{1}{\sqrt{\epsilon_k^2 + \Delta_{SDW}^2}} \right] \tanh \left\{ \frac{\beta\sqrt{\epsilon_k^2 + \Delta_{SDW}^2}}{2} \right\} &= I_1 + I_2 \\ &= \ln 1.13 \left(\frac{\hbar\omega_b}{2k_B T_C} \right) - \left(\frac{\Delta_{SDW}}{\pi k_B T_C} \right)^2 \frac{8.414}{8} \end{aligned} \quad (4.2.60)$$

\implies The second integral of equation (4.2.56) becomes;

$$I_3 = \int_0^{\hbar\omega_b} d\epsilon \left[\frac{\Delta_{SDW}}{\Delta_S \sqrt{\epsilon_k^2 + (\Delta_S + \Delta_{SDW})^2}} \right] \tanh \left\{ \frac{\beta\sqrt{\epsilon_k^2 + (\Delta_S + \Delta_{SDW})^2}}{2} \right\}$$

Applying l'Hopital's rule

$$\begin{aligned}
&= \int_0^{\hbar\omega_b} \lim_{\Delta_S \rightarrow 0} \left\{ \frac{d}{d\Delta_S} \left(d\epsilon \left[\frac{\Delta_{SDW}}{\Delta_S \sqrt{\epsilon_k^2 + (\Delta_S + \Delta_{SDW})^2}} \tanh \frac{\beta \sqrt{\epsilon_k^2 + (\Delta_S + \Delta_{SDW})^2}}{2} \right] \right) \right\} \\
&\quad \frac{d}{d\Delta_S} \left(\tanh \left(\frac{\beta \sqrt{\epsilon_k^2 + (\Delta_S + \Delta_{SDW})^2}}{2} \right) \right) \\
&= \text{Sech}^2 \left\{ \frac{\beta \sqrt{\epsilon_k^2 + (\Delta_S + \Delta_{SDW})^2}}{2} \right\} \left\{ \frac{\beta (\Delta_S + \Delta_{SDW})}{2 \sqrt{\epsilon_k^2 + (\Delta_S + \Delta_{SDW})^2}} \right\}
\end{aligned}$$

And

$$\frac{d}{d\Delta_S} \left(\Delta_S \sqrt{\epsilon_k^2 + (\Delta_S + \Delta_{SDW})^2} \right) = \sqrt{\epsilon_k^2 + (\Delta_S + \Delta_{SDW})^2} + \Delta_S \left\{ \frac{2\beta (\Delta_S + \Delta_{SDW})}{2 \sqrt{\epsilon_k^2 + (\Delta_S + \Delta_{SDW})^2}} \right\}$$

Substituting the above derivatives in (I_3) yields;

$$\begin{aligned}
I_3 &= \int_0^{\hbar\omega_b} \lim_{\Delta_S \rightarrow 0} \left\{ \frac{d\epsilon \Delta_{SDW} \frac{\text{Sech}^2 \left\{ \frac{\beta \sqrt{\epsilon_k^2 + (\Delta_S + \Delta_{SDW})^2}}{2} \right\} \left\{ \frac{\beta (\Delta_S + \Delta_{SDW})}{2 \sqrt{\epsilon_k^2 + (\Delta_S + \Delta_{SDW})^2}} \right\}}{\sqrt{\epsilon_k^2 + (\Delta_S + \Delta_{SDW})^2} + \Delta_S \left\{ \frac{2\beta (\Delta_S + \Delta_{SDW})}{2 \sqrt{\epsilon_k^2 + (\Delta_S + \Delta_{SDW})^2}} \right\}} \right\} \\
I_3 &= \int_0^{\hbar\omega_b} d\epsilon \frac{\Delta_{SDW}^2 \beta \text{Sech}^2 \frac{\beta}{2} \sqrt{\epsilon_k^2 + \Delta_{SDW}^2}}{2(\epsilon_k^2 + \Delta_{SDW}^2)} \tag{4.2.61}
\end{aligned}$$

Therefore combining equations (4.2.60) and (4.2.61) gives;

$$I = \ln 1.13 \left(\frac{\hbar\omega_b}{2k_B T} \right) - \left(\frac{\Delta_{SDW}}{\pi k_B T_C} \right)^2 \frac{8.414}{8} + \int_0^{\hbar\omega_b} d\epsilon \frac{\Delta_{SDW}^2 \beta \text{Sech}^2 \left(\frac{\beta}{2} \sqrt{\epsilon_k^2 + \Delta_{SDW}^2} \right)}{2(\epsilon_k^2 + \Delta_{SDW}^2)} \tag{4.2.62}$$

Using the relation $\Rightarrow \text{Sech}^2 x = 1 - \tanh^2 x$

$$\begin{aligned}
I &= \ln 1.13 \left(\frac{\hbar\omega_b}{2k_B T_C} \right) - \Delta_{SDW}^2 \left(\frac{1}{\pi k_B T_C} \right)^2 \frac{8.414}{8} + \int_0^{\hbar\omega_b} d\epsilon \frac{\Delta_{SDW}^2}{2k_B T_C (\epsilon_k^2 + \Delta_{SDW}^2)} \\
&\quad - \int_0^{\hbar\omega_b} d\epsilon \frac{\Delta_{SDW}^2 \tanh^2 \left(\frac{\beta}{2} \sqrt{\epsilon_k^2 + \Delta_{SDW}^2} \right)}{2k_B T_C (\epsilon_k^2 + \Delta_{SDW}^2)} \tag{4.2.63}
\end{aligned}$$

From the integral of special functions and the help of FORTRAN language;

$$\int_0^{\hbar\omega_b} d\epsilon \frac{\Delta_{SDW}^2}{2k_B T_C (\epsilon_k^2 + \Delta_{SDW}^2)} = \frac{\Delta_{SDW}^2}{2k_B T_C} \arctan \left(\frac{\hbar\omega_b}{\Delta_{SDW}} \right)$$

$$= \frac{\Delta_{SDW}}{4k_B T_C} \ln \left| \frac{\hbar\omega_b + \Delta_{SDW}}{\hbar\omega_b - \Delta_{SDW}} \right| \quad (4.2.64)$$

Similarly, let us solve for L

$$L = \left[\frac{\left(1 - \frac{\Delta_{SDW}}{\Delta_S}\right)}{\sqrt{\epsilon_k^2 + (\Delta_S - \Delta_{SDW})^2}} \tanh\left(\frac{\beta\sqrt{\epsilon_k^2 + (\Delta_S - \Delta_{SDW})^2}}{2}\right) \right]$$

$$L = \int_0^{\hbar\omega_b} d\epsilon \left[\frac{1}{\sqrt{\epsilon_k^2 - (\Delta_S - \Delta_{SDW})^2}} \right] \tanh\left\{ \frac{\beta\sqrt{\epsilon_k^2 + (\Delta_S - \Delta_{SDW})^2}}{2} \right\}$$

$$- \int_0^{\hbar\omega_b} d\epsilon \left[\frac{\Delta_{SDW}}{\Delta_S \sqrt{\epsilon_k^2 + (\Delta_S - \Delta_{SDW})^2}} \right] \tanh\left\{ \frac{\beta\sqrt{\epsilon_k^2 + (\Delta_S - \Delta_{SDW})^2}}{2} \right\} \quad (4.2.65)$$

At $T = T_C, \Delta_S = 0$

The first integral of equation (4.2.65) can be calculated by applying the previous method;

For $\Delta_S = 0$

$$\int_0^{\hbar\omega_b} d\epsilon \left[\frac{1}{\sqrt{\epsilon_k^2 + \Delta_{SDW}^2}} \right] \tanh\left\{ \frac{\beta\sqrt{\epsilon_k^2 + \Delta_{SDW}^2}}{2} \right\}$$

$$= \int_0^{\hbar\omega_b} d\epsilon \frac{2}{\beta} \sum_{n=-\infty}^{\infty} \frac{1}{\omega_n^2 + \epsilon_k^2 + \Delta_{SDW}^2} \quad (4.2.66)$$

Since, $\frac{\tanh(\frac{x}{2})}{2x} = \sum_n \frac{1}{(2n+1)^2\pi^2 + x^2}$, where $\omega_n = \frac{(2n+1)\pi}{\beta}$

Using Laplace's transform and Matsubara frequency, $\omega_n = \frac{(2n+1)\pi}{\beta}$, the above integral becomes;

$$= \int_0^{\hbar\omega_b} d\epsilon \frac{2}{\beta} \sum_{n=-\infty}^{\infty} \frac{1}{\omega_n^2 + \epsilon^2} - \int_0^{\hbar\omega_b} \Delta_{SDW}^2 d\epsilon \frac{2}{\beta} \sum_{n=-\infty}^{\infty} \frac{1}{(\omega_n^2 + \epsilon^2)^2} + \dots$$

$$= \int_0^{\hbar\omega_b} d\epsilon \frac{\tanh\left(\frac{\beta\epsilon}{2}\right)}{\epsilon} - \int_0^{\hbar\omega_b} \Delta_{SDW}^2 d\epsilon \frac{2}{\beta} \sum_{n=-\infty}^{\infty} \frac{1}{\left\{ \left(\frac{(2n+1)\pi}{\beta} \right)^2 + \epsilon^2 \right\}^2} + \dots$$

But the sum becomes;

$$\sum_{n=-\infty}^{\infty} \frac{1}{\left\{ \left(\frac{(2n+1)\pi}{\beta} \right)^2 + \epsilon^2 \right\}^2} = 2 \sum_{n=0}^{\infty} \frac{1}{\left\{ \left(\frac{(2n+1)\pi}{\beta} \right)^2 + \epsilon^2 \right\}^2}$$

And from the expression;

$$2 \sum_{n=0}^{\infty} \frac{1}{(a^2 + \epsilon^2)^2} = 2 \sum_{n=0}^{\infty} \frac{1}{a^4 \left(1 + \frac{\epsilon^2}{a^2}\right)^2} = 2 \sum_{n=0}^{\infty} \frac{1}{a^4 (1 + x^2)^2}$$

Where,

$$x^2 = \frac{\epsilon^2}{a^2}, \quad a = \frac{(2n+1)\pi}{\beta}$$

Then,

$$\begin{aligned} & \int_0^{\hbar\omega_b} d\epsilon \left[\frac{1}{\sqrt{\epsilon_k^2 + \Delta_{SDW}^2}} \right] \tanh \left\{ \frac{\beta \sqrt{\epsilon_k^2 + \Delta_{SDW}^2}}{2} \right\} \\ &= \int_0^{\hbar\omega_b} d\epsilon \frac{\tanh\left(\frac{\beta\epsilon}{2}\right)}{\epsilon} - \int_0^{\hbar\omega_b} \Delta_{SDW}^2 d\epsilon \frac{2}{\beta} 2 \sum_{n=0}^{\infty} \frac{1}{a^4 (1 + x^2)^2} \end{aligned}$$

Let

$$\begin{aligned} L_1 &= \int_0^{\hbar\omega_b} d\epsilon \frac{\tanh\left(\frac{\beta\epsilon}{2}\right)}{\epsilon} \\ L_2 &= - \int_0^{\hbar\omega_b} \Delta_{SDW}^2 d\epsilon \frac{4}{\beta} \sum_{n=0}^{\infty} \frac{1}{a^4 (1 + x^2)^2} \end{aligned}$$

The value of L_1 and L_2 can be obtained using the method that we have used previously to solve equation I (from page 49-51);Then we have

$$L_1 = \ln 1.13 \left(\frac{\hbar\omega_b}{k_B T_C} \right) \quad (4.2.67)$$

$$L_2 = - \left(\frac{\Delta_{SDW}}{\pi k_B T_C} \right)^2 \frac{8.414}{8} \quad (4.2.68)$$

Therefore equation (4.2.66) becomes the sum of equation (4.2.67) and (4.2.68)i.e;

$$\begin{aligned} & \int_0^{\hbar\omega_b} d\epsilon \left[\frac{1}{\sqrt{\epsilon_k^2 + \Delta_{SDW}^2}} \right] \tanh \left\{ \frac{\beta \sqrt{\epsilon_k^2 + \Delta_{SDW}^2}}{2} \right\} = L_1 + L_2 \\ &= \ln 1.13 \left(\frac{\hbar\omega_b}{k_B T_C} \right) - \left(\frac{\Delta_{SDW}}{\pi k_B T_C} \right)^2 \frac{8.414}{8} \end{aligned} \quad (4.2.69)$$

\implies The second integral of equation (4.2.65) becomes;

$$L_3 = - \int_0^{\hbar\omega_b} d\epsilon \left[\frac{\Delta_{SDW}}{\Delta_S \sqrt{\epsilon_k^2 + (\Delta_S - \Delta_{SDW})^2}} \right] \tanh \left\{ \frac{\beta \sqrt{\epsilon_k^2 + (\Delta_S - \Delta_{SDW})^2}}{2} \right\}$$

Applying l'Hopital's rule

$$\begin{aligned}
L_3 &= - \int_0^{\hbar\omega_b} \lim_{\Delta_S \rightarrow 0} \left\{ \frac{d}{d\Delta_S} \left(d\epsilon \left[\frac{\Delta_{SDW}}{\Delta_S \sqrt{\epsilon_k^2 + (\Delta_S - \Delta_{SDW})^2}} \tanh \frac{\beta \sqrt{\epsilon_k^2 + (\Delta_S - \Delta_{SDW})^2}}{2} \right] \right) \right\} \\
&\quad \frac{d}{d\Delta_S} \left(\tanh \left(\frac{\beta \sqrt{\epsilon_k^2 + (\Delta_S - \Delta_{SDW})^2}}{2} \right) \right) \\
&= \text{Sech}^2 \left\{ \frac{\beta \sqrt{\epsilon_k^2 + (\Delta_S - \Delta_{SDW})^2}}{2} \right\} \left\{ \frac{\beta (\Delta_S - \Delta_{SDW})}{2 \sqrt{\epsilon_k^2 + (\Delta_S - \Delta_{SDW})^2}} \right\}
\end{aligned}$$

And

$$\frac{d}{d\Delta_S} \left(\Delta_S \sqrt{\epsilon_k^2 + (\Delta_S - \Delta_{SDW})^2} \right) = \sqrt{\epsilon_k^2 + (\Delta_S - \Delta_{SDW})^2} - \Delta_S \left\{ \frac{2\beta (\Delta_S - \Delta_{SDW})}{2 \sqrt{\epsilon_k^2 + (\Delta_S - \Delta_{SDW})^2}} \right\}$$

Substituting the above derivatives in equation (L_3) yields;

$$\begin{aligned}
L_3 &= \int_0^{\hbar\omega_b} \lim_{\Delta_S \rightarrow 0} \left\{ \frac{d\epsilon \Delta_{SDW} \frac{\text{Sech}^2 \left\{ \frac{\beta \sqrt{\epsilon_k^2 + (\Delta_S - \Delta_{SDW})^2}}{2} \right\} \left\{ \frac{\beta (\Delta_S - \Delta_{SDW})}{2 \sqrt{\epsilon_k^2 + (\Delta_S - \Delta_{SDW})^2}} \right\}}{\sqrt{\epsilon_k^2 + (\Delta_S - \Delta_{SDW})^2} + \Delta_S \left\{ \frac{2\beta (\Delta_S - \Delta_{SDW})}{2 \sqrt{\epsilon_k^2 + (\Delta_S - \Delta_{SDW})^2}} \right\}} \right\} \\
L_3 &= \int_0^{\hbar\omega_b} d\epsilon \frac{\Delta_{SDW}^2 \beta \text{Sech}^2 \frac{\beta}{2} \sqrt{\epsilon_k^2 + \Delta_{SDW}^2}}{2(\epsilon_k^2 + \Delta_{SDW}^2)} \tag{4.2.70}
\end{aligned}$$

Therefore combining equations (4.2.69) and (4.2.70) gives;

$$L = \ln 1.13 \left(\frac{\hbar\omega_b}{k_B T} \right) - \left(\frac{\Delta_{SDW}}{\pi k_B T_C} \right)^2 \frac{8.414}{8} + \int_0^{\hbar\omega_b} d\epsilon \frac{\Delta_{SDW}^2 \beta \text{Sech}^2 \left(\frac{\beta}{2} \sqrt{\epsilon_k^2 + \Delta_{SDW}^2} \right)}{2(\epsilon_k^2 + \Delta_{SDW}^2)} \tag{4.2.71}$$

Using the relation $\implies \text{Sech}^2 x = 1 - \tanh^2 x$

$$\begin{aligned}
L &= \ln 1.13 \left(\frac{\hbar\omega_b}{k_B T_C} \right) - \Delta_{SDW}^2 \left(\frac{1}{\pi k_B T_C} \right)^2 \frac{8.414}{8} + \int_0^{\hbar\omega_b} d\epsilon \frac{\Delta_{SDW}^2}{2k_B T_C (\epsilon_k^2 + \Delta_{SDW}^2)} \\
&\quad - \int_0^{\hbar\omega_b} d\epsilon \frac{\Delta_{SDW}^2 \tanh^2 \left(\frac{\beta}{2} \sqrt{\epsilon_k^2 + \Delta_{SDW}^2} \right)}{2k_B T_C (\epsilon_k^2 + \Delta_{SDW}^2)} \tag{4.2.72}
\end{aligned}$$

From the integral of special functions and the help of FORTRAN language;

$$\int_0^{\hbar\omega_b} d\epsilon \frac{\Delta_{SDW}^2}{2k_B T_C (\epsilon_k^2 + \Delta_{SDW}^2)} = \frac{\Delta_{SDW}^2}{2k_B T_C} \arctan \left(\frac{\hbar\omega_b}{\Delta_{SDW}} \right)$$

$$= \frac{\Delta_{SDW}}{4k_B T_C} \ln \left| \frac{\hbar\omega_b + \Delta_{SDW}}{\hbar\omega_b - \Delta_{SDW}} \right| \quad (4.2.73)$$

since, $\frac{2}{\lambda} = I + L$

Using equation(4.2.63) and (4.2.72) we have,

$$\begin{aligned} \frac{2}{\lambda} = & 2 \ln 1.13 \left(\frac{\hbar\omega_b}{k_B T_C} \right) - 2\Delta_{SDW}^2 \left(\frac{1}{\pi k_B T_C} \right)^2 \frac{8.414}{8} + 2 \int_0^{\hbar\omega_b} d\epsilon \frac{\Delta_{SDW}^2}{2k_B T_C (\epsilon_k^2 + \Delta_{SDW}^2)} \\ & - 2 \int_0^{\hbar\omega_b} d\epsilon \frac{\Delta_{SDW}^2 \tanh^2 \left(\frac{\beta}{2} \sqrt{\epsilon_k^2 + \Delta_{SDW}^2} \right)}{2k_B T_C (\epsilon_k^2 + \Delta_{SDW}^2)} \end{aligned} \quad (4.2.74)$$

Using equation (4.2.73), equation (4.2.74) can be written as;

$$\begin{aligned} \frac{1}{\lambda} = & \ln 1.13 \left(\frac{\hbar\omega_b}{k_B T} \right) + \frac{\Delta_{SDW}}{4k_B T_C} \ln \left| \frac{\Delta_{SDW} + \hbar\omega_b}{\Delta_{SDW} - \hbar\omega_b} \right| \\ & - \Delta_{SDW}^2 \left(\frac{1}{\pi k_B T_C} \right)^2 \frac{8.414}{8} - \int_0^{\hbar\omega_b} d\epsilon \frac{\Delta_{SDW}^2 \tanh^2 \left(\frac{\beta}{2} \sqrt{\epsilon_k^2 + \Delta_{SDW}^2} \right)}{2k_B T_C (\epsilon_k^2 + \Delta_{SDW}^2)} \end{aligned} \quad (4.2.75)$$

Let

$$a = \frac{1}{4k_B T_C} \ln \left| \frac{\Delta_{SDW} + \hbar\omega_b}{\Delta_{SDW} - \hbar\omega_b} \right| \quad m = \left(\frac{1}{\pi k_B T_C} \right)^2 \frac{8.414}{8}$$

$$n = \int_0^{\hbar\omega_b} d\epsilon \frac{\tanh^2 \left(\frac{\beta}{2} \sqrt{\epsilon_k^2 + \Delta_{SDW}^2} \right)}{2k_B T_C (\epsilon_k^2 + \Delta_{SDW}^2)}$$

$$\frac{1}{\lambda} = \ln 1.13 \left(\frac{\hbar\omega_b}{2k_B T} \right) + a\Delta_{SDW} - m\Delta_{SDW}^2 - n\Delta_{SDW}^2 \quad (4.2.76)$$

$$\left(\frac{1}{\lambda} + m\Delta_{SDW}^2 + n\Delta_{SDW}^2 - a\Delta_{SDW} \right) = \ln 1.13 \left(\frac{\hbar\omega_b}{2k_B T_C} \right)$$

$$k_B T_C = 1.13 \hbar\omega_b \exp - \left(\frac{1}{\lambda} + m\Delta_{SDW}^2 + n\Delta_{SDW}^2 - a\Delta_{SDW} \right)$$

$$k_B T_C = 1.13 \hbar\omega_b e^{- \left(\frac{1}{\lambda} + m\Delta_{SDW}^2 + n\Delta_{SDW}^2 - a\Delta_{SDW} \right)} \quad (4.2.77)$$

4.2.2 For the spin density wave order parameter and temperature

From equation (4.2.52) we have;

$$\langle\langle C_{k+Q\downarrow}, C_{k\uparrow}^\dagger \rangle\rangle = \frac{(\Delta_S + \Delta_{SDW})}{2[\omega^2 - \epsilon_k^2 - (\Delta_S + \Delta_{SDW})^2]} + \frac{(\Delta_{SDW} - \Delta_S)}{2[\omega^2 - \epsilon_k^2 - (\Delta_S - \Delta_{SDW})^2]}$$

Where Δ_S is the superconducting order parameter (analogous to the BCS order parameter) and Δ_{SDW} is the magnetic order parameter.

Using the relation for Δ_{SDW} i.e;

$$\Delta_{SDW} = \frac{U}{\beta} \sum_{k,n} \langle\langle C_{k+Q\downarrow}, C_{k\uparrow}^\dagger \rangle\rangle$$

And the sum may be changed in to an integral by introducing the density of states, $N(\epsilon)$,

$$\frac{1}{U} \sum_k \longrightarrow \frac{1}{(2\pi)^3} \int d^3k = \int_{-E_F}^{\infty} d\epsilon N(\epsilon)$$

The summation with respect to k and n extends over all allowed pair states. Therefore;

$$\Delta_{SDW} = \frac{U}{\beta} \sum_{k,n} \int_{-\epsilon_F}^{\infty} d\epsilon N(\epsilon) \left[\frac{(\Delta_S + \Delta_{SDW})}{2[\omega_n^2 - \epsilon_k^2 - (\Delta_S + \Delta_{SDW})^2]} - \frac{(\Delta_S - \Delta_{SDW})}{2[\omega_n^2 - \epsilon_k^2 - (\Delta_S - \Delta_{SDW})^2]} \right]$$

Attractive interaction is effective for the region $-\hbar\omega_b < \epsilon < \hbar\omega_b$ Assuming the density of states doesn't vary over this integral. Then the expression becomes;

$$\Delta_{SDW} = 2N(\epsilon) \frac{u}{\beta} \sum_{k,n} \int_0^{\hbar\omega_b} d\epsilon \left[\frac{(\Delta_S + \Delta_{SDW})}{2[\omega_n^2 - \epsilon_k^2 - (\Delta_S + \Delta_{SDW})^2]} - \frac{(\Delta_S - \Delta_{SDW})}{2[\omega_n^2 - \epsilon_k^2 - (\Delta_S - \Delta_{SDW})^2]} \right]$$

Now changing $\omega \longrightarrow \omega_n$, and using the Matsubara frequency; $\omega_n = \frac{(2n+1)\pi}{\beta}$, $\omega_n^2 = -\frac{(2n+1)^2\pi^2}{\beta^2}$

and the relation ;

$$\frac{\tanh\left(\frac{x}{2}\right)}{2x} = \sum_n \frac{1}{(2n+1)^2\pi^2 + x^2}$$

$$2\Delta_{SDW} = 2N(0)U\beta \sum_n \int_0^{\hbar\omega_b} d\epsilon \left\{ -(\Delta_S + \Delta_{SDW}) \frac{\tanh\left(\frac{\beta\tilde{E}_1}{2}\right)}{2\beta\tilde{E}_1} + (\Delta_S - \Delta_{SDW}) \frac{\tanh\left(\frac{\beta\tilde{E}_2}{2}\right)}{2\beta\tilde{E}_2} \right\}$$

Where, $\tilde{E}_1^2 = \epsilon_k^2 + (\Delta_S + \Delta_{SDW})^2$, and $\tilde{E}_2^2 = \epsilon_k^2 + (\Delta_S - \Delta_{SDW})^2$

Let $N(0)U = \lambda_1$;

$$\begin{aligned} \frac{2\Delta_{SDW}}{\lambda_1} &= \sum_n \int_0^{\hbar\omega_b} d\epsilon \left\{ \left[\frac{-(\Delta_S + \Delta_{SDW})}{\sqrt{\epsilon_k^2 + (\Delta_S + \Delta_{SDW})^2}} \right] \tanh\left(\frac{\beta\sqrt{\epsilon_k^2 + (\Delta_S + \Delta_{SDW})^2}}{2}\right) \right\} \\ &+ \int_0^{\hbar\omega_b} d\epsilon \left\{ \left[\frac{\Delta_S - \Delta_{SDW}}{\sqrt{\epsilon_k^2 + (\Delta_S - \Delta_{SDW})^2}} \right] \tanh\left(\frac{\beta\sqrt{\epsilon_k^2 + (\Delta_S - \Delta_{SDW})^2}}{2}\right) \right\} \end{aligned} \quad (4.2.78)$$

Let us study the above equation for the case $T \rightarrow T_{SDW}$

As $T \rightarrow T_{SDW}$, $\Delta_{SDW} \rightarrow 0$

Using equation (4.2.78),

$$\begin{aligned} \frac{2\Delta_{SDW}}{\lambda_1} &= \sum_n \int_0^{\hbar\omega_b} d\epsilon \left\{ \left[\frac{-(\Delta_S + \Delta_{SDW})}{\sqrt{\epsilon_k^2 + (\Delta_S + \Delta_{SDW})^2}} \right] \tanh\left(\frac{\beta\sqrt{\epsilon_k^2 + (\Delta_S + \Delta_{SDW})^2}}{2}\right) \right\} \\ &+ \int_0^{\hbar\omega_b} d\epsilon \left\{ \left[\frac{\Delta_S - \Delta_{SDW}}{\sqrt{\epsilon_k^2 + (\Delta_S - \Delta_{SDW})^2}} \right] \tanh\left(\frac{\beta\sqrt{\epsilon_k^2 + (\Delta_S - \Delta_{SDW})^2}}{2}\right) \right\} \\ \frac{2}{\lambda_1} &= \int_0^{\hbar\omega_b} d\epsilon \left[\frac{-\left(1 + \frac{\Delta_S}{\Delta_{SDW}}\right)}{\sqrt{\epsilon_k^2 + (\Delta_S + \Delta_{SDW})^2}} \right] \tanh\left(\frac{\beta\sqrt{\epsilon_k^2 + (\Delta_S + \Delta_{SDW})^2}}{2}\right) \\ &- \int_0^{\hbar\omega_b} d\epsilon \left[\frac{\left(1 - \frac{\Delta_S}{\Delta_{SDW}}\right)}{\sqrt{\epsilon_k^2 + (\Delta_S - \Delta_{SDW})^2}} \right] \tanh\left(\frac{\beta\sqrt{\epsilon_k^2 + (\Delta_S - \Delta_{SDW})^2}}{2}\right) \end{aligned} \quad (4.2.79)$$

$$\text{Let, } \frac{2}{\lambda} = I + R \quad (4.2.80)$$

Where

$$\begin{aligned} I &= \int_0^{\hbar\omega_b} d\epsilon \left[\frac{-\left(1 + \frac{\Delta_S}{\Delta_{SDW}}\right)}{\sqrt{\epsilon_k^2 + (\Delta_S + \Delta_{SDW})^2}} \tanh\left(\frac{\beta\sqrt{\epsilon_k^2 + (\Delta_S + \Delta_{SDW})^2}}{2}\right) \right] \\ R &= - \int_0^{\hbar\omega_b} d\epsilon \left[\frac{\left(1 - \frac{\Delta_S}{\Delta_{SDW}}\right)}{\sqrt{\epsilon_k^2 + (\Delta_S - \Delta_{SDW})^2}} \tanh\left(\frac{\beta\sqrt{\epsilon_k^2 + (\Delta_S - \Delta_{SDW})^2}}{2}\right) \right] \end{aligned}$$

LET US SOLVE FOR I

$$I = - \int_0^{\hbar\omega_b} d\epsilon \left[\frac{1}{\sqrt{\epsilon_k^2 + (\Delta_S + \Delta_{SDW})^2}} \right] \tanh \left\{ \frac{\beta \sqrt{\epsilon_k^2 + (\Delta_S + \Delta_{SDW})^2}}{2} \right\} \\ - \int_0^{\hbar\omega_b} d\epsilon \left[\frac{\Delta_S}{\Delta_{SDW} \sqrt{\epsilon_k^2 + (\Delta_S + \Delta_{SDW})^2}} \right] \tanh \left\{ \frac{\beta \sqrt{\epsilon_k^2 + (\Delta_S + \Delta_{SDW})^2}}{2} \right\} \quad (4.2.81)$$

Where

$$I = - \int_0^{\hbar\omega_b} d\epsilon \left[\frac{1}{\sqrt{\epsilon_k^2 + (\Delta_S + \Delta_{SDW})^2}} \right] \tanh \left\{ \frac{\beta \sqrt{\epsilon_k^2 + (\Delta_S + \Delta_{SDW})^2}}{2} \right\} \\ I_3 = - \int_0^{\hbar\omega_b} d\epsilon \left[\frac{\Delta_S}{\Delta_{SDW} \sqrt{\epsilon_k^2 + (\Delta_S - \Delta_{SDW})^2}} \right] \tanh \left\{ \frac{\beta \sqrt{\epsilon_k^2 + (\Delta_S - \Delta_{SDW})^2}}{2} \right\}$$

At $T = T_{SDW}$, $\Delta_{SDW} = 0$

Let us solve for I ;

$$I = - \int_0^{\hbar\omega_b} d\epsilon \left[\frac{1}{\sqrt{\epsilon_k^2 + (\Delta_S + \Delta_{SDW})^2}} \right] \tanh \left\{ \frac{\beta \sqrt{\epsilon_k^2 + (\Delta_S + \Delta_{SDW})^2}}{2} \right\}$$

For $\Delta_{SDW} = 0$

$$I_1 = - \int_0^{\hbar\omega_b} d\epsilon \left[\frac{1}{\sqrt{\epsilon_k^2 + \Delta_S^2}} \right] \tanh \left\{ \frac{\beta \sqrt{\epsilon_k^2 + \Delta_S^2}}{2} \right\} \\ = - \int_0^{\hbar\omega_b} d\epsilon \frac{2}{\beta} \sum_{n=-\infty}^{\infty} \frac{1}{\omega_n^2 + \epsilon_k^2 + \Delta_S^2}$$

Since, $\tilde{E}^2 = \epsilon_k^2 + (\Delta_S + \Delta_{SDW})^2$ and $\frac{\tanh(\frac{x}{2})}{2x} = \sum_n \frac{1}{(2n+1)^2\pi^2 + x^2}$, where $\omega_n = \frac{(2n+1)\pi}{\beta}$

Using Laplace's transform and Matsubara frequency, $\omega_n = \frac{(2n+1)\pi}{\beta}$, the above integral becomes;

$$= - \left(\int_0^{\hbar\omega_b} d\epsilon \frac{2}{\beta} \sum_{n=-\infty}^{\infty} \frac{1}{\omega_n^2 + \epsilon^2} - \int_0^{\hbar\omega_b} \Delta_S^2 d\epsilon \frac{2}{\beta} \sum_{n=-\infty}^{\infty} \frac{1}{(\omega_n^2 + \epsilon^2)^2} + \dots \right) \\ = - \left(\int_0^{\hbar\omega_b} d\epsilon \frac{\tanh(\frac{\beta\epsilon}{2})}{\epsilon} - \int_0^{\hbar\omega_b} \Delta_S^2 d\epsilon \frac{2}{\beta} \sum_{n=-\infty}^{\infty} \frac{1}{\left\{ \left(\frac{(2n+1)\pi}{\beta} \right)^2 + \epsilon^2 \right\}^2} + \dots \right)$$

But the sum becomes;

$$\sum_{n=-\infty}^{\infty} \frac{1}{\left\{ \left(\frac{(2n+1)\pi}{\beta} \right)^2 + \epsilon^2 \right\}^2} = 2 \sum_{n=0}^{\infty} \frac{1}{\left\{ \left(\frac{(2n+1)\pi}{\beta} \right)^2 + \epsilon^2 \right\}^2}$$

And from the expression;

$$2 \sum_{n=0}^{\infty} \frac{1}{(a^2 + \epsilon^2)^2} = 2 \sum_{n=0}^{\infty} \frac{1}{a^4 \left(1 + \frac{\epsilon^2}{a^2} \right)^2} = 2 \sum_{n=0}^{\infty} \frac{1}{a^4 (1 + x^2)^2}$$

Where,

$$x^2 = \frac{\epsilon^2}{a^2} \quad a = \frac{(2n+1)\pi}{\beta}$$

Then,

$$\begin{aligned} & - \int_0^{\hbar\omega_b} d\epsilon \left[\frac{1}{\sqrt{\epsilon_k^2 + \Delta_S^2}} \right] \tanh \left\{ \frac{\beta \sqrt{\epsilon_k^2 + \Delta_S^2}}{2} \right\} \\ &= - \left(\int_0^{\hbar\omega_b} d\epsilon \frac{\tanh\left(\frac{\beta\epsilon}{2}\right)}{\epsilon} - \int_0^{\hbar\omega_b} \Delta_S^2 d\epsilon \frac{2}{\beta} 2 \sum_{n=0}^{\infty} \frac{1}{a^4 (1 + x^2)^2} \right) \end{aligned}$$

Let

$$\begin{aligned} I_1 &= - \int_0^{\hbar\omega_b} d\epsilon \frac{\tanh\left(\frac{\beta\epsilon}{2}\right)}{\epsilon} \\ I_2 &= \int_0^{\hbar\omega_b} \Delta_S^2 d\epsilon \frac{4}{\beta} \sum_{n=0}^{\infty} \frac{1}{a^4 (1 + x^2)^2} \end{aligned}$$

By Applying the method we have used previously we can obtain the value of I_1 and I_2 .

Therefore;

$$I_1 = - \ln 1.13 \left(\frac{\hbar\omega_b}{k_B T_{SDW}} \right) \quad (4.2.82)$$

$$I_2 = \left(\frac{\Delta_S}{\pi k_B T_C} \right)^2 \frac{8.414}{8} \quad (4.2.83)$$

Therefore combining equation (4.2.82) and (4.2.83)i.e;

$$- \int_0^{\hbar\omega_b} d\epsilon \left[\frac{1}{\sqrt{\epsilon_k^2 + \Delta_S^2}} \right] \tanh \left\{ \frac{\beta \sqrt{\epsilon_k^2 + \Delta_S^2}}{2} \right\} = I_1 + I_2$$

$$I = -\ln 1.13 \left(\frac{\hbar\omega_b}{k_B T} \right) + \left(\frac{\Delta_S}{\pi k_B T_C} \right)^2 \frac{8.414}{8} \quad (4.2.84)$$

\implies The second integral of equation (4.2.81) becomes;

$$I_3 = - \int_0^{\hbar\omega_b} d\epsilon \left[\frac{\Delta_S}{\Delta_{SDW} \sqrt{\epsilon_k^2 + (\Delta_S + \Delta_{SDW})^2}} \right] \tanh \left\{ \frac{\beta \sqrt{\epsilon_k^2 + (\Delta_S + \Delta_{SDW})^2}}{2} \right\}$$

Applying l'Hopital's rule

$$\begin{aligned} I_3 &= - \int_0^{\hbar\omega_b} \lim_{\Delta_{SDW} \rightarrow 0} \left\{ \frac{d}{d\Delta_{SDW}} \left(d\epsilon \left[\frac{\Delta_S}{\Delta_{SDW} \sqrt{\epsilon_k^2 + (\Delta_S + \Delta_{SDW})^2}} \tanh \frac{\beta \sqrt{\epsilon_k^2 + (\Delta_S + \Delta_{SDW})^2}}{2} \right] \right) \right\} \\ &= \frac{d}{d\Delta_{SDW}} \left(\tanh \left(\frac{\beta \sqrt{\epsilon_k^2 + (\Delta_S + \Delta_{SDW})^2}}{2} \right) \right) \\ &= \text{Sech}^2 \left\{ \frac{\beta \sqrt{\epsilon_k^2 + (\Delta_S + \Delta_{SDW})^2}}{2} \right\} \left\{ \frac{\beta (\Delta_S + \Delta_{SDW})}{2 \sqrt{\epsilon_k^2 + (\Delta_S + \Delta_{SDW})^2}} \right\} \end{aligned}$$

And

$$\frac{d}{d\Delta_{SDW}} \left(\Delta_S \sqrt{\epsilon_k^2 + (\Delta_S + \Delta_{SDW})^2} \right) = \sqrt{\epsilon_k^2 + (\Delta_S + \Delta_{SDW})^2} + \Delta_{SDW} \left\{ \frac{2\beta (\Delta_S + \Delta_{SDW})}{2 \sqrt{\epsilon_k^2 + (\Delta_S + \Delta_{SDW})^2}} \right\}$$

Substituting the above derivatives in equation (I_3) yields;

$$\begin{aligned} I_3 &= - \int_0^{\hbar\omega_b} \lim_{\Delta_{SDW} \rightarrow 0} \left\{ \frac{\text{Sech}^2 \left\{ \frac{\beta \sqrt{\epsilon_k^2 + (\Delta_S + \Delta_{SDW})^2}}{2} \right\} \left\{ \frac{\beta (\Delta_S + \Delta_{SDW})}{2 \sqrt{\epsilon_k^2 + (\Delta_S + \Delta_{SDW})^2}} \right\}}{\sqrt{\epsilon_k^2 + (\Delta_S + \Delta_{SDW})^2} + \Delta_{SDW} \left\{ \frac{2\beta (\Delta_S + \Delta_{SDW})}{2 \sqrt{\epsilon_k^2 + (\Delta_S + \Delta_{SDW})^2}} \right\}} \right\} \\ I_3 &= - \int_0^{\hbar\omega_b} d\epsilon \frac{\Delta_S^2 \beta \text{Sech}^2 \frac{\beta}{2} \sqrt{\epsilon_k^2 + \Delta_S^2}}{2(\epsilon_k^2 + \Delta_S^2)} \quad (4.2.85) \end{aligned}$$

Therefore combining equations (4.2.84) and (4.2.85) gives;

$$I = -\ln 1.13 \left(\frac{\hbar\omega_b}{k_B T_{SDW}} \right) + \left(\frac{\Delta_S}{\pi k_B T_{SDW}} \right)^2 \frac{8.414}{8} - \int_0^{\hbar\omega_b} d\epsilon \frac{\Delta_S^2 \beta \text{Sech}^2 \left(\frac{\beta}{2} \sqrt{\epsilon_k^2 + \Delta_S^2} \right)}{2(\epsilon_k^2 + \Delta_S^2)} \quad (4.2.86)$$

Using the relation $\implies \text{Sech}^2 x = 1 - \tanh^2 x$

$$I = -\ln 1.13 \left(\frac{\hbar\omega_b}{2k_B T_{SDW}} \right) + \Delta_S^2 \left(\frac{1}{\pi k_B T_{SDW}} \right)^2 \frac{8.414}{8} - \int_0^{\hbar\omega_b} d\epsilon \frac{\Delta_S^2}{2k_B T_{SDW} (\epsilon_k^2 + \Delta_S^2)}$$

$$+ \int_0^{\hbar\omega_b} d\epsilon \frac{\Delta_S^2 \tanh^2 \left(\frac{\beta}{2} \sqrt{\epsilon_k^2 + \Delta_S^2} \right)}{2k_B T_{SDW} (\epsilon_k^2 + \Delta_S^2)} \quad (4.2.87)$$

From the integral of special functions and the help of FORTRAN language;

$$\begin{aligned} \int_0^{\hbar\omega_b} d\epsilon \frac{\Delta_S^2}{2k_B T_{SDW} (\epsilon^2 + \Delta_S^2)} &= \frac{\Delta_S^2}{2k_B T_{SDW}} \arctan\left(\frac{\hbar\omega_b}{\Delta_S}\right) \\ &= \frac{\Delta_S}{4k_B T_C} \ln \left| \frac{\hbar\omega_b + \Delta_S}{\hbar\omega_b - \Delta_S} \right| \end{aligned} \quad (4.2.88)$$

Similarly, let us solve for R

$$\begin{aligned} R &= - \int_0^{\hbar\omega_b} d\epsilon \left[\frac{\left(1 - \frac{\Delta_S}{\Delta_{SDW}}\right)}{\sqrt{\epsilon_k^2 + (\Delta_S - \Delta_{SDW})^2}} \tanh\left(\frac{\beta\sqrt{\epsilon_k^2 + (\Delta_S - \Delta_{SDW})^2}}{2}\right) \right] \\ &= - \int_0^{\hbar\omega_b} d\epsilon \left[\frac{1}{\sqrt{\epsilon_k^2 - (\Delta_S - \Delta_{SDW})^2}} \right] \tanh \left\{ \frac{\beta\sqrt{\epsilon_k^2 + (\Delta_S - \Delta_{SDW})^2}}{2} \right\} \\ &+ \int_0^{\hbar\omega_b} d\epsilon \left[\frac{\Delta_S}{\Delta_{SDW} \sqrt{\epsilon_k^2 + (\Delta_S - \Delta_{SDW})^2}} \right] \tanh \left\{ \frac{\beta\sqrt{\epsilon_k^2 + (\Delta_S - \Delta_{SDW})^2}}{2} \right\} \end{aligned} \quad (4.2.89)$$

At $T = T_{SDW}$, $\Delta_{SDW} = 0$

The first integral of equation (4.2.89) will be;

$$= - \int_0^{\hbar\omega_b} d\epsilon \left[\frac{1}{\sqrt{\epsilon_k^2 + (\Delta_S - \Delta_{SDW})^2}} \right] \tanh \left\{ \frac{\beta\sqrt{\epsilon_k^2 + (\Delta_S - \Delta_{SDW})^2}}{2} \right\}$$

For $\Delta_{SDW} = 0$

$$\begin{aligned} &= - \int_0^{\hbar\omega_b} d\epsilon \left[\frac{1}{\sqrt{\epsilon_k^2 + \Delta_S^2}} \right] \tanh \left\{ \frac{\beta\sqrt{\epsilon_k^2 + \Delta_S^2}}{2} \right\} \\ &= - \int_0^{\hbar\omega_b} d\epsilon \frac{2}{\beta} \sum_{n=-\infty}^{\infty} \frac{1}{\omega_n^2 + \epsilon_k^2 + \Delta_S^2} \end{aligned} \quad (4.2.90)$$

Since, $\tilde{E}_2^2 = \epsilon_k^2 + (\Delta_S - \Delta_{SDW})^2$ and $\frac{\tanh\left(\frac{x}{2}\right)}{2x} = \sum_n \frac{1}{(2n+1)^2\pi^2 + x^2}$, where $\omega_n = \frac{(2n+1)\pi}{\beta}$

Using Laplace's transform and Matsubara frequency, $\omega_n = \frac{(2n+1)\pi}{\beta}$, the above integral

becomes;

$$= - \left(\int_0^{\hbar\omega_b} d\epsilon \frac{2}{\beta} \sum_{n=-\infty}^{\infty} \frac{1}{\omega_n^2 + \epsilon^2} - \int_0^{\hbar\omega_b} \Delta_S^2 d\epsilon \frac{2}{\beta} \sum_{n=-\infty}^{\infty} \frac{1}{(\omega_n^2 + \epsilon^2)^2} + \dots \right)$$

$$= - \left(\int_0^{\hbar\omega_b} d\epsilon \frac{\tanh(\frac{\beta\epsilon}{2})}{\epsilon} - \int_0^{\hbar\omega_b} \Delta_S^2 d\epsilon \frac{2}{\beta} \sum_{n=-\infty}^{\infty} \frac{1}{\left\{ \left(\frac{(2n+1)\pi}{\beta} \right)^2 + \epsilon^2 \right\}^2} + \dots \right)$$

But the sum becomes;

$$\sum_{n=-\infty}^{\infty} \frac{1}{\left\{ \left(\frac{(2n+1)\pi}{\beta} \right)^2 + \epsilon^2 \right\}^2} = 2 \sum_{n=0}^{\infty} \frac{1}{\left\{ \left(\frac{(2n+1)\pi}{\beta} \right)^2 + \epsilon^2 \right\}^2}$$

And from the expression;

$$2 \sum_{n=0}^{\infty} \frac{1}{(a^2 + \epsilon^2)^2} = 2 \sum_{n=0}^{\infty} \frac{1}{a^4 \left(1 + \frac{\epsilon^2}{a^2} \right)^2} = 2 \sum_{n=0}^{\infty} \frac{1}{a^4 (1 + x^2)^2}$$

Where,

$$x^2 = \frac{\epsilon^2}{a^2} \quad a = \frac{(2n+1)\pi}{\beta}$$

Then,

$$\begin{aligned} & - \int_0^{\hbar\omega_b} d\epsilon \left[\frac{1}{\sqrt{\epsilon_k^2 + \Delta_S^2}} \right] \tanh \left\{ \frac{\beta \sqrt{\epsilon_k^2 + \Delta_S^2}}{2} \right\} \\ &= - \int_0^{\hbar\omega_b} d\epsilon \frac{\tanh(\frac{\beta\epsilon}{2})}{\epsilon} + \int_0^{\hbar\omega_b} \Delta_S^2 d\epsilon \frac{2}{\beta} 2 \sum_{n=0}^{\infty} \frac{1}{a^4 (1 + x^2)^2} \end{aligned}$$

Let

$$\begin{aligned} R_1 &= - \int_0^{\hbar\omega_b} d\epsilon \frac{\tanh(\frac{\beta\epsilon}{2})}{\epsilon} \\ R_2 &= \int_0^{\hbar\omega_b} \Delta_S^2 d\epsilon \frac{4}{\beta} \sum_{n=0}^{\infty} \frac{1}{a^4 (1 + x^2)^2} \end{aligned}$$

Applying similar method as we have done previously;

$$R_1 = - \ln 1.13 \left(\frac{\hbar\omega_b}{k_B T_{SDW}} \right) \quad (4.2.91)$$

$$R_2 = \left(\frac{\Delta_S}{\pi k_B T_C} \right)^2 \frac{8.414}{8} \quad (4.2.92)$$

Therefore equation (4.2.90) becomes the sum of equations (4.2.91) and (4.2.92)i.e;

$$\begin{aligned} - \int_0^{\hbar\omega_b} d\epsilon \left[\frac{1}{\sqrt{\epsilon_k^2 + \Delta_S^2}} \right] \tanh \left\{ \frac{\beta\sqrt{\epsilon_k^2 + \Delta_S^2}}{2} \right\} &= R_1 + R_2 \\ &= -\ln 1.13 \left(\frac{\hbar\omega_b}{k_B T} \right) + \left(\frac{\Delta_S}{\pi k_B T_C} \right)^2 \frac{8.414}{8} \end{aligned} \quad (4.2.93)$$

\implies The second integral of equation (4.2.89) becomes;

$$R_3 = \int_0^{\hbar\omega_b} d\epsilon \left[\frac{\Delta_S}{\Delta_{SDW} \sqrt{\epsilon_k^2 + (\Delta_S - \Delta_{SDW})^2}} \right] \tanh \left\{ \frac{\beta\sqrt{\epsilon_k^2 + (\Delta_S - \Delta_{SDW})^2}}{2} \right\}$$

Applying l'Hopital's rule

$$\begin{aligned} R_3 &= \int_0^{\hbar\omega_b} \lim_{\Delta_{SDW} \rightarrow 0} \left\{ \frac{d}{d\Delta_{SDW}} \left(d\epsilon \left[\frac{\Delta_S}{\Delta_{SDW} \sqrt{\epsilon_k^2 + (\Delta_S - \Delta_{SDW})^2}} \tanh \frac{\beta\sqrt{\epsilon_k^2 + (\Delta_S - \Delta_{SDW})^2}}{2} \right] \right) \right\} \\ &\quad \frac{d}{d\Delta_{SDW}} \left(\tanh \left(\frac{\beta\sqrt{\epsilon_k^2 + (\Delta_S - \Delta_{SDW})^2}}{2} \right) \right) \\ &= \text{Sech}^2 \left\{ \frac{\beta\sqrt{\epsilon_k^2 + (\Delta_S - \Delta_{SDW})^2}}{2} \right\} \left\{ \frac{-\beta(\Delta_S - \Delta_{SDW})}{2\sqrt{\epsilon_k^2 + (\Delta_S - \Delta_{SDW})^2}} \right\} \end{aligned}$$

And

$$\begin{aligned} &\frac{d}{d\Delta_{SDW}} \left(\Delta_{SDW} \sqrt{\epsilon_k^2 + (\Delta_S - \Delta_{SDW})^2} \right) \\ &= \sqrt{\epsilon_k^2 + (\Delta_S - \Delta_{SDW})^2} - \Delta_{SDW} \left\{ \frac{-2\beta(\Delta_S - \Delta_{SDW})}{2\sqrt{\epsilon_k^2 + (\Delta_S - \Delta_{SDW})^2}} \right\} \end{aligned}$$

Rearranging yields;

$$\begin{aligned} R_3 &= \int_0^{\hbar\omega_b} \lim_{\Delta_{SDW} \rightarrow 0} \left\{ d\epsilon \Delta_S \frac{\text{Sech}^2 \left\{ \frac{\beta\sqrt{\epsilon_k^2 + (\Delta_S - \Delta_{SDW})^2}}{2} \right\} \left\{ \frac{-\beta(\Delta_S - \Delta_{SDW})}{2\sqrt{\epsilon_k^2 + (\Delta_S - \Delta_{SDW})^2}} \right\}}{\sqrt{\epsilon_k^2 + (\Delta_S - \Delta_{SDW})^2} + \Delta_{SDW} \left\{ \frac{-2\beta(\Delta_S - \Delta_{SDW})}{2\sqrt{\epsilon_k^2 + (\Delta_S - \Delta_{SDW})^2}} \right\}} \right\} \\ R_3 &= - \int_0^{\hbar\omega_b} d\epsilon \frac{\Delta_S^2 \beta \text{Sech}^2 \frac{\beta}{2} \sqrt{\epsilon_k^2 + \Delta_S^2}}{2(\epsilon_k^2 + \Delta_S^2)} \end{aligned} \quad (4.2.94)$$

Therefore combining the result of the first and the second integral (4.2.93) and (4.2.94)

respectively) gives;

$$R = -\ln 1.13 \left(\frac{\hbar\omega_b}{2k_B T} \right) + \left(\frac{\Delta_S}{\pi k_B T_C} \right)^2 \frac{8.414}{8} - \int_0^{\hbar\omega_b} d\epsilon \frac{\Delta_S^2 \beta \text{Sech}^2 \left(\frac{\beta}{2} \sqrt{\epsilon_k^2 + \Delta_S^2} \right)}{2(\epsilon_k^2 + \Delta_S^2)}$$

Using the relation $\implies \text{Sech}^2 x = 1 - \tanh^2 x$

$$R = -\ln 1.13 \left(\frac{\hbar\omega_b}{2k_B T_{SDW}} \right) + \Delta_S^2 \left(\frac{1}{\pi k_B T_{SDW}} \right)^2 \frac{8.414}{8} - \int_0^{\hbar\omega_b} d\epsilon \frac{\Delta_S^2}{2k_B T_C (\epsilon_k^2 + \Delta_S^2)} + \int_0^{\hbar\omega_b} d\epsilon \frac{\Delta_S^2 \tanh^2 \left(\frac{\beta}{2} \sqrt{\epsilon_k^2 + \Delta_S^2} \right)}{2k_B T_{SDW} (\epsilon_k^2 + \Delta_S^2)} \quad (4.2.95)$$

From the integral of special functions and the help of FORTRAN language;

$$\int_0^{\hbar\omega_b} d\epsilon \frac{\Delta_S^2}{2k_B T_{SDW} (\epsilon^2 + \Delta_S^2)} = \frac{\Delta_S^2}{2k_B T_{SDW}} \arctan \left(\frac{\hbar\omega_b}{\Delta_S} \right) = \frac{\Delta_S}{4k_B T_{SDW}} \ln \left| \frac{\hbar\omega_b + \Delta_S}{\hbar\omega_b - \Delta_S} \right| \quad (4.2.96)$$

since, $\frac{2}{\lambda_1} = I + R$

Using equations 4.2.87 and 4.2.95, we have;

$$-\frac{2}{\lambda_1} = 2 \ln 1.13 \left(\frac{\hbar\omega_b}{2k_B T_{SDW}} \right) - 2\Delta_S^2 \left(\frac{1}{\pi k_B T_{SDW}} \right)^2 \frac{8.414}{8} + 2 \int_0^{\hbar\omega_b} d\epsilon \frac{\Delta_S^2}{2k_B T_{SDW} (\epsilon_k^2 + \Delta_S^2)} - 2 \int_0^{\hbar\omega_b} d\epsilon \frac{\Delta_S^2 \tanh^2 \left(\frac{\beta}{2} \sqrt{\epsilon_k^2 + \Delta_S^2} \right)}{2k_B T_{SDW} (\epsilon_k^2 + \Delta_S^2)}$$

Generally;

$$-\frac{1}{\lambda_1} = \ln 1.13 \left(\frac{\hbar\omega_b}{2k_B T_{SDW}} \right) - \Delta_S^2 \left(\frac{1}{\pi k_B T_{SDW}} \right)^2 \frac{8.414}{8} + \frac{\Delta_S}{4k_B T_{SDW}} \ln \left| \frac{\hbar\omega_b + \Delta_S}{\hbar\omega_b - \Delta_S} \right| - \int_0^{\hbar\omega_b} d\epsilon \frac{\Delta_S^2 \tanh^2 \left(\frac{\beta}{2} \sqrt{\epsilon_k^2 + \Delta_S^2} \right)}{2k_B T_{SDW} (\epsilon_k^2 + \Delta_S^2)} \quad (4.2.97)$$

Let;

$$X = \frac{1}{4k_B T_{SDW}} \ln \left| \frac{\hbar\omega_b + \Delta_S}{\hbar\omega_b - \Delta_S} \right| \quad Y = \int_0^{\hbar\omega_b} d\epsilon \frac{\tanh^2 \left(\frac{\beta}{2} \sqrt{\epsilon_k^2 + \Delta_S^2} \right)}{2k_B T_{SDW} (\epsilon_k^2 + \Delta_S^2)}$$

$$Z = \left(\frac{1}{\pi k_B T_{SDW}} \right)^2 \frac{8.414}{8}$$

$$-\frac{1}{\lambda_1} = \ln 1.13 \left(\frac{\hbar\omega_b}{k_B T_{SDW}} \right) - \Delta_S^2 Z + \Delta_S X - \Delta_S^2 Y$$

$$\begin{aligned}
-\frac{1}{\lambda_1} + \Delta_S^2 Z + \Delta_S^2 Y - \Delta_S X &= \ln 1.13 \left(\frac{\hbar\omega_b}{k_B T_{SDW}} \right) \\
k_B T_{SDW} &= 1.13 \hbar\omega_b e^{\left(\frac{1}{\lambda_1} - \Delta_S^2 Z - \Delta_S^2 Y + \Delta_S X \right)}
\end{aligned} \tag{4.2.98}$$

4.2.3 For pure superconducting state

For pure superconducting system ($\Delta_{SDW} = 0$ or magnetic effect is zero), We can ignore the Δ_{SDW} term from equation(4.2.53), we get,

$$\frac{\Delta_S}{\lambda} = \int_0^\infty \frac{\Delta_S \tanh\left(\frac{\beta\sqrt{\epsilon_k^2 + \Delta_S^2}}{2}\right)}{\sqrt{\epsilon_k^2 + \Delta_S^2}} d\epsilon_k \tag{4.2.99}$$

To obtain temperature dependent of energy gap of equation(4.2.99).we used the same technique to solve the first equation ,

$$\begin{aligned}
\frac{1}{\lambda} &= \int_0^\infty \frac{\tanh\left(\frac{\beta\sqrt{\epsilon_k^2 + \Delta^2}}{2}\right)}{\sqrt{\epsilon_k^2 + \Delta^2}} d\epsilon_k \\
\frac{1}{\lambda} &= \ln\left(1.13 \frac{\hbar\omega_b}{k_B T_c}\right) - \left(\frac{\Delta}{\pi k_B T}\right)^2 \frac{8.414}{8}
\end{aligned}$$

From BCS at $T = T_C$, $\frac{1}{\lambda} = \ln\left(1.13 \frac{\hbar\omega_b}{k_B T_c}\right)$

$$\ln\left(\frac{T}{T_c}\right) = -\Delta^2 \left(\frac{1}{\pi k_B T}\right)^2 \frac{8.414}{8}$$

Using $\ln(1-x) = -x - \frac{x^2}{2} - \dots$

$$\ln\left(\frac{T}{T_c}\right) = \ln\left(1 - \left(1 - \frac{T}{T_c}\right)\right) = -\left(1 - \frac{T}{T_c}\right)$$

$$-\left(1 - \frac{T}{T_c}\right) = -\Delta^2 \left(\frac{1}{\pi k_B T}\right)^2 \frac{8.414}{8}$$

$$\frac{(\pi k_B T_c)^2}{1.05175} \left(1 - \frac{T}{T_c}\right) = \Delta^2$$

$$10.3353 T_c^2 \left(1 - \frac{T}{T_c}\right) = \Delta^2$$

$$\Delta(T) = 3.21 T_c \left(1 - \frac{T}{T_c}\right)^{\frac{1}{2}} \tag{4.2.100}$$

4.2.4 For pure SDW State

For pure SDW system ($\Delta_S = 0$) we can ignore the Δ_S term from equation (4.2.78).we get;

$$\frac{2\Delta_{SDW}}{\lambda_1} = -2 \int_0^\infty \frac{\Delta_{SDW} \tanh\left(\frac{\beta \sqrt{\epsilon_k^2 + \Delta_{SDW}^2}}{2}\right)}{\sqrt{\epsilon_k^2 + \Delta_{SDW}^2}} d\epsilon_k \quad (4.2.101)$$

$$\frac{-1}{\lambda_1} = \int_0^\infty \frac{\tanh\left(\frac{\beta \sqrt{\epsilon_k^2 + \Delta_{SDW}^2}}{2}\right)}{\sqrt{\epsilon_k^2 + \Delta_{SDW}^2}} d\epsilon_k$$

For the case, $T \rightarrow T_{SDW}$, $\Delta_{SDW} \rightarrow 0$

$$\frac{-1}{\lambda_1} = \int_0^\infty \frac{\tanh\left(\frac{\beta}{2}\epsilon\right)}{\epsilon} d\epsilon$$

Let, $x = \frac{\epsilon}{2k_B T_{SDW}}$ since $\beta = \frac{1}{k_B T_{SDW}}$

$$\frac{-1}{\lambda_1} = \int_0^\infty \frac{\tanh(x)}{x} dx$$

Integrating as we have done previously gives,

$$\frac{-1}{\lambda_1} = \ln\left(1.13 \frac{\hbar\omega_b}{k_B T_{SDW}}\right)$$

Then,

$$k_B T_{SDW} = 1.13 \hbar\omega_b e^{\frac{1}{\lambda_1}}$$

$$T_{SDW} = 1.13 \theta_D e^{\frac{1}{\lambda_1}} \quad (4.2.102)$$

Where $\theta_D = \frac{\hbar\omega_b}{k_B}$

Chapter 5

Results and Discussions

The interplay between the Sc and SDW state is mainly studied by self consistently solving the gap equations with fixed set of parameters. Two distinct set of results are obtained. *i)* The superconducting transition temperatures (T_C) as a function of magnetic order parameter (Δ_{SDW}) and *ii)* The magnetic ordering temperature (T_{SDW}) as a function of superconducting order parameter (Δ_S). Furthermore, in computing the self self consistent solutions of equations for the cases $\Delta_S = 0$ and $\Delta_{SDW} = 0$, pure SC and pure SDW states are also obtained.

The magnetically ordered state of some materials vanish abruptly with the appearance of superconductivity, in others superconductivity emerges precisely as the magnetic order is destroyed, and still others exhibit coexistence between the magnetically ordered and superconducting states. This issue of phase coexistence in doped, $LaFeAsO_{1-x}F_x$, $Ba(Fe_{1-x}Co_x)_2As_2$ and $Fe_{1.03}Te_{1-x}Se_x$ has been most carefully examined in this paper. The transition temperatures T_C and T_{SDW} has been calculated numerically as a function of order parameters using equations (4.2.78) and (4.2.98) respectively, assuming constant density of states around Fermi level with cut off energies $\hbar\omega_b$. Taking $\hbar\omega_b = 0.0862\text{ev}$.

To map out the phase boundary between the SDW and SC phases, we first calculate $T_C(\Delta_{SDW})$ which is determined using equation (4.2.77). We consider the cases $\lambda_S = 0.2, 0.26,$ and 0.28 for doped compounds, $LaFeAsO_{1-x}F_x, Ba(Fe_{1-x}Co_x)_2As_2$ and $Fe_{1.03}Te_{1-x}Se_x$ respectively and corresponding $T_C(\Delta_{SDW})$ are shown in fig.(5.3).

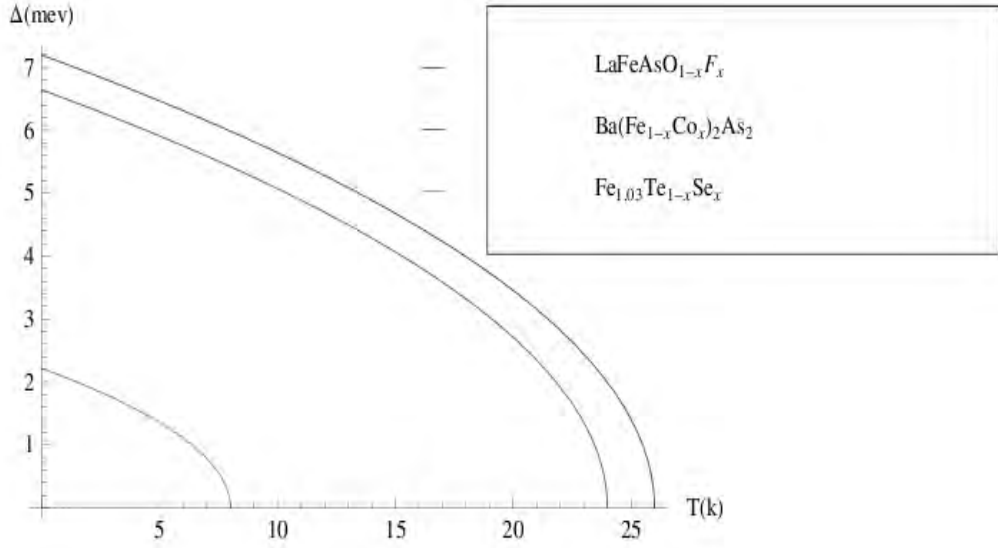


Figure 5.1: A graph of energy gap (Δ) Vs Temperature(T) for doped $LaFeAsO_{1-x}F_x$ (Blue color), $Ba(Fe_{1-x}Co_x)_2As_2$ (Red color) and $Fe_{1.03}Te_{1-x}Se_x$ (Yellow color)

$T_{SDW}(\Delta_S)$ is also calculated numerically using equation (4.2.98) considering $\lambda_M = 0.47, 0.48$ and 0.35 for doped compounds , $LaFeAsO_{1-x}F_x, Ba(Fe_{1-x}Co_x)_2As_2$ and $Fe_{1.03}Te_{1-x}Se_x$ respectively and corresponding $T_C(\Delta_{SDW})$ are shown in fig.(5.4).The computation of $T_C(\Delta_{SDW})$ and $T_{SDW}(\Delta_S)$ yields that; Both temperatures decreases with the increase of the order parameters.

Now we will discuss the results of our model calculations. The expression we get for pure superconductors (equation 4.2.134) are similar with BCS expression and it is clear that the energy gap (Δ) which is the measure of pairing energy, decreases with increasing temperatures (T) until it vanishes at transition temperature (T_C) as shown in fig (5.1).

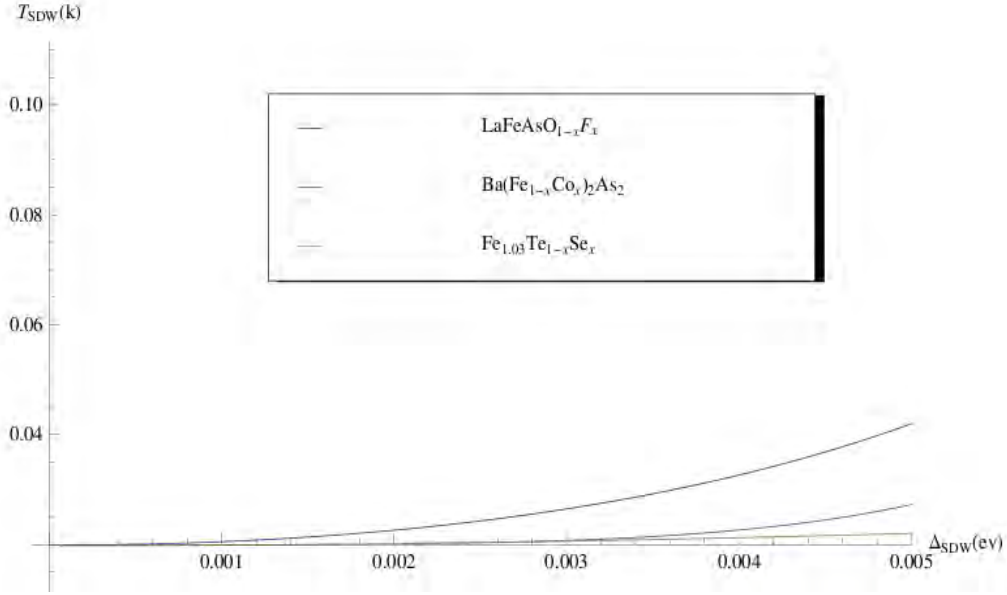


Figure 5.2: A graph of magnetic ordering temperature (T_{SDW}) Vs magnetic order parameter (Δ_{SDW}) for doped $LaFeAsO_{1-x}F_x$ (Blue color), $Ba(Fe_{1-x}Co_x)_2As_2$ (Red color) and $Fe_{1.03}Te_{1-x}Se_x$ (Yellow color)

In figure 5.2, T_{SDW} Vs Δ_{SDW} is plotted for $LaFeAsO_{1-x}F_x$, $Ba(Fe_{1-x}Co_x)_2As_2$ and $Fe_{1.03}Te_{1-x}Se_x$. It is clear from fig.5.2 that the magnetic ordering temperature T_{SDW} increases with Δ_{SDW} . Although increase in T_{SDW} for small values of Δ_{SDW} is small but increase is rapid for higher values of Δ_{SDW} . In any case our results shows enhancement of T_{SDW} with magnetic order parameter (Δ_{SDW}).

Figure 5.3 below shows variation of transition temperature T_C with Δ_{SDW} . Although the transition temperatures of the three doped compounds are different, it is clear from fig.5.3 that transition temperatures decreases with the increase of the magnetic order parameter (Δ_{SDW}). Therefore the figure demonstrates the influence of the SDW order parameter (Δ_{SDW}) on the SC transition temperatures (T_C).

Comparing the figure 5.2 and 5.3 we find that the magnetic order parameter suppresses the superconducting transition temperatures and it enhances the magnetic ordering temperatures.

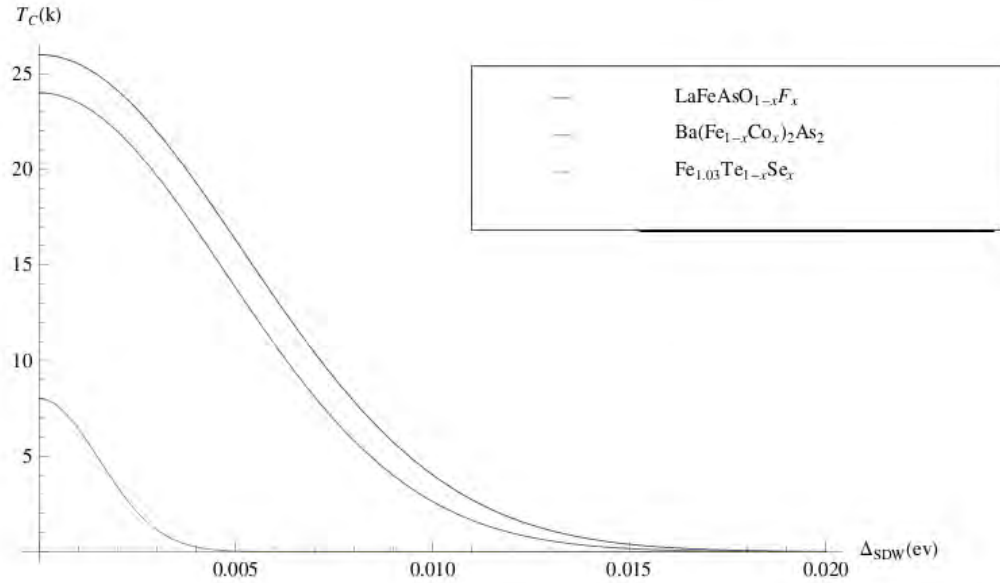


Figure 5.3: A graph of superconducting transition temperature (T_C) Vs magnetic order parameter (Δ_{SDW}) for doped $LaFeAsO_{1-x}F_x$ (Blue color), $Ba(Fe_{1-x}Co_x)_2As_2$ (Red color) and $Fe_{1.03}Te_{1-x}Se_x$ (Yellow color)

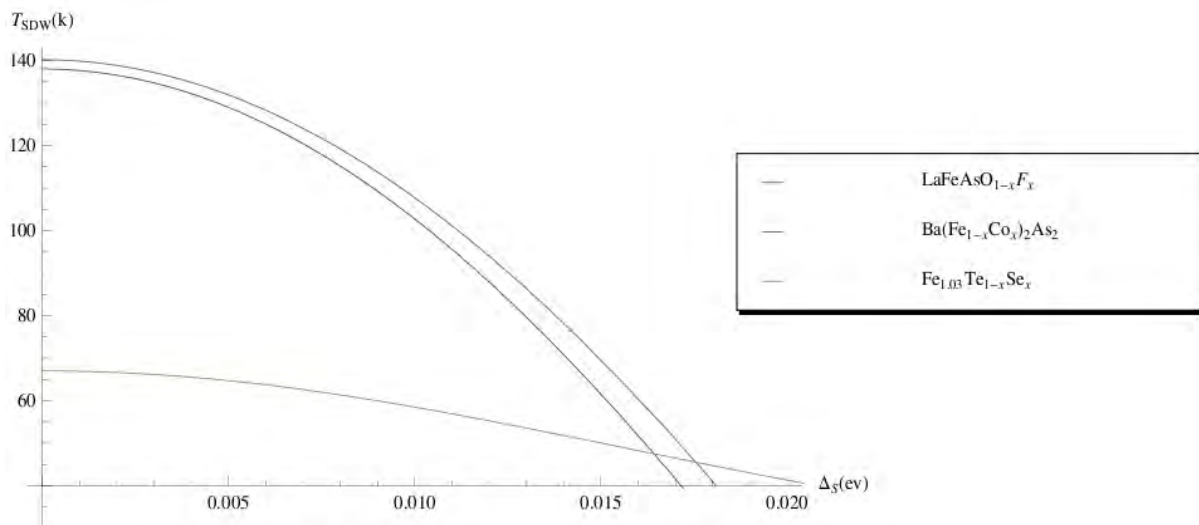


Figure 5.4: A graph of magnetic ordering temperature (T_{SDW}) Vs superconducting order parameter (Δ_S) for doped $LaFeAsO_{1-x}F_x$ (Blue color), $Ba(Fe_{1-x}Co_x)_2As_2$ (Red color) and $Fe_{1.03}Te_{1-x}Se_x$ (Yellow color)

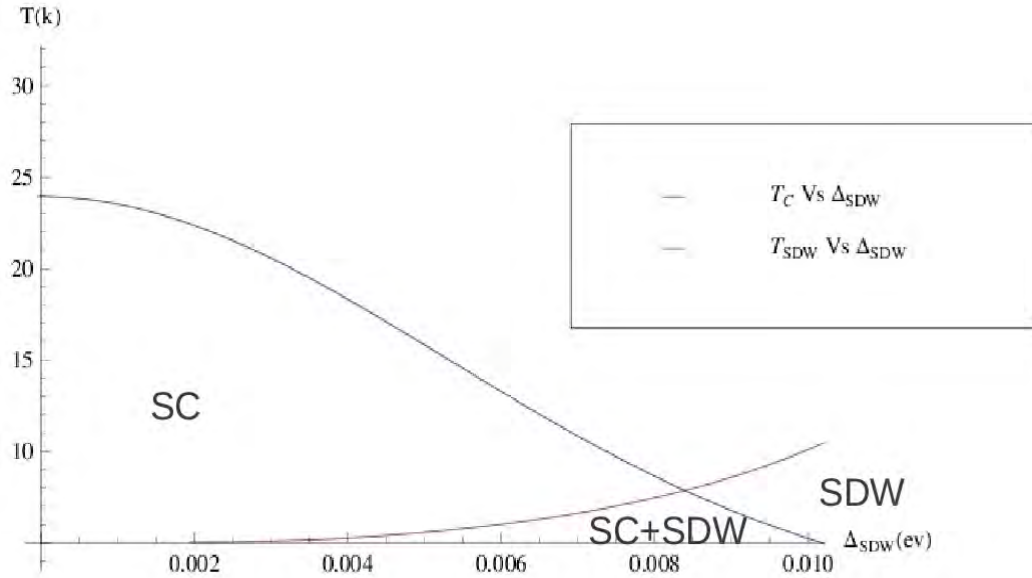


Figure 5.5: The phase diagram of the SDW and SC for doped $Ba(Fe_{1-x}Co_x)_2As_2$

Figure 5.4, Also shows the graph of magnetic ordering temperature (T_{SDW}) Vs the superconducting order parameter (Δ_S). Although the compounds have different values of T_{SDW} , the magnetic ordering temperature (T_{SDW}) of all doped compounds decreases with the increase of the superconducting order parameters (Δ_S) as shown in fig 5.4. Generally fig 5.4 shows the superconducting order parameters (Δ_S) suppresses the magnetic ordering temperatures (T_{SDW}).

In fig 5.5 we have plotted the superconducting transition temperatures (T_C) and magnetic ordering temperatures (T_{SDW}) evaluated at $T_C = 26$ k and $T_{SDW} = 140$ k Vs magnetic order parameters (Δ_{SDW}) for doped $LaFeAsO_{1-x}F_x$. Clearly the figure demonstrates the strong competition between the SC and SDW phases emphasizing the coexistence of SDW and superconductivity at low magnetic order parameter. More precisely an extended region of phase coexistence with $0.002 \leq \Delta_{SDW} \leq 0.009$ with the maximum transition temperature inside this region of ~ 9 k is observed. When the magnetic order parameter is further increased we obtained pure SDW phase for $0.009 \leq \Delta_{SDW} \leq 0.021$.

In fig 5.6 also we have plotted the superconducting transition temperatures (T_C) and

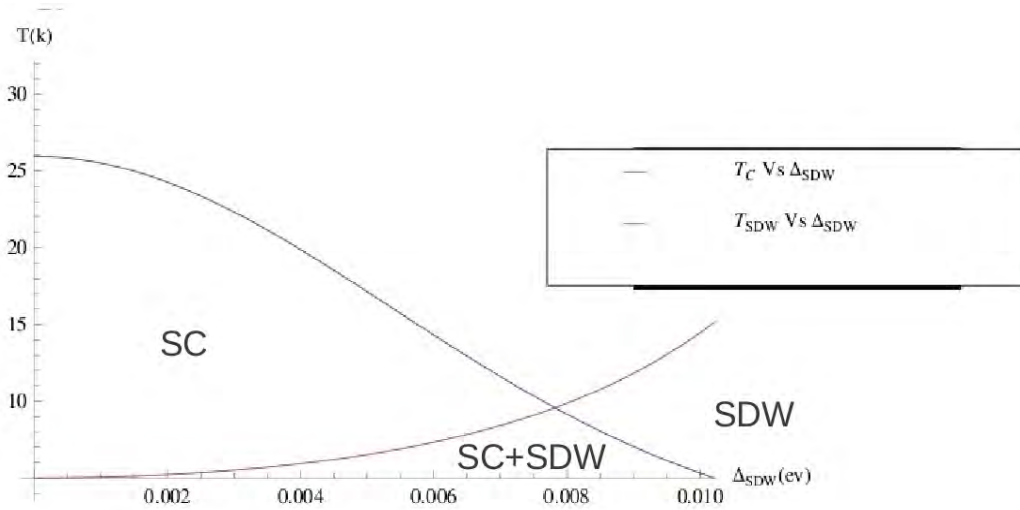


Figure 5.6: The phase diagram of the SDW and SC for doped $LaFeAsO_{1-x}F_x$

magnetic ordering temperatures (T_{SDW}) evaluated at $T_C = 24$ k and $T_{SDW} = 138$ k Vs magnetic order parameters (Δ_{SDW}) for doped $Ba(Fe_{1-x}Co_x)_2As_2$. Here we find that, the coexistence of the SDW and SC phases at low magnetic order parameters for $T_C < T_{SDW}$. In fact the SC phase is dominant in the low magnetic order parameter region where as SDW phase is observed at large magnetic order parameter values. More precisely, the graph shows the coexistence of the SDW and SC phases in the region of $0.004 \leq \Delta_{SDW} \leq 0.010$ and the maximum T_C of 8 k is seen for $\Delta_{SDW} \sim 0.0085$ in this region. As a result in the region $0.010 \leq \Delta_{SDW} \leq 0.020$ we have observed a pure SDW phase. This result nicely corresponds to the doped 122 compounds.

In fig 5.7 we have presented the phase diagram of the SDW and SC phases for doped $Fe_{1.03}Te_{1-x}Se_x$. Clearly the figure demonstrates the SDW and SC phases coexist microscopically in the region $0.0022 \leq \Delta_{SDW} \leq 0.0044$. Also the superconducting transition temperatures T_C is very small ~ 0.5 k in this region. When $\Delta_{SDW} > 0.0044$ superconductivity disappears and we obtain a pure SDW phase. As shown from fig.5.7 the region of coexistence is small as compared to other doped compounds. The phase coexistence of the SDW and SC phases in ferropnictides have been reported in many papers. This fact is evident from our results, which clearly shows, superconductivity is destroyed by increasing the

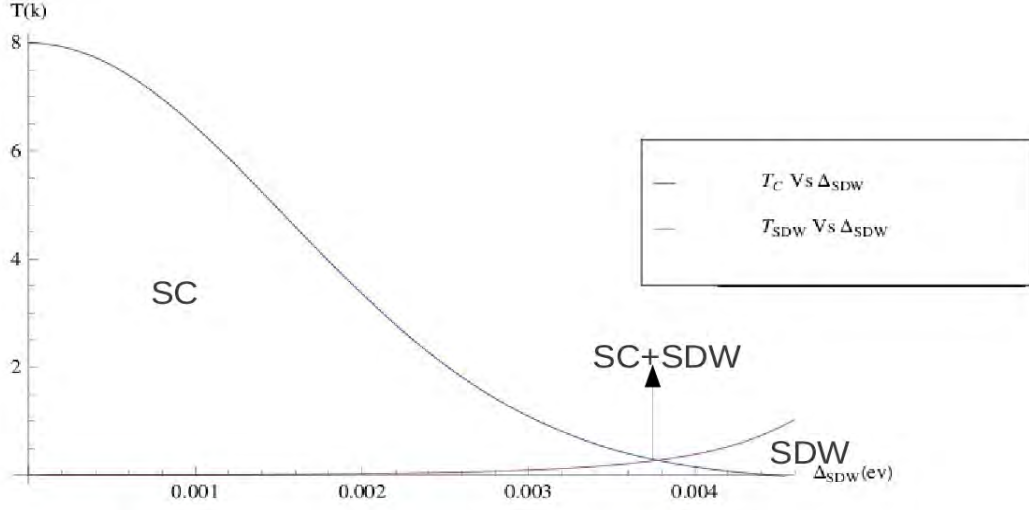


Figure 5.7: The phase diagram of the SDW and SC for doped $Fe_{1.03}Te_{1-x}Se_x$

magnetic order parameter (Δ_{SDW}), which is in agreement with ref. [112].

In conclusion we can say that our theoretical model provides a microscopic ground work towards explaining the interplay of superconductivity and SDW in Fe based superconductors.

It is a very well known fact that the first evidence of interplay between the SDW and SC in the Fe pnictide superconductors was the presence of magnetism in the concentration dependent phase diagram. This fact is also evident from our results, which clearly shows, the presence of magnetism in the magnetic order parameter (Δ_{SDW}) dependent phase diagram.

Considering the case of interplay between SDW and SC we therefore find that the magnetic order parameter suppresses the superconducting transition temperature and as a result both the SDW and SC phases coexist at low magnetic order parameter for $T_C < T_{SDW}$ and separate for $T_C > T_{SDW}$.

Chapter 6

Conclusion

In this paper, we examine the interplay between the Spin density wave and superconductivity in Fe pnictide superconductors. We have obtained the self consistent gap equations, and the expressions for the transition temperatures and order parameters with the combination of Green function technique. By calculating the temperatures as a function of order parameters, we have presented possible cases of phase coexistence /separation among the SDW and superconducting phases.

In our study the issue of interplay between SDW and superconducting state Such as been most carefully examine in doped $LaFeAsO_{1-x}F_x, Ba(Fe_{1-x}Co_x)_2As_2$ and $Fe_{1.03}Te_{1-x}Se_x$ and they exhibits coexistence between the magnetically ordered and the superconducting states which is similar with most experimental measurements.

The phase coexistence of SDW and Sc for $T_C < T_{SDW}$ in $LaFeAsO_{1-x}F_x, Ba(Fe_{1-x}Co_x)_2As_2$ and $Fe_{1.03}Te_{1-x}Se_x$ was shown in fig. 5.5, 5.6 and 5.7 respectively. In doing so, we employed a systematic way of determining the phase separation/coexistence between SDW and SC orders. We found that if T_C is larger than T_{SDW} then, the two orders phase separate, but coexist for $T_C < T_{SDW}$.

The phase diagram in the $T_C - \Delta_{SDW}$ and $T_{SDW} - \Delta_{SDW}$ plane, the Δ_{SDW} dependence of the superconducting transition temperature(T_C) and the magnetic ordering temperature (T_{SDW}) were shown, Here we found that the superconducting transition

temperature(T_C) decrease with the increase of order parameter (Δ_{SDW}),while the magnetic order temperature (T_{SDW})increases with increasing magnetic order parameter.

Further more when the magnetic ordering parameters is further increased we observe that the superconducting transition temperature decreases sufficiently rapidly from its maximum value.

In general,our results clearly shows the fact that,superconductivity is destroyed by increasing the magnetic order parameter (Δ_{SDW}).On the other hand,the suppression of magnetic order parameter(Δ_{SDW}) is important for the emergence of superconductivity and for enhancing the superconducting transition temperature(T_C).

Therefore the present paper presents as extensive study of a very strong interplay and coexistence between the SDW and superconductivity. We would like to further point out that,there are some differences in the magnetic order dependent phase diagrams of various Fe- based superconductors,inspection of phase diagrams for pnictide family shows that there are some common features.

All compounds exhibit a magnetically ordered state,which suppresses the the superconducting states.Therefore this shows an evidence for the interplay between SDW and Superconductivity in Fe pnictide superconductors.

Finally,we remark that the shape of the electron Fermi surfaces take quite different forms for different class of the pnictides,the effect of the FS shapes on the phase coexistence was studied in ref.[116].Also the effect of magnetism on the phase separation/coexistence will be interesting.We are currently applying the present method to understand how the phase coexistence/separation phenomenon depends on magnetic ordering state.

Bibliography

- [1] Kamihara Y, Watanabe T, Hirano M and Hosono H 2008 Iron-based layered superconductor $La[O_{1-x}Fx]FeAs$ ($x = 0.050.12$) with $T_C = 26$ K J. Am. Chem. Soc. 130 3296
- [2] Ren Z A et al 2008 Superconductivity in the iron-based F-doped layered quaternary compound $Nd[O_{1-x}Fx]FeAs$ Europhys. Lett. 82 57002
- [3] Ren Z A, Yang J, Lu W, Yi W, Che G C, Dong X L, Sun L L and Zhao Z X 2008 Superconductivity at 52 K in iron based F doped layered quaternary compound $Pr[O_{1-x}Fx]FeAs$ Mater. Res. Innov. 12 1056
- [4] Ren Z A et al 2008 Superconductivity at 55 K in iron-based F-doped layered quaternary compound $Sm[O_{1-x}Fx]FeAs$ Chin. Phys. Lett. 25 22156
- [5] Chen G F, Li Z, Wu D, Li G, Hu W Z, Dong J, Zheng P, Luo J L and Wang N L 2008 Superconductivity at 41 K and its competition with spin-density-wave instability in layered $CeO_{1-x}FxFeAs$ Phys. Rev. Lett. 100 247002
- [6] H,K,Onnes,Leiden comm.124c(1911)
- [7] G.Ascherman,E.Friederich,E.Justi and -J.Kramer,Pys.Zeir.,42349(1941)
- [8] J.Bardeen,LN.Cooper and J.R.Schriffer,Phys.Rev.106,162 (1957);Phys.Rev.108,1175(1957)
- [9] Bos J W G, Penny G B S, Rodgers J A, Sokolov D A,Huxley A D and Attfield J P 2008 High pressure synthesis of late rare earth $RFeAs(O, F)$ superconductors; R = Tb and Dy Chem. Commun. 36345
- [10] Wang C et al 2008 Thorium-doping-induced superconductivity up to 56 K in $Gd_{1-x}ThxFeAsO$ Europhys. Lett. 83 67006
- [11] Ren Z A et al 2008 Superconductivity and phase diagram in iron-based arsenic-oxides $ReFeAsO_{1-\delta}$ (Re = rare-earth metal) without fluorine doping Europhys. Lett. 83 17002
- [12] Miyazawa K, Kihou K, Shirage P M, Lee C H, Kito H, Eisaki H and Iyo A 2009 Superconductivity above 50 K in $LnFeAsO_{(1-y)}$ (Ln = Nd, Sm, Gd, Tb, and Dy) synthesized

by high-pressure technique J. Phys. Soc. Japan 78 034712

[13] Kito H, Eisaki H and Iyo A 2008 Superconductivity at 54 K in F-free $NdFeAsO_{1-y}$ J. Phys. Soc. Japan 77 063707

[14] Yang J et al 2008 Superconductivity at 53.5 K in $GdFeAsO_{1-\delta}$ Supercond. Sci. Technol. 21 082001

[15] de la Cruz C et al 2008 Magnetic order close to superconductivity in the iron-based layered $LaO_{1-x}F_xFeAs$ systems Nature 453 899902

[16] Rotter M, Tegel M and Johrendt D 2008 Superconductivity at 38 K in the iron arsenide $(Ba_{1-x}Kx)Fe_2As_2$ Phys. Rev. Lett. 101 107006

[17] Sefat A S, Huq A, McGuire M A, Jin R Y, Sales B C, Mandrus D, Cranswick L M D, Stephens P W and Stone K H 2008 Superconductivity in $LaFe_{1-x}Co_xAsO$ Phys. Rev. B 78 104505

[18] Sefat A S, Jin R Y, McGuire M A, Sales B C, Singh D J and Mandrus D 2008 Superconductivity at 22 K in Co-doped $BaFe_2As_2$ crystals Phys. Rev. Lett. 101 117004

[19] Li L J et al 2009 Superconductivity induced by Ni doping in $BaFe_2As_2$ single crystals New J. Phys. 11 025008

[20] Ni N, Thaler A, Kracher A, Yan J Q, Budko S L and Canfield P C 2009 Phase diagrams of $Ba(Fe_{1-x}Mx)_2As_2$ single crystals (M = Rh and Pd) Phys. Rev. B 80 024511

[21] Han F et al 2009 Superconductivity and phase diagrams of the 4d- and 5d-metal-doped iron arsenides $SrFe_{2-x}MxAs_2$ (M = Rh, Ir, Pd) Phys. Rev. B 80 024506

[22] H.R.Ott, H. Rudiger, Z. Fisk and J.L. Smith. Phys. Rev. Lett. 50, 1595 (1983)

[23] Qi Y P, Wang L, Gao Z S, Wang D L, Zhang X P and Ma Y W 2009 Superconductivity induced by doping Ru in $SrFe_{2-x}Ru_xAs_2$ Physica C 469 19214

[24] Canfield P C, Budko S L, Ni N, Yan J Q and Kracher A 2009 Decoupling of the superconducting and magnetic/structural phase transitions in electron-doped $BaFe_2As_2$ Phys. Rev. B 80 060501

[25] Sefat A S, Singh D J, VanBebber L H, Mozharivskyj Y, McGuire M A, Jin R Y, Sales B C, Keppens V and Mandrus D 2009 Absence of superconductivity in hole-doped $BaFe_{2-x}Cr_xAs_2$ single crystals Phys. Rev. B 79 224524

[26] B.D. Joesefson, Phys. Lett. 1, 251 (1962)

[27] J.D. Dew Hughes and V.D. Linee, J. Appl. Phys. 50, 3500 (1979)

- [28] F. Steglich, J. Aarts, C. D. Bredl, W. Leike, D. Meschede, W. Franz and H. Schafer, *phys. rev. lett* 43, 1892 (1979)
- [29] D. C. Johnston, H. Prakash, W. H. Zachariasen and R. Viswanathan, *Mat. Res. Bull.* 8, 777 (1973)
- [30] A. W. Seight, J. L. Gillson and P. E. Bierstedt. *Sol. State. Comm*, 17, 27 (1975)
- [31] L. B. Colman, M. J. Cohen, D. J. Sandman, F. G. Yamagishi, A. F. Garito and A. J. Heeper, *Solid state Comm*, 12, 1125 (1973)
- [32] D. Jerome, A. Mazaud, M. Ribault, and K. Beechgaard; *J. Phys. (Paris) Lett.* 41, L95 (1980)
- [33] V. N. Tauklin, E. E. Khostyuchenko, Yu. V. Sushko, I. F. Schnegolve, and E. B. Yagubskii, *PismaZh. Ekip. Teor. Fiz*, 41, 68 (1985)
- [34] J. F. Schooley, W. R. Hoster, E. Ambler, J. H. Becker, M. L. Cohen and C. S. Koonce, *Phys. Rev. Lett* 14, 305 (1965)
- [35] M. k. Wu, J. R. Ashburn, C. J. Torng, P. H. Hor, R. L. Meng, L. Gao, Z. J. Huang, Y. G. Wang, and C. W. Chu, *Phys. Rev. Lett*, 58, 908 (1987)
- [36] J. G. Bednorz and K. A. Muller, *Z. Phys. B* 64, 189 (1986)
- [37] Tapp J H, Tang Z J, Lv B, Sasmal K, Lorenz B, Chu P C W and Guloy A M 2008 *LiFeAs*: an intrinsic FeAs-based superconductor with $T_C = 18$ K *Phys. Rev. B* 78 060505
- [38] Wang X C, Liu Q Q, Lv Y X, Gao W B, Yang L X, Yu R C, Li F Y and Jin C Q 2008 The superconductivity at 18 K in *LiFeAs* system *Solid State Commun.* 148 53840
- [39] Pitcher M J, Parker D R, Adamson P, Herkelrath S J C, Boothroyd A T, Ibberson R M, Brunelli M and Clarke S J 2008 Structure and superconductivity of *LiFeAs* *Chem. Commun.* 591820
- [40] Chu C W, Chen F, Gooch M, Guloy A M, Lorenz B, Lv B, Sasmal K, Tang Z J, Tapp J H and Xue Y Y 2009 The synthesis and characterization of *LiFeAs* and *NaFeAs* *Physica C* 469 32631
- [41] M. D. Lumsden and A. D. Christenson, *J. Phys. Condens. Matter* 22 (2010) 203203 (26PP)
- [42] Hsu F C et al 2008 Superconductivity in the *PbO*-type structure α -*FeSe* *Proc. Natl Acad. Sci. USA* 105 142624
- [43] Subedi A, Zhang L J, Singh D J and Du M H 2008 Density functional study of *FeS*, *FeSe*, and *FeTe*: electronic structure, magnetism, phonons, and superconductivity *Phys. Rev. B* 78 134514

- [44] Bao W *etal* 2009 Tunable ($\delta\Pi, \delta\Pi$)-type antiferromagnetic order in α -Fe(Te, Se) superconductors *Phys. Rev. Lett.* 102 247001
- [45] Bao W et al 2009 Tunable ($\delta\Pi, \delta\Pi$)-type antiferromagnetic order in α -Fe(Te, Se) superconductors *Phys.Rev.Lett.* 102 247001
- [46] Zhu X Y, Han F, Mu G, Cheng P, Shen B, Zeng B and Wen H H 2009 Transition of stoichiometric Sr_2VO_3FeAs to a superconducting state at 37.2 K *Phys.Rev. B* 79 220512
- [47] Chen G F, Xia T-L, Yang H X, Li J Q, Zheng P, Luo J L and Wang N L 2009 Possible high temperature superconductivity in a Ti-doped $A\text{ScFeAsO}$ ($A = \text{Ca}, \text{Sr}$) system *Supercond.Sci.Technol.* 22 072001
- [48] Boeri L, Dolgov O V and Golubov A A 2008 Is $LaFeAsO_{1-x}Fx$ an electronphonon superconductor? *Phys.Rev.Lett.* 101 026403
- [49] Christianson A D *etal* 2008 Phonon density of states of $LaFeAsO_{1-x}Fx$ *Phys.Rev.Lett.* 101 157004
- [50] McGuire M A *etal* 2008 Phase transitions in $LaFeAsO$: structural, magnetic, elastic, and transport properties, heat capacity and Mössbauer spectra *Phys.Rev. B* 78 094517
- [51] Nomura T, Kim S W, Kamihara Y, Hirano M, Sushko P V, Kato K, Takata M, Shluger A L and Hosono H 2008 Crystallographic phase transition and high- T_c superconductivity in $LaFeAsO:F$ *Supercond.Sci.Technol.* 21 125028
- [52] Luetkens H *etal* 2009 The electronic phase diagram of the $LaO_{1-x}FxFeAs$ superconductor *Nat.Mater.* 8 3059
- [53] Zhao J *etal* 2008 Structural and magnetic phase diagram of $CeFeAsO_{1-x}Fx$ and its relation to high-temperature superconductivity *Nat.Mater.* 7 9539
- [54] Drew A J et al 2009 Coexistence of static magnetism and superconductivity in $SmFeAsO_{1-x}Fx$ as revealed by muon spin rotation *Nat.Mater.* 8 3104
- [55] de la Cruz C et al 2008 magnetic order close to superconductivity in the iron based layered $LaO_{1-x}FxFeAs$ system *Nature* 453 ,899-902
- [56] Rotundu C R, Keane D T, Freelon B, Wilson S D, Kim A, Valdivia P N, Bourret-Courchesne E and Birgeneau R J 2009 Phase diagram of the $PrFeAsO_{1-x}Fx$ superconductor arXiv:0907.1308
- [57] Margadonna S, Takabayashi Y, McDonald M T, Brunelli M, Wu G, Liu R H, Chen

- X H and Prassides K 2009 Crystal structure and phase transitions across the metalsuperconductor boundary in the $SmFeAsO_{1-x}Fx$ ($0 \leq x \leq 0.20$) family *Phys.Rev. B* 79 014503
- [58] Chen G F, Li Z, Wu D, Dong J, Li G, Hu W Z, Zheng P, Luo J L and Wang N L 2008 Element substitution effect in transition metal oxypnictide $Re(O_{1-x}F_x)TAs$ (Re = rare earth, T = transition metal) *Chin.Phys.Lett.* 25 22358
- [59] Rotter M, Tegel M, Johrendt D, Schellenberg I, Hermes W and Pottgen R 2008 Spin-density-wave anomaly at 140 K in the ternary iron arsenide $BaFe_2As_2$ *Phys.Rev. B* 78 020503
- [60] Huang Q, Qiu Y, Bao W, Green M A, Lynn J W, Gasparovic Y C, Wu T, Wu G and Chen X H 2008 Neutron-diffraction measurements of magnetic order and a structural transition in the parent $BaFe_2As_2$ compound of FeAs-based high-temperature superconductors *Phys.Rev.Lett.* 101 257003
- [61] Kofu M, Qiu Y, Bao W, Lee S H, Chang S, Wu T, Wu G and Chen X H 2009 Neutron scattering investigation of the magnetic order in single crystalline $BaFe_2As_2$ *NewJ.Phys.* 11 055001
- [62] Rotter M, Pangerl M, Tegel M and Johrendt D 2008 Superconductivity and crystal structures of $(Ba_{1-x}K_x)Fe_2As_2$ ($x = 0-1$) *Angew.Chem.Int.Edn* 47 794952
- [63] Chen H et al 2009 Coexistence of the spin-density wave and superconductivity in $Ba_{1-x}K_xFe_2As_2$ *Europhys.Lett.* 85 17006
- [64] Wang X F, Wu T, Wu G, Liu R H, Chen H, Xie Y L and Chen X H 2009 The peculiar physical properties and phase diagram of $BaFe_{2-x}Co_xAs_2$ single crystals *NewJ.Phys.* 11 045003
- [65] Ni N, Tillman M E, Yan J Q, Kracher A, Hannahs S T, Budko S L and Canfield P C 2008 Effects of Co substitution on thermodynamic and transport properties and anisotropic Hc_2 in $Ba(Fe_{1-x}Co_x)_2As_2$ single crystals *Phys.Rev. B* 78 214515
- [66] Pratt D K, Tian W, Kreyssig A, Zarestky J L, Nandi S, Ni N, Budko S L, Canfield P C, Goldman A I and McQueeney R J 2009 Coexistence of competing antiferromagnetic and superconducting phases in the underdoped $Ba(Fe_{0.953}Co_{0.047})_2As_2$ compound using x-ray and neutron scattering techniques *Phys.Rev.Lett.* 103 087001
- [67] Christianson A D, Lumsden M D, Nagler S E, MacDougall G J, McGuire M A, Sefat

- A S, Jin R, Sales B C and Mandrus D 2009 Static and dynamic magnetism in underdoped superconductor $BaFe_{1.92}Co_{0.08}As_2$ *Phys.Rev.Lett.* 103 087002
- [68] Chevrel R, Hirrien M and Sergent M 1986 Superconducting Chevrel phases: prospects and perspectives *Polyhedron* 5 8794
- [69] Müller K-H and Narozhnyi V N 2001 Interaction of superconductivity and magnetism in borocarbide superconductors *Rep.Prog.Phys.* 64 943
- [70] Metoki N, Haga Y, Koike Y and Onuki Y 1998 Superconducting energy gap observed in the magnetic excitation spectra of a heavy fermion superconductor UPd_2Al_3 *Phys.Rev.Lett.* 80 5417
- [71] Isaacs E D, Zschack P, Broholm C L, Burns C, Aeppli G, Ramirez A P, Palstra T T M, Erwin R W, Stücheli N and Bucher E 1995 Antiferromagnetism and its relation to the superconducting phases of UPt_3 *Phys.Rev.Lett.* 75 1178
- [72] Fukazawa H et al 2009 As- 75 NMR study of hole-doped superconductor $Ba_{1-x}K_xFe_2As_2$ (T_C similar or equal to 38 K) *J.Phys.Soc.Japan* 78 033704
- [73] Park J T *etal* 2009 Electronic phase separation in the slightly underdoped iron pnictide superconductor $Ba_{1-x}K_xFe_2As_2$ *Phys.Rev.Lett.* 102 117006
- [74] Inosov D S et al 2009 Suppression of the structural phase transition and lattice softening in slightly underdoped $Ba_{1-x}K_xFe_2As_2$ with electronic phase separation *Phys.Rev.B* 79 224503
- [75] Rotter M, Tegel M, Schellenberg I, Schappacher F M, Pottgen R, Deisenhofer J, Gunther A, Schrettle F, Loidl A and Johrendt D 2009 Competition of magnetism and superconductivity in underdoped $(Ba_{1-x}K_x)Fe_2As_2$ *NewJ.Phys.* 11 025014
- [76] Laplace Y, Bobroff J, Rullier-Albenque F, Colson D and Forget A 2009 Atomic coexistence of superconductivity and incommensurate magnetic order in the pnictide $Ba(Fe_{1-x}Co_x)_2As_2$ *Phys.Rev. B* 80 140501
- [77] Bernhard C et al 2009 Muon spin rotation study of magnetism and superconductivity in $BaFe_{2-x}Co_xAs_2$ and $Pr_{1-x}Sr_xFeAsO$ *NewJ.Phys.* 11 055050
- [78] Julien M H, Mayaffre H, Horvatic M, Berthier C, Zhang X D, Wu W, Chen G F, Wang N L and Luo J L 2009 Homogeneous versus inhomogeneous coexistence of magnetic order and superconductivity probed by NMR in Co- and K-doped iron pnictides *Europhys.Lett.* 87 37001

- [79] Sales B C, Sefat A S, McGuire M A, Jin R Y, Mandrus D and Mozharivskyj Y 2009 Bulk superconductivity at 14 K in single crystals of $Fe_{1+y}Te_xSe_{1-x}$ *Phys.Rev. B* 79 094521
- [80] Paulose P L, Yadav C S and Subhedar K M 2009 Magnetic phase diagram of $Fe_{1+y}Te_{1-x}Se_x$ system: coexistence of spin glass behavior with superconductivity? arXiv:0907.3513
- [81] Klingeler R et al 2010 Local antiferromagnetic correlations in the iron pnictide superconductors $LaFeAsO_{1-x}F_x$ and $Ca(Fe_{1-x}Co_x)_2As_2$ as seen via normal-state susceptibility *Phys.Rev. B* 81 024506
- [82] Wang X F, Wu T, Wu G, Chen H, Xie Y L, Ying J J, Yan Y J, Liu R H and Chen X H 2009 Anisotropy in the electrical resistivity and susceptibility of superconducting $BaFe_2As_2$ single crystals *Phys.Rev.Lett.* 102 117005
- [83] Yan J Q et al 2008 Structural transition and anisotropic properties of single-crystalline $SrFe_2As_2$ *Phys.Rev. B* 78 024516
- [84] Zhang G M, Su Y H, Lu Z Y, Weng Z Y, Lee D H and Xiang T 2009 Universal linear-temperature dependence of static magnetic susceptibility in iron pnictides *Europhys.Lett.* 86 37006
- [85] Sales B C, McGuire M A, Sefat A S and Mandrus D 2010 A model of the normal state susceptibility and transport properties of $Ba(Fe_{1-x}Co_x)_2As_2$: an explanation of the increase of magnetic susceptibility with temperature *Physica C* 470 304
- [86] McGuire T R and Kriessman C J 1952 The magnetic susceptibility of chromium *Phys.Rev.* 85 452
- [87] Huang Q, Zhao J, Lynn J W, Chen G F, Luo J L, Wang N L and Dai P C 2008 Doping evolution of antiferromagnetic order and structural distortion in $LaFeAsO_{1-x}F_x$ *Phys.Rev. B* 78 054529
- [88] Singh D J and Du M H 2008 Density functional study of $LaFeAsO_{1-x}F_x$: a low carrier density superconductor near itinerant magnetism *Phys.Rev.Lett.* 100 237003
- [89] Mazin I I, Singh D J, Johannes M D and Du M H 2008 Unconventional superconductivity with a sign reversal in the order parameter of $LaFeAsO_{1-x}F_x$ *Phys.Rev.Lett.* 101 057003
- [90] Dong J et al 2008 Competing orders and spin-density-wave instability in $LaO_{1-x}F_xFeAs$ *Europhys.Lett.* 83 27006

- [91] Yildirim T 2008 Origin of the 150 K anomaly in *LaFeAsO*: competing antiferromagnetic interactions, frustration, and a structural phase transition *Phys.Rev.Lett.* 101 057010
- [92] Ma F J, Lu Z Y and Xiang T 2009 Arsenic-bridged antiferromagnetic superexchange interactions in *LaFeAsO* (vol 78, art no 224517, 2008) *Phys.Rev. B* 79 224517
- [93] Si Q M and Abrahams E 2008 Strong correlations and magnetic frustration in the high T_C iron pnictides *Phys.Rev.Lett.* 101 076401
- [94] Chen Y, Lynn J W, Li J, Li G, Chen G F, Luo J L, Wang N L, Dai P C, de la Cruz C and Mook H A 2008 Magnetic order of the iron spins in *NdFeAsO* *Phys.Rev. B* 78 064515
- [95] Zhao J et al 2008 Lattice and magnetic structures of *PrFeAsO*, *PrFeAsO_{0.85}F_{0.15}*, and *PrFeAsO_{0.85}* *Phys.Rev. B* 78 132504
- [96] Ryan D H, Cadogan J M, Ritter C, Canepa F, Palenzona A and Putti M 2009 Coexistence of long-ranged magnetic order and superconductivity in the pnictide superconductor *SmFeAsO_{1-x}F_x* ($x=0, 0.15$) *Phys.Rev. B* 80 220503
- [97] Kimber S A J *etal* 2008 Magnetic ordering and negative thermal expansion in *PrFeAsO* *Phys.Rev. B* 78 140503
- [98] Qiu Y et al 2008 Crystal structure and antiferromagnetic order in *NdFeAsO_{1-x}F_x* ($x = 0.0$ and 0.2) superconducting compounds from neutron diffraction measurements *Phys.Rev.Lett.* 101 257002
- [99] Klauss H H et al 2008 Commensurate spin density wave in *LaFeAsO*: a local probe study *Phys.Rev.Lett.* 101 077005
- [100] Kitao S, Kobayashi Y, Higashitaniguchi S, Saito M, Kamihara Y, Hirano M, Mitsui T, Hosono H and Seto M 2008 Spin ordering in *LaFeAsO* and its suppression in superconductor *LaFeAsO_{0.89}F_{0.11}* probed by Mössbauer spectroscopy *J.Phys.Soc.Japan* 77 103706
- [101] Sanchez D R, Alzamora M, Munevar J, Wang N L, Cheng G F and Baggio-Saitovitch E 2009 Mössbauer study of superconducting *NdFeAsO_{0.88}F_{0.12}* and its parent compound *NdFeAsO* *J.Phys. : Condens.Matter* 21 455701
- [102] Su Y et al 2009 Antiferromagnetic ordering and structural phase transition in *Ba₂Fe₂As₂* with Sn incorporated from the growth flux *Phys.Rev. B* 79 064504

- [103] Zhao J, Ratcliff W, Lynn J W, Chen G F, Luo J L, Wang N L, Hu J P and Dai P C 2008 Spin and lattice structures of single-crystalline $SrFe_2As_2$ *Phys.Rev. B* 78 140504
- [104] Kaneko K, Hoser A, Caroca-Canales N, Jesche A, Krellner C, Stockert O and Geibel C 2008 Columnar magnetic structure coupled with orthorhombic distortion in the anti-ferromagnetic iron arsenide $SrFe_2As_2$ *Phys.Rev. B* 78 212502
- [105] Jesche A et al 2008 Strong coupling between magnetic and structural order parameters in $SrFe_2As_2$ *Phys.Rev. B* 78 180504
- [106] Tegel M, Rotter M, Weiss V, Schappacher F, Pottgen R and Johrendt D 2008 Structural and magnetic phase transitions in the ternary iron arsenides $SrFe_2As_2$ and $EuFe_2As_2$ *J.Phys. : Condens.Matter* 20 452201
- [107] Li S L et al 2009 First-order magnetic and structural phase transitions in $Fe_{1+y}Se_xTe_{1-x}$ *Phys.Rev. B* 79 054503
- [108] Bonville P, Rullier-Albenque F, Colson D and Forget A 2010 Incommensurate spin density wave in Co-doped $BaFe_2As_2$ arXiv:1002.0931
- [109] Krellner C, Burkhardt U and Geibel C 2009 Interplay between 3d and 4f magnetism in $CeCoPO$ *Physica B* 404 32069
- [110] Schuster W, Mikler H and Komarek K L 1979 Transition metal-chalcogen systems, VII: the iron-selenium phase diagram *Monatsh.Chem.* 110 1153
- [111] Mcqueen T M et al 2009 Extreme sensitivity of superconductivity to stoichiometry in $Fe_{1+\delta}Se$ *Phys.Rev. B* 79 014522
- [112] Fang M H, Pham H M, Qian B, Liu T J, Vehstedt E K, Liu Y, Spinu L and Mao Z Q 2008 Superconductivity close to magnetic instability in $Fe(Se_{1-x}Te_x)_{0.82}$ *Phys.Rev. B* 78 224503
- [113] T. Ishiguro, K. Yamaji and G.saito, Organic superconductors ; Springer series in Solid state Sciences, Vol. 48, p-99, Berlin, Heidelberg, New York ; Springer 1990.
- [114] Stuart A. Wolf, and Vidamir Z.Kresin, Novel Superconductivity.
- [115] M.D Lumsden and A.D.Christianson, 2010 magnetism in Fe based superconductors. *J.Phys:Condens.Matter* 22,203203
- [116] P.Singh J.supercon.Novel Magnetism.24,945

Declaration

This thesis is my original work, has not been presented for a degree in any other University and that all the sources of material used for the thesis have been dully acknowledged.

Name: Wubishet Ahmed

Signature:— — — — —

Place and time of submission: Addis Ababa University, June 2011

This thesis has been submitted for examination with my approval as University advisor.

Name: Prof.P.Singh

Signature:— — — — —